

**THE LIVER IN UROPORPHYRIA**  
**A BIOCHEMICAL AND MORPHOLOGICAL STUDY**

Peter D. Siersema

Financial support for the publication of this thesis was generously provided by:  
Glaxo, Brocades Pharma Nederland, Tramedico, Byk Nederland, Duphar Nederland,  
Nourypharma and Ciba Geigy.

Cover: "Venaesectione Inamorata"

Engraving; Artist unknown; Printed by Petrus Schenk (1660-1713)  
(Rijksmuseum, Amsterdam, The Netherlands)

CIP-GEGEVENS KONINKLIJKE BIBLIOTHEEK, DEN HAAG

Siersema, Peter Derk

The liver in uroporphyrria: a biochemical and  
morphological study / Peter Derk Siersema. - [S.l.:  
s.n.] - [1].

Proefschrift Rotterdam. - Met lit. opg., reg.

ISBN 90-9006261-0

NUGI 743

Trefw.: porfyrria cutanea tarda / uroporfyrrie / lever.

© 1993, Peter D. Siersema. No part of this book may be reproduced in any form or by any  
means without permission of the author.

Printed by Haveka BV, Alblasserdam, The Netherlands

**THE LIVER IN UROPORPHYRIA**  
**A BIOCHEMICAL AND MORPHOLOGICAL STUDY**

DE LEVER BIJ UROPORFYRIE  
een biochemische en morfologische studie

**Proefschrift**

Ter verkrijging van de graad van doctor  
aan de Erasmus Universiteit  
op gezag van de rector magnificus  
Prof.Dr P.W.C. Akkermans M.Lit.  
en volgens het besluit van het college van dekanen.  
De openbare verdediging zal plaatsvinden op  
woensdag 27 oktober 1993 om 15.45 uur

door

**Peter Derk Siersema**

Geboren te Delft

**Promotiecommissie:**

Promotores: Prof.Dr H.G. van Eijk  
Prof. J.H.P. Wilson

Overige leden: Prof.Dr F.J.W. ten Kate  
Prof.Dr J.F. Koster

The studies reported in this thesis were performed at the Departments of Chemical Pathology, Erasmus University Rotterdam (Head: Prof.Dr H.G. van Eijk), Internal Medicine II, University Hospital Rotterdam-Dijkzigt (Head: Prof. J.H.P. Wilson), Pathology, Erasmus University Rotterdam (Head: Prof.Dr F.T. Bosman) and Pathology, Academical Medical Centre, Amsterdam (Head: Prof.Dr F.J.W. ten Kate), The Netherlands.

*Alle Toekomst is Gebouwd op het Verleden*

*Confucius (550 v. Chr.)*

Uit: Beschouwingen over de Porphyria Cutanea Tarda  
Door: Dr Tio Tiong Hoo (Academisch Proefschrift 1956)

## TABLE OF CONTENTS

	page
List of abbreviations and of international enzyme nomenclature	1
<b>Chapter 1</b>	<b>3</b>
Uroporphyrin: A Review of the Literature	
1.0 Introduction	
1.1 The heme biosynthetic pathway	
1.2 The porphyrias	
1.3 Porphyria cutanea tarda	
1.4 Experimental uroporphyrin	
1.5 Aims of the study	
<b>Chapter 2</b>	<b>23</b>
Materials & Methods	
<b>PART A. EXPERIMENTAL UROPORPHYRIA</b>	<b>35</b>
<b>Chapter 3</b>	<b>37</b>
Ferritin Iron Accumulation and Uroporphyrin Crystal Formation in Hepatocytes of C57BL/10 mice: A Biochemical and Morphological Study	
<b>Chapter 4</b>	<b>57</b>
The Effect of Desferrioxamine on Iron Metabolism, Lipid Peroxidation and Porphyrin Metabolism in Hepatocytes of C57BL/10 Mice with Uroporphyrin	

	<b>page</b>
<b>PART B. PORPHYRIA CUTANEA TARDA</b>	<b>71</b>
<b>Chapter 5</b>	<b>73</b>
The Liver in Porphyria Cutanea Tarda: A Morphological and Morphometrical Study	
<b>Chapter 6</b>	<b>91</b>
Porphobilinogen Deaminase Activity in Erythrocytes of Patients with Porphyria Cutanea Tarda	
<b>Chapter 7</b>	<b>101</b>
General Discussion and Summary	
<b>Chapter 8</b>	<b>111</b>
Samenvatting (Summary in Dutch)	
<b>Chapter 9</b>	<b>115</b>
References	
<b>List of publications related to this thesis</b>	<b>131</b>
<b>Curriculum Vitae (in Dutch)</b>	<b>133</b>
<b>Verantwoording (Acknowledgement in Dutch)</b>	<b>135</b>





## List of abbreviations

AIP	Acute Intermittent Porphyria
ALA	5-Aminolevulinic Acid
ALA-S	5-Aminolevulinic Acid Synthase
CYP1A2	Cytochrome P-4501A2
Cyt P-450	Cytochrome P-450
DFx	Desferrioxamine
EM	Electron Microscopy
EPP	Erythropoietic Protoporphyria
F-PCT	Familial Porphyria Cutanea Tarda
HBV	Hepatitis B Virus
HC	Hereditary Coproporphyria
HCB	Hexachlorobenzene
HCC	Hepatocellular Carcinoma
HCV	Hepatitis C Virus
HEP	Hepatoerythropoietic Porphyria
Ig PBG-D	Total Amount of Immuno-Detectable PBG-D
Ig PBG-D/100 U	Immuno-Detectable PBG-D per 100 Units of PBG-D Activity
IMF	Ferrihydroxide-Dextran (Imferon <sup>®</sup> )
IP	Intraperitoneal
LM	Light Microscopy
LMW	Low Molecular Weight
MC	3-Methylcholanthrene
MDA	Malondialdehyde
PAH	Polyhalogenated Aromatic Hydrocarbon
PBG	Porphobilinogen
PBG-D	Porphobilinogen Deaminase
PCT	Porphyria Cutanea Tarda
SD	Standard Deviation
S-PCT	Sporadic Porphyria Cutanea Tarda
TCDD	2,3,7,8,-Tetrachlorodibenzo- <i>p</i> -Dioxin
URO-D	Uroporphyrinogen Decarboxylase
VP	Variegate Porphyria

## List of the international nomenclature of the heme biosynthetic enzymes

EC 2.3.1.37	5-Aminolevulinic Acid Synthase
EC 4.2.1.24	5-Aminolevulinic Acid Dehydratase
EC 4.3.1.8	Porphobilinogen Deaminase
EC 4.2.1.75	Uroporphyrinogen-III-Synthase
EC 4.1.1.37	Uroporphyrinogen Decarboxylase
EC 1.3.3.3	Coproporphyrinogen Oxidase
EC 1.3.3.4	Protoporphyrinogen Oxidase
EC 4.99.1.1	Ferrochelatase



## CHAPTER 1

### Uroporphyrin: A Review of the Literature

Contents	page
1.0 Introduction	4
1.1 The heme biosynthetic pathway	4
1.2 The porphyrias	7
1.3 Porphyria cutanea tarda	9
1.4 Experimental uroporphyrin	16
1.5 Aims of the study	21

Parts of this chapter are based on:

Siersema PD, Wilson JHP.  
De porfyrieën.  
Ned Tijdschr Geneesk 1989; 133: 2542-2547.

Wilson JHP, Siersema PD.  
Geneesmiddelen bij acute porfyrie.  
Geneesmiddelenbulletin 1990; 24: 35-40.

Siersema PD, de Rooij FWM, Wilson JHP, van Helvoirt RP, van Eijk HG.  
De porfyrieën in klinisch-chemisch perspectief.  
Tijdschr NVKC 1991; 16: 16-22.

De Verneuil H, Bourgeois F, de Rooij F, Siersema PD, Wilson JHP, Grandchamp B, Nordmann Y.  
Characterization of a new mutation (R292G) and a deletion at the human uroporphyrinogen  
decarboxylase locus in two patients with hepatoerythropoietic porphyria.  
Hum Genet 1992; 89: 548-552.

Siersema PD, de Man RA, Wilson JHP, Alleman MA, Mulder AH, de Rooij FWM.  
Porphyria cutanea tarda and focal nodular hyperplasia: the role of estrogens.  
Eur J Gastroenterol Hepatol 1993, in press.

## 1.0 Introduction

Porphyria cutanea tarda (PCT) is the most common form of all porphyrias with an estimated prevalence of at least 1:25,000 in the western part of Europe (1).

The basic biochemical defect in PCT is a defective uroporphyrinogen decarboxylation in the liver (2-4). This leads to the overproduction and accumulation of uroporphyrins and heptacarboxylporphyrins in hepatocytes, followed by the accumulation in the skin. PCT can occur in families as an inherited disorder (2,4), but can also be produced in humans and animals by exposure to certain chemicals (1). Recent studies in humans with PCT and in animal models with uroporphyrin suggest that the changes in uroporphyrinogen decarboxylase (URO-D) activity and the accumulation of porphyrins to the levels at which overt uroporphyrin develops, requires the interaction between a number of inherited and acquired factors (1).

One of the most important factors is iron, and indeed iron removal by repeated phlebotomy remains the mainstay of treatment of PCT, as shown by Ippen in 1962 (5). Although many studies confirmed the important role for iron in the pathogenesis of PCT and experimental uroporphyrin, the mechanism by which iron influences porphyrin metabolism has not been elucidated.

### 1.1 The heme biosynthetic pathway

The principal sites for heme biosynthesis in humans are the bone marrow and the liver. Heme serves as the prosthetic group of hemoproteins, which mediate oxygen transport and storage, the generation of cellular energy, the formation of certain steroid hormones and some reduction reactions and detoxifications. Heme is also involved in the regulation of protein synthesis and modifies cell development in experimental systems (6).

#### 1.1.1 Heme biosynthesis

The synthesis of one molecule of heme requires 8 molecules of glycine and 8 molecules of succinyl CoA. The 8 enzyme steps required for heme synthesis are distributed between the mitochondrial and cytosolic compartments. The first and the last 3 steps occur in the mitochondrion and the intervening 4 steps in the cytosol (Figure 1).

All the enzymes have been purified and their kinetic parameters have been described (6). Moreover, the genes for 6 of the 8 enzymes have also been identified (7), allowing the

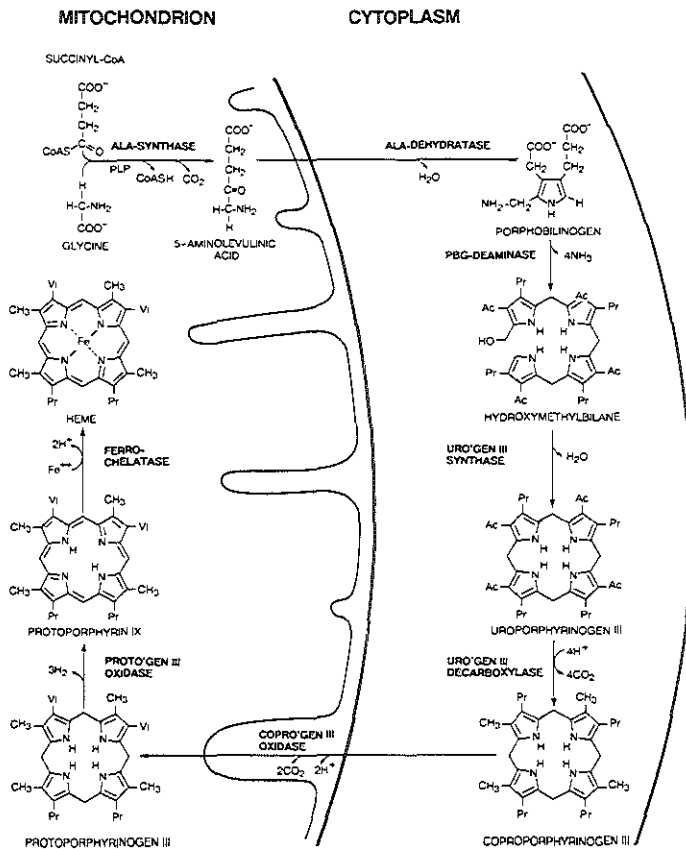


**Figure 1.** The heme biosynthetic pathway.

PLP, pyridoxal-5-phosphate; ALA, 5-Aminolevulinic Acid; PBG, Porphobilinogen; URO'gen, Uroporphyrinogen; COPRO'gen, Coproporphyrinogen; PROTO'gen, Protoporphyrinogen; Ac, Acetate; Pr, Propionate; Vi, Vinyl

(by courtesy of Dr S.S. Bottomley)

characterization of genetic defects of the pathway (the porphyrias) at the molecular level.

Under normal circumstances, the sequence of the enzymatic reactions proceeds with little accumulation of substrates and less than 2.5% of the 5-aminolevulinic acid (ALA) has been estimated to be lost during heme biosynthesis (1).

### 1.1.2 Regulation of heme biosynthesis

Intracellular heme is involved in the regulation of its own synthesis by a negative feedback mechanism exercised at the level of ALA synthase (ALA-S). Presumably, "free" heme concentrations determine this effect. The regulatory "free" heme pool can be visualized as a relatively small pool with a rapid turnover rate. The size of this pool is determined by rates of synthesis of heme and rates of withdrawal of heme for combination with the apoproteins of cytochromes and other hemoproteins, and by the rate-limiting enzyme of its degradation, heme oxygenase (6).

Certain steroids, drugs and chemical compounds induce hepatic ALA-S activity by inhibiting repression and in that way activating the transcription and increasing the amount of m-RNA for ALA-S (8). The induction probably results largely from depletion of the regulatory pool of heme by one or more of the following mechanisms (9):

1. Accelerated depletion of heme (e.g., depletion or inactivation of cytochrome P-450 by chemicals or drugs).
2. Inhibition of heme biosynthesis by inhibiting one or more of the enzymes of the heme pathway or by removal of the substrate of the enzyme.
3. Increased rate of combination of heme with apoproteins for synthesis or reconstitution of hemoproteins.

### 1.1.3 Porphyrins

Porphyrinogens and porphyrins are cyclic tetrapyrroles. The intermediate products formed in the heme biosynthetic pathway are the reduced forms of porphyrins, porphyrinogens (Figure 1). Porphyrinogens undergo rapid oxidation on exposure to oxygen to become porphyrins, which are the usual forms of the cyclic tetrapyrroles found in biologic specimens. With the exception of protoporphyrin, which is the substrate for ferrochelatase, all other enzymatic steps require porphyrinogens as substrate. Porphyrinogens have unique photo-optical properties. They are readily excited by light at around 400 nm to emit intense red fluorescence. In contrast, heme (Fe-protoporphyrin) does not emit fluorescence (1).

The water-solubility of porphyrins decreases with reduction in the number of carboxylic acid side-chains. Thus, uroporphyrin (with 8 carboxylic groups) is most water-soluble and protoporphyrin (with 2 carboxylic groups) is least water-soluble. Protoporphyrin is

excreted only in bile, while uroporphyrin and coproporphyrin are excreted mainly in urine.

Free porphyrins do not appear to have useful biologic functions. However, light activation of porphyrinogens causes cell damage: a) by injuring plasma and lysosomal membranes in the presence of oxygen-related free radicals (10), and b) by activating enzymes such as the complement system (11). In contrast, heme, chlorophyll and corrins, which are Fe, Mg, and Co chelates of porphyrins have important biologic functions.

## 1.2 The porphyrias

### 1.2.1 Different types of porphyria

The porphyrias have traditionally been classified according to whether the liver or the bone marrow is the main source of excess porphyrin production. Nowadays, a classification is preferred based on whether patients suffer acute attacks, cutaneous manifestations, or both (Table 1) (1,6,12).

Clinically indistinguishable attacks of acute porphyria occur in ALA dehydratase deficiency, acute intermittent porphyria (AIP), hereditary coproporphyrin (HC) and in variegate porphyria (VP). All the disorders causing an acute attack of porphyria have in

Table 1.  
The different types of porphyria.

Disorder	Enzyme deficiency	Clinical features		Site of porphyrin production	Inheritance
		Acute attacks	Skin symptoms		
ALA <sup>1</sup> dehydratase deficiency	ALA dehydratase	+	-	liver	Aut.-Rec. <sup>6</sup>
Acute intermittent porphyria	PBG <sup>2</sup> deaminase	+	-	liver	Aut.-Dom. <sup>7</sup>
Cong. erythropoietic porphyria	URO'gen <sup>3</sup> -III-synthase	-	+	bone marrow	Aut.-Rec.
Porphyria cutanea tarda	URO'gen decarboxylase	-	+	liver	Aut.-Dom.
Hereditary coproporphyrin	COPRO'gen <sup>4</sup> oxidase	+	+	liver	Aut.-Dom.
Variegate porphyria	PROTO'gen <sup>5</sup> oxidase	+	+	liver	Aut.-Dom.
Erythropoietic protoporphyria	Ferrochelatase	-	+	bone marrow and/or liver	Aut.-Dom.

ALA<sup>1</sup>, 5-Aminolevulinic Acid; PBG<sup>2</sup>, Porphobilinogen; URO'gen<sup>3</sup>, Uroporphyrinogen; COPRO'gen<sup>4</sup>, Coproporphyrinogen; PROTO'gen<sup>5</sup>, Protoporphyrinogen; Aut.-Dom.<sup>6</sup>, Autosomal-Dominant; Aut.-Rec.<sup>7</sup>, Autosomal-Recessive

common the overproduction of the porphyrin precursors, ALA and porphobilinogen (PBG), and the liver is the main site of overproduction of these precursors. Almost all acute attacks start with symptoms of abdominal pain, which may be accompanied by psychiatric abnormalities and peripheral neuropathy (13). At least 75% of attacks are precipitated by drugs, alcohol, fasting or endocrine factors (13,14). Five percent of attacks that are severe enough to require hospitalization end fatally (1).

Cutaneous manifestations caused by photosensitization due to porphyrinogens occur in all types of porphyria, except AIP and ALA dehydratase deficiency. Porphyrinogen photosensitization produces two distinct clinical syndromes:

1. Acute photosensitivity on exposure to sunlight with erythema and oedema, which subsides between episodes to leave few visible changes of the skin.
2. A syndrome in which subepidermal bullae, erosions, hypertrichosis and pigmentation occur in sun-exposed areas of the skin.

The first of these is seen only in erythropoietic protoporphyria (EPP) and the second in all cutaneous porphyrias. In VP and HC, acute porphyric attacks and skin lesions may occur together or separately (15).

### *1.2.2 Enzyme defects in porphyrias*

Each of the porphyrias results from a partial deficiency of one of the enzymes of heme biosynthesis. The porphyrias, with the exception of some types of PCT (see also paragraph 1.3), are inherited in either an autosomal-dominant or autosomal-recessive fashion (Table 1).

In each type of porphyria, the decreased rate of heme synthesis is compensated by the induction of ALA-S, which results in an increase in the concentration of the substrate of the defective enzyme. Intracellular accumulation and subsequent excretion of the substrate produces a pattern of liver, plasma, erythrocyte, urine and feces porphyrin precursors and porphyrins that is characteristic for that enzyme deficiency (1,6).

Individuals who inherit the gene for one of the autosomal-dominant porphyrias have quantitatively similar enzyme deficiencies, yet probably <10% ever develop symptoms. The remaining individuals in this group have "latent" or "subclinical" porphyria. All individuals who carry the gene for one of the autosomal-dominant acute hepatic porphyrias (AIP, VP or HC) are at risk of developing acute attacks in response to drugs



and other precipitants (1).

Latency may be a life-long state or follow a symptomatic phase. In PCT, urinary, fecal and plasma uroporphyrin concentrations may return to normal in some patients within a year of clinical remission. In AIP, VP and HC, evidence of heme precursor overproduction usually persists for many years after remission, but may eventually return to normal in some patients (1).

A number of clinical variants have been described. Most of these appear to be homozygous forms of the autosomal-dominant porphyrias, for example hepatoerythropoietic porphyria (HEP), the homozygous form of PCT (16) (see also paragraph 1.3.10). Homozygous forms of HC (17), VP (18), EPP (19) and AIP (20) have also been identified. All these cases have in common that: a) symptoms appear in childhood; b) enzyme activities are usually around 10% of normal; c) sustained overproduction of porphyrins occurs from an early age; and d) erythrocyte protoporphyrin production is increased. This last characteristic provides a useful indicator to its existence (21).

Very occasionally patients with porphyria may have porphyrin excretion patterns that suggest the presence of more than one enzyme defect. For example, the co-existence of two types of cutaneous porphyria, VP and PCT, has been reported from South Africa (22). In addition, more than one type of acute porphyria, AIP and VP, has been described in a family in the United Kingdom (23).

### 1.3 Porphyria cutanea tarda

PCT is the commonest of the porphyrias and refers to a heterogeneous group of porphyrias, characterized by cutaneous photosensitivity due to the increased production of uroporphyrinogens and heptacarboxylporphyrinogens and a 50% reduction of URO-D activity in the liver (2-4).

Different types of PCT have been distinguished:

1. Sporadic PCT/ type I PCT (S-PCT), where decreased URO-D activity is restricted to the liver and not detectable in erythrocytes. There is no family history of PCT (3,24).
2. Familial PCT/ type II PCT (F-PCT), which is transmitted as an autosomal-dominant disorder, where the enzymatic defect is apparently present in all tissues (2,4,24).
3. Recently, a few patients with at least one other family member with PCT, but with a

normal URO-D activity in erythrocytes, have been reported (25-28). This form of PCT has been termed type III PCT. It has been suggested that these patients may have inherited an atypical form of URO-D that has enhanced susceptibility to inactivation by a liver-specific process, but which is indistinguishable from normals by standard kinetic and immunochemical measurements. An alternative possibility is that these patients have a normal URO-D gene, but inherited a factor which interferes with URO-D activity (28,29).

The combined prevalence of familial forms of PCT has been reported to vary between 22.5 and 51% of cases in different series (1,6,25-29). The remainder of patients can be classified as S-PCT.

### 1.3.1 Enzymology

URO-D catalyses the sequential removal of the 4 carboxylic groups of the acetic acid side-chains of uroporphyrinogen to yield coproporphyrinogen (30). Mukerji and Pimstone provided evidence for the existence of 2 separate URO-D isoenzymes in human erythrocytes (31). However, at present, it seems most likely that only one URO-D enzyme (32-36), with 2 (32) or 4 (35) active sites, mediates the 4 decarboxylation steps.

URO-D decarboxylates *in vitro* all 4 isomers of uroporphyrinogen, but the naturally most abundant type III isomer is decarboxylated most rapidly, followed by types IV, II and I isomers in decreasing order (37). Whether the decarboxylation mechanism of uroporphyrinogen type III isomer is clockwise (30,38) or random (39) has not been established.

URO-D, purified from human erythrocytes, has a molecular mass of 40,800 (33,35,40), an isoelectric point of 4.6 and a specific activity of 9970 U/mg protein, using uroporphyrinogen III as substrate (35).

### 1.3.2 Genetics & Molecular biology

A cDNA complementary to URO-D mRNA from human erythroid cells has been cloned and sequenced (40) and the structure of the gene has been determined (36). URO-D is encoded at a single locus on the short arm of chromosome 1 (41-43). The gene contains 10 exons spread over 3 kb and appears to be transcribed from the same promoter of all tissues to give major and minor mRNA species that arise from initiation start sites that

are 6 bases apart. The proportions of the two species are the same in erythroid and non-erythroid cells (36).

In patients with F-PCT, two point mutations have been described (44,45). One mutation (gly → val at amino-acid position 281) could not be identified in other unrelated pedigrees with F-PCT (44), however the other mutation (deletion of exon 6) could be detected in 5 of 22 unrelated pedigrees with F-PCT (45).

### *1.3.3 Activity of other heme biosynthetic enzymes*

Whether the activity of the rate-limiting enzyme, ALA-S, is increased in PCT has been disputed (46). However, Moore et al. (47) convincingly reported an increased hepatic ALA-S activity in patients with PCT. After ALA-S, porphobilinogen deaminase (PBG-D) has the next lowest endogenous activity of all enzymes in the heme biosynthetic pathway (1). An increased PBG-D activity in erythrocytes (48-52) and in livers (48,52) of patients with PCT has been described. Increased ALA-S and PBG-D activities suggest that these enzymes are probably necessary to maintain heme biosynthesis in PCT (1).

In contrast to ALA-S and PBG-D, the activity of ALA dehydratase in liver biopsy specimens is decreased in PCT. However, ALA dehydratase activity greatly surpasses ALA-S activity in human liver, therefore, this is unlikely to interfere with heme biosynthesis (53).

### *1.3.4 Clinical features*

Lesions on sun-exposed skin are the most consistent clinical feature. The commonest lesions are superficial erosions from mechanical skin fragility, subepidermal bullae, hypertrichosis and pigmentation (54,55). Sclerodermatous changes, alopecia and onycholysis may occur in long-standing disease. Erosions and bullae, which may become infected, heal slowly with crusting, scars and milia. Long-term effects may range from minor scars to severe photomutilation, especially in sunny climates (55,56). Acute photosensitivity is uncommon. Histological changes and immunopathological findings of the skin are distinctive enough to be useful in PCT (57).

PCT is uncommon before the age of 20 and most patients develop symptoms in the 5th decade or later. Patients tend to present in the early summer, before the skin has any protective pigmentation (46,54,58).

Both S-PCT and F-PCT are often triggered by environmental factors. The most frequently incriminated agents are: a) ethanol; b) estrogens; c) polyhalogenated aromatic hydrocarbons; and d) iron.

a) Ethanol has long been recognized to exacerbate PCT. The incidence of ethanol-intake in different series of PCT patients varies from 25 to 100% (54,55,58). The degree of ethanol-intake may range from one or two drinks daily to frank alcoholism. The mechanism by which ethanol exacerbates PCT is not clear, but ethanol has been reported to increase the uptake of iron in patients with PCT (59), but also in normal subjects (60), and to increase liver iron content (see also paragraph 1.3.5). Moreover, ethanol has also been shown to stimulate the activity of ALA-S in livers of PCT patients (61) and to decrease URO-D activity in livers of rats (62).

b) Estrogen administration to patients with carcinoma of the prostate, for postmenopausal replacement therapy or for contraceptive purposes has been associated with aggravation or precipitation of PCT (63). Pregnancy has also been reported to precipitate PCT (64). Interestingly, alcoholics sometimes display signs of hyperestrogenization (60). Increased hepatic ALA-S activity has been demonstrated in males receiving stilbestrol for carcinoma of the prostate (65), but otherwise few clues concerning the mechanism of these estrogen effects in PCT have been found.

c) Polyhalogenated aromatic hydrocarbons (PAH's) have been associated with the development of PCT in humans. The best known example is a massive outbreak of about 4000 cases of PCT from 1956 to 1961 in Turkey following the widespread ingestion of hexachlorobenzene-treated wheat (66). A 20 to 30 year follow-up study on 204 of these patients still found some patients with uroporphyrin (67). A variety of other PAH's, used in industry, have also been implicated (68,69). Studies in laboratory animals have indicated that PAH's decrease activity of URO-D by an iron-dependent and a cytochrome P-450 system-dependent mechanism (see also paragraph 1.4).

### *1.3.5 Role of iron*

Many observations point to an important role of iron in the pathogenesis of PCT. Most patients have increased hepatic iron stores: a variable degree of hepatic siderosis is present in 72-100% of patients with PCT (54,70-76). Moreover, phlebotomy or treatment with desferrioxamine leads to clinical and biochemical remission (5,71,75,77-80),

whereas replenishment of iron stores after phlebotomy induces symptoms again (81-83).

The explanation for hepatic siderosis in PCT is not clear. Data on iron-absorption are conflicting. Some studies have described an increased absorption of iron in PCT (84,85), while others have not found a consistent ferrokinetic abnormality (86,87). There are a few reports linking PCT to hemochromatosis (88,89), and it has been proposed that the inheritance of at least one allele for HLA-linked hemochromatosis is responsible for hepatic siderosis in PCT (90,91). Others have not confirmed this suggestion (92).

Investigations on the interactions of ferrous and ferric iron with preparations of URO-D enzyme from human and other mammalian tissues have shown inhibition (93-97), activation (98) or no effect (35,99,100).

Elder et al. (101) measured URO-D activities and URO-D protein concentrations in liver tissue of patients with S-PCT and F-PCT. In S-PCT, patients in remission following phlebotomy had normal URO-D activities and URO-D protein concentrations, whereas in symptomatic patients before phlebotomy, URO-D activities were decreased and URO-D protein concentrations increased. In F-PCT, patients in remission following phlebotomy had 50% reduced URO-D activities and URO-D protein concentrations, with a further fall in URO-D activities and a slight increase in URO-D protein concentrations in symptomatic patients. An inherited defect of URO-D, as in F-PCT, is clearly an important factor in determining susceptibility, but is not sufficient by itself to produce overt PCT. In S-PCT, genetic factors may also play a role, but these are not clearly defined (29,101). However, in both forms, clinically-overt PCT is possibly precipitated by an iron-dependent process, which inactivates the active site(s) of URO-D molecule(s) in the liver (102). Whether this is a direct effect of iron on URO-D is not clear. Recent research has suggested that for the inactivation of URO-D additional factors might be important, such as the formation of reactive oxygen species and/or the formation of an inhibitor of URO-D. This will be discussed more extensively in paragraph 1.4.

#### *1.3.6 Associated disorders*

Some authors describe an association of PCT with systemic lupus erythematosus (54,73,103-105) and with diabetes mellitus (54,73,106-108). However, it is not clear why the incidence of these disorders is increased in PCT.

PCT has been described to occur more often in patients with renal failure than in the

normal population (109-113). In addition, in 58% to 100% of patients with renal failure, mildly elevated plasma uroporphyrin levels have been reported without clinical or biochemical evidence of PCT (109,114,115). The mechanism remains obscure.

### *1.3.7 Liver disturbances*

Livers of patients with PCT reveal a broad spectrum of histological lesions ranging from minimal changes to cirrhosis (54,70,73,74,76,116-119), in addition to a variable degree of hepatic siderosis (54,70-76). Of these findings, only the presence of needle-like structures in hepatocytes, representing uroporphyrin crystals (73), is characteristic (73,116-123).

Serologic markers of a past or present hepatitis B virus (HBV) infection have been found in up to 47% of patients with PCT (54,124-127) and antibodies against hepatitis C virus (HCV) have been detected in 82% of Italian patients with PCT (128). In addition, 17 cases of an association between PCT and human immunodeficiency virus (HIV) infection have been described [summarized in (129)]. This suggests that the virus infection is a precipitating factor, which could unmask the underlying porphyrin metabolism disorder.

Ethanol, viral hepatitis and iron overload can all cause chronic hepatitis, fibrosis and cirrhosis, which makes it difficult to assess the role of porphyrin accumulation by itself, in the liver damage in patients with PCT. In these patients, more than one factor may be present.

Many investigators have found an increased frequency of hepatocellular carcinoma in PCT (126,127,130-132), but this has not been confirmed in other series (54,70,74,76,123,133).

### *1.3.8 Diagnosis*

The clinical picture of PCT is fairly specific but can obviously be confused with other porphyrias (e.g., VP) and with non-porphyrin diseases (e.g., systemic lupus erythematosus).

The diagnosis of PCT is established by showing an increased excretion of uroporphyrins and heptacarboxylporphyrins in the urine, and an increased excretion of isocoproporphyrins and heptacarboxylporphyrins in the feces (12). Measurement of the

activity of URO-D in erythrocytes differentiates S-PCT patients from F-PCT patients, and detects latent forms of F-PCT (12,51).

In children with PCT-like skin lesions, levels of erythrocyte protoporphyrins should always be measured, because in patients with HEP, erythrocyte protoporphyrin concentrations are abnormal (21).

### 1.3.9 *Therapy*

PCT has been shown to respond to two therapeutic approaches:

1. Depletion of iron stores by phlebotomy or subcutaneous infusion with desferrioxamine (5,71,75,77-80,134). Interestingly, phlebotomy has been described to be also effective in the absence of a siderotic state (134).
2. Low-dose chloroquine (135,136). Chloroquine complexes with uroporphyrinogens and promotes its release from the liver, possibly by stimulating exocytosis. Chloroquine may also inhibit porphyrin formation (135). Higher doses of chloroquine may cause severe hepatotoxicity when given to patients with PCT (136).

Both treatments are effective, however, since iron plays an important role in the pathogenesis of PCT, depleting iron stores seems a more rational treatment.

### 1.3.10 *Hepatoerythropoietic porphyria*

HEP is a rare homozygous form of F-PCT with severe cutaneous symptoms that develops in early childhood. Twenty cases have been reported worldwide as of 1992 [summarized in (137)]. The activity of URO-D in erythrocytes is markedly decreased (5-27% of normal) (16). In contrast to patients with PCT, serum and liver iron concentrations are usually normal in patients with HEP (1).

Seven different mutations of the URO-D gene have been described in patients with HEP (137). A mutation at one amino-acid position has been described both in F-PCT and HEP patients. In the F-PCT patient, the mutation at position 281 resulted in the substitution of a valine residue for the glycine residue (44). In the HEP patient, the mutation at position 281 involved the substitution of a glutamic acid residue for the glycine residue (138).

Avoidance of the sun and the use of topical sunscreens is essentially all that can be offered to these patients at present. Response to phlebotomy has not been observed in patients with HEP (139).

#### 1.4 Experimental uroporphyrria

Following an outbreak of human uroporphyrria in Turkey, the fungicidal agent hexachlorobenzene (HCB), a PAH, was suspected to be the cause. HCB was subsequently shown to induce hepatic uroporphyrria in rodents (68). A low hepatic URO-D activity and the accumulation and excretion of uroporphyrins and heptacarboxylporphyrins were found to be important features of HCB-induced porphyria (140). A number of other PAH's have since been shown to have similar effects, both in experimental animals and in humans (68,69). In all cases, the biochemical and clinical manifestations are the same as in S-PCT (3,24). Both conditions can be exacerbated or precipitated by estrogens (63,141). Abnormalities in liver pathology are commonly encountered in the drug-induced condition in animals (142-146), as well as in S-PCT (54,70,72-76,116-123,126,127,130-133), ranging from minor degrees of hepatocellular damage to cirrhosis. Different species and strains vary remarkably in their susceptibility to the porphyrinogenic effects of PAH's (46), and a genetic predisposition of some kind has also been suspected in S-PCT (29). Both in HCB-induced uroporphyrria (97,146-153) and in S-PCT (5,54,70-83), the condition is aggravated by iron overload, while iron deficiency (whether induced by phlebotomy or treatment with desferrioxamine) prevents the overproduction of porphyrinogens in both conditions.

In view of the similarities between HCB-induced uroporphyrria and human S-PCT, HCB-induced uroporphyrria has been used as an appropriate experimental animal model for the human condition. In the following, the more recent work on the possible mechanism(s) of experimental uroporphyrria will be considered.

##### *1.4.1 Reactive drug-metabolite hypothesis*

In 1974 Sinclair and Grannick put forward the hypothesis that, in order to produce uroporphyrria, PAH's had to be converted by cytochrome P-450 (Cyt P-450) enzymes to metabolites capable of inhibiting URO-D (154). This hypothesis is supported by the following findings:

- a) Pretreatment of animals or cultured hepatocytes with certain inducers of Cyt P-450 increases the degree of uroporphyrria induced by PAH's (155-158).
- b) HCB, 2,3,7,8,-tetrachlorodibenzo-*p*-dioxin (TCDD) and polychlorinated or polybrominated biphenyls are themselves inducers of several forms of Cyt P-450 (159).



c) The responsiveness of two inbred strains of mice, the C57BL/6 strain and the DBA/2 strain and of their crosses, to the porphyria-inducing property of TCDD can be correlated with inducibility of certain forms of Cyt P-450 (159).

d) In microsomal incubation experiments, HCB has been shown to be converted into one or more reactive metabolites capable of becoming covalently bound to proteins and therefore potentially able to modify URO-D (160,161).

Metabolism of HCB however, has not been shown to correlate with *in vivo* toxicity (162,163). Moreover, the hypothesis fails to account for the ability of iron to worsen the metabolic condition (97,147-153).

#### 1.4.2 *Involvement of the cytochrome P-450 system*

As the initial biochemical event, PAH's have been shown to interact with a soluble protein in hepatocytes known as the *Ah* receptor, the regulatory gene product of the *Ah* locus (164,165). This interaction results in the nucleus of the cell in the transcriptional activation of certain genes, leading to the induction of an isoenzyme of the Cyt P-450 system: Cyt P-4501A2 (166,167). This isoenzyme was formerly called Cyt P<sub>3</sub>-450 in mice, Cyt P-450d or Cyt P-448 in rats and Cyt P<sub>3</sub>-450 or Cyt P-450d in humans, but the recommended nomenclature at present is CYP1A2 (168).

In *Ah*-responsive mouse strains, such as the C57BL/10 strain, the receptor has a much higher affinity for PAH's than in *Ah*-non-responsive strains, such as the DBA/2 strain, where the receptor is either absent or has a much lower affinity for PAH's (164,165). Moreover, there is a marked difference between the different PAH's in receptor-binding affinity: TCDD is a strong, but HCB is a weak agonist for the *Ah* receptor (169). Mixtures of some PAH's have been reported to induce hepatic cytosolic binding components that are distinct from the *Ah* receptor, however their role remains to be established (170). Some PAH's, like 3,4,5,3',4',5'-hexabromobiphenyl, with the capacity to induce CYP1A2, bind to the cytochrome and inhibit catalytic activity of the cytochrome (171).

Several chemically-unrelated drugs, such as the polycyclic aromatic hydrocarbons, like 3-methylcholanthrene (MC), are also capable of inducing CYP1A2, without interacting with the *Ah* receptor and produce a HCB-type porphyria, both in hepatocyte cultures (151) and in intact rodents (172). Therefore, apart from the *Ah*-responsiveness, other

regulatory mechanisms must be involved in PAH-induced uroporphyrin. In addition, both the effect of iron and the sex difference on the porphyrinogenic process are also independent of the *Ah* phenotype (173).

#### 1.4.3 Role of iron

Iron has been implicated in the pathogenesis of PAH-induced uroporphyrin; uroporphyrin develops faster if animals are made siderotic (97,146-153,174). Iron deficiency due to bleeding (150) or treatment with desferrioxamine (153) diminishes or completely prevents the development of uroporphyrin.

There is evidence for strain differences in sensitivity to PAH's, which is, at least partly, based on liver iron content (175). Moreover, female rats are much more susceptible than male rats to HCB-induced porphyria (176). A possible explanation for the increased susceptibility of female rats is that hepatic ferritin iron turnover is significantly greater in female than in male rats (177).

#### 1.4.4 Uroporphyrin accumulation by URO-D inhibition

As has been described before, both polycyclic aromatic hydrocarbons, like MC (151,172), and PAH's, like HCB and TCDD (166,167), induce CYP1A2. Treatment with these compounds either *in vivo* (178,179) or *in vitro* (163,166,167,180,181), using hepatic microsomes from chick embryos, rats and mice, induces the hepatic oxidation of uroporphyrinogen to uroporphyrin in the liver. At the same time, a marked inhibition of hepatic URO-D activity has been found by several investigators (182-186).

At present, the hepatic accumulation of uroporphyrins and the inhibition of URO-D activity in experimental uroporphyrin has been attributed to one or more of the following proposed mechanisms:

1. Oxidation of uroporphyrinogen to uroporphyrin by cytochrome P-4501A2 (163,166,167,180-182,187).
2. Iron-mediated oxidative formation of a specific inhibitor of URO-D (183-186).
3. Iron-mediated direct damage to URO-D enzyme (95,96).

##### 1.4.4.1 Uroporphyrinogen oxidation by cytochrome P-4501A2

Uroporphyrinogen has been shown to be a substrate of (PAH-induced or MC-induced)

CYP1A2, leading to the oxidation of uroporphyrinogen to uroporphyrin (163,166,167, 180-182,187). Because uroporphyrin is not a substrate for URO-D, accumulation of uroporphyrins results (188). Binding of the inducer is not required for rodent CYP1A2 to catalyze oxidation of uroporphyrinogen (189). The hypothesis of uroporphyrinogen oxidation, catalyzed by induced CYP1A2, is supported by the following observations:

- a) If uroporphyrinogen is a substrate of CYP1A2, then other substrates of CYP1A2 might competitively inhibit uroporphyrinogen oxidation. This has been shown for phenacetin and ketoconazole (167).
- b) Inhibitors of CYP1A2, like piperonyl butoxide, stop the accumulation of uroporphyrins in cultured chick embryo hepatocytes (163).
- c) The conversion of uroporphyrinogen to uroporphyrin follows saturation kinetics (190).

The mechanism of uroporphyrinogen oxidation by itself does not explain a marked inhibition of hepatic URO-D activity, which can be observed simultaneously (182-186). Recently, it has been described that, under *in vitro* conditions, oxidation of uroporphyrinogen could lead to the generation of a uroporphyrinogen oxidation product, which could act as an inhibitor of URO-D (182). This inhibitor has been supposed to be a labile product, since inhibition of the oxidation reaction by ketoconazole restores URO-D enzyme decarboxylation capacity (167).

#### 1.4.4.2 *The iron-mediated oxidative mechanism*

Precipitating drugs, like HCB, may interact with the NADPH-dependent reductase/cytochrome P-450 system of hepatocytes, leading to the production of reactive oxygen species (191). Evidence in favour of a drug-dependent, oxidative mechanism has been obtained from three different laboratories with the demonstration that, *in vitro*, liver microsomes from PAH-treated rats, in the presence of NADPH, produce increased amounts of reactive oxygen species compared with microsomes from control rats (192). Liver microsomes from similarly-induced chick embryos, in the presence of NADPH, will catalyze the oxidation of porphyrinogens, especially when challenged with small amounts of a powerful uroporphyrinogen-inducing chemical (180,181). From these experiments it can be concluded that two different drug actions are required for the microsomal oxidation of porphyrinogens: a) the drug first acts as an inducer of CYP1A2; b) it then interacts with the induced cytochrome to produce reactive oxygen species.

The role of iron in this mechanism can be explained by its known ability to participate in peroxidative and free-radical reactions (151,152,181,191-198). If in hepatocytes as a result of Cyt P-450 induction, reactive oxygen species are produced and "free" iron is also present, highly reactive oxygen-related free radicals could be formed by the Haber-Weiss reaction (193,198). In the presence of free radicals, a variety of reactions can be initiated, such as the peroxidation of membrane lipids (199). Recently, it has been suggested that the process of lipid peroxidation is involved in the pathogenesis of experimental uroporphyrinemia (152,196).

Accelerated oxidation of porphyrinogens to porphyrins by iron is compatible with a peroxidase-type mechanism involving electron transfer and hydrogen transfer, but the resulting accumulation of uroporphyrins is unlikely by itself to explain the inhibition of URO-D and the formation of an inhibitor of the enzyme by iron. However, in the microsomal system (191), iron has also been found to promote modification of the porphyrinogen pigment, leading to a marked loss of its Soret absorbance. This indicates that degradation products might be produced (possibly following oxidative attack by hydroxyl radicals), which could act as inhibitors of URO-D (174,200). When the oxidative derivatives of uroporphyrinogens, which lack Soret absorbance, are tested *in vivo* for their effect on URO-D, they have been found to inhibit the enzyme, thus supporting the concept that iron is implicated in the oxidative conversion of uroporphyrinogen into an inhibitor of the enzyme (200).

Evidence for an iron-mediated oxidative formation of a specific heat-stable inhibitor of URO-D has been provided from several laboratories (183-186,200). However, it has also been shown (see paragraph 1.4.4.1) that URO-D inhibition by an uroporphyrinogen oxidation product, without the generation of reactive oxygen species (201,202), can occur (182). Therefore, it seems likely that URO-D inhibition in experimental uroporphyrinemia can occur by different mechanisms depending on the concentration of reactive ferrous iron.

#### 1.4.5 *Iron-mediated damage to URO-D enzyme*

Investigations on the interactions of ferrous or ferric iron with preparations of URO-D from human and other mammalian tissues have shown inhibition (93-97), activation (98), or no effect of iron on URO-D (35,99,100). Mukerji et al. (95,96) postulated on the basis of *in vitro* experiments, that URO-D inhibition by iron can occur without the involvement

of an induced hepatic Cyt P-450 system. Two mechanisms have been postulated:

1. An oxygen-independent inhibition, where iron directly interacts with essential sulfhydryl group(s) at the catalytic site(s) of the URO-D enzyme (95,96).
2. An oxygen-dependent inhibition, where iron is generating free radicals in the presence of cysteine, thereby damaging the URO-D enzyme (95).

It is not clear whether the direct interaction of ferrous iron with URO-D also occurs *in vivo*. Moreover, Mukerji et al. (95,96) have found that ferrous iron concentrations in the range of 0.1 - 1.0 mM are required *in vitro* to reduce the activity of partially purified URO-D. However, it seems unlikely that these ferrous iron concentrations can be met *in vivo* (203).

### 1.5 Aims of the study

The aim of the work described in this thesis was to examine further the mechanisms involved in the accumulation of uroporphyrins in the liver, i.e., the role of iron and an increased activity of one of the preceding enzymes in the heme biosynthetic pathway, PBG-D, in the porphyrinogenic process in experimental uroporphyrinuria and in PCT.

In the previous paragraphs, the proposed role of iron in the development of uroporphyrinuria has been discussed. However, a study on the time-sequence relationship between iron accumulation and uroporphyrin production in the liver has not been performed. In addition, the nature of the iron pool involved in this process has not been established. The role of iron in uroporphyrinuria has been explained by its ability to participate in peroxidative and free radical reactions. Desferrioxamine, an iron chelator, has been described to diminish uroporphyrin accumulation in the liver. At present, the specific effects of desferrioxamine on iron accumulation, free radical-mediated reactions, uroporphyrin accumulation and URO-D activity in the liver have not been studied in experimental uroporphyrinuria.

It has been reported that the activity of the enzyme PBG-D is increased in erythrocytes and livers of patients with PCT. It is not clear whether this increased PBG-D activity can be observed both in animals with experimental uroporphyrinuria and in humans with sporadic and familial forms of PCT. An increased PBG-D activity could explain the absence of acute attacks in PCT. Moreover, an increased PBG-D activity could also provide an additional explanation for uroporphyrin accumulation in experimental and human

uroporphyrin.

Therefore, in the following chapters we investigated:

1. The site within the liver where iron accumulation and uroporphyrin production takes place, both in livers of C57BL/10 mice with experimental uroporphyrin (Chapter 3) and in livers of patients with PCT (Chapter 5).
2. The effects of desferrioxamine on iron metabolism, lipid peroxidation, porphyrin accumulation and URO-D activity in livers of C57BL/10 mice with experimental uroporphyrin (Chapter 4).
3. The role of an intracellular pool of low molecular weight iron in livers of C57BL/10 mice with experimental uroporphyrin (Chapter 4).
4. The activity of the enzyme PBG-D in livers of C57BL/10 mice with experimental uroporphyrin (Chapter 4) and in erythrocytes of patients with sporadic and familial forms of PCT (Chapter 6), and its possible role in the overproduction of uroporphyrins in uroporphyrin.
5. The mechanism of an increased erythrocyte PBG-D activity in patients with PCT (Chapter 6).

**CHAPTER 2****Materials & Methods**

<b>Contents</b>	<b>page</b>
2.1 Materials	24
2.2 Biochemical methods	25
2.3 Histological study (Light microscopy)	31
2.4 Ultrastructural study (Electron microscopy)	32
2.5 Morphometrical analysis	33
2.6 Statistical analysis	34

## 2.1 Materials

### 2.1.1 Animals

Male C57BL/10 mice (Centraal Proefdier Bedrijf, Zeist, The Netherlands) were 9 to 11 weeks of age and weighed 20 gm at the beginning of the experiments.

All animal studies were performed according to the "Regulations for use of laboratory animals in the Erasmus University Rotterdam" laid down by the Laboratory Animal Committee of the Erasmus University Rotterdam, The Netherlands.

#### 2.1.1.1 Treatment

Treatment with hexachlorobenzene (HCB; Merck, Darmstadt, Germany) consisted of two intraperitoneal (ip) injections of 8 mg HCB (400 mg/kg body weight), dissolved in 0.25 ml warm corn oil, with 1 week interval. Mice treated with iron dextran (Imferon<sup>R</sup> (IMF); Fisons Pharmaceuticals B.V., Leusden, The Netherlands) received a single ip injection of 12 mg (600 mg/kg body weight). When mice were treated with HCB and IMF, IMF was given three days after the second injection of HCB. HCB and IMF were injected under Enfluraan (Ethrane<sup>R</sup>, Abbott B.V., Amstelveen, The Netherlands) anesthesia.

Treatment with desferrioxamine (Desferal<sup>R</sup> (DFx), Ciba-Geigy B.V., Arnhem, The Netherlands) consisted of daily intramuscular injections of 5 mg DFx (250 mg/kg bodyweight), dissolved in 0.05 ml sterile water, injected alternately in one of the hind-legs.

#### 2.1.1.2 Perfusion of livers for biochemical determinations

In order to obtain blood-free livers, the vena cava inferior was cannulated and the liver was perfused with isotonic saline (NaCl, 0.15 mol/l) at room temperature, until the fluid leaving the liver was clear (the average perfusion time was 3 minutes). The procedure was performed under Enfluraan anesthesia.

#### 2.1.1.3 Perfusion of livers for morphological studies

The portal vein was cannulated and the liver was perfused with 3% glutaraldehyde in cacodylate buffer (0.14 mol/l, pH 7.4, 275 mOsm). A perfusion rate of 10 ml/min, a perfusion pressure of 15 cm Hg and a perfusion temperature of 37 °C were maintained



throughout the procedure. For the frozen sections, unperfused livers were removed and immediately frozen in liquid nitrogen. These procedures were performed under Enfluraan anesthesia.

### 2.1.2 Patients

A diagnosis of the familial form of porphyria cutanea tarda (PCT) was based on a positive family history, skin symptoms and a characteristic pattern of porphyrins produced from porphobilinogen (PBG) by hemolysates (see paragraph 2.2.3). Patients with the sporadic form of PCT had a negative family history, characteristic skin-symptoms and an indirect uroporphyrinogen decarboxylase (URO-D) activity comparable to controls. Studies were performed in patients with skin-symptoms and an increased urinary excretion of uroporphyrins and heptacarboxylporphyrins before phlebotomy, and in patients without skin-symptoms and a normal urinary excretion of porphyrins following phlebotomy.

Evaluation of each patient included a careful history. Serum bilirubin, aspartate transferase, alanine transferase, gamma-glutamyl transpeptidase, alkaline phosphatase, iron, ferritin and transferrin saturation were measured, and serum was assayed for  $\alpha$ -fetoprotein (increased at levels of  $\geq 20$  ng/ml), using standard clinical chemistry laboratory methods.

In some patients a percutaneous liver biopsy was performed. Most liver specimens of patients were obtained with a True-Cut<sup>®</sup> needle (Travenol Lab, USA). A small number of liver biopsies was taken with the Menghini needle. Liver biopsies were processed for light microscopy (LM) and electron microscopy (EM).

### 2.1.3 Hemolysates

Erythrocytes in heparinized blood samples were washed three times in isotonic saline (NaCl, 0.15 mol/l) at 4 °C. The cells were diluted 4 times with distilled water and incubated for 30 min at 0 °C.

## 2.2 Biochemical methods

Determinations of the amount of porphyrins in urine and in liver tissue, the indirect URO-D activity in erythrocytes and the URO-D activity in liver tissue, the activity of porphobilinogen deaminase (PBG-D) in erythrocytes and in liver tissue, the amount of

immuno-detectable PBG-D/100 units PBG-D activity in erythrocytes and the total amount of immuno-detectable PBG-D in erythrocytes were performed at the Department of Internal Medicine II, Academical Hospital Rotterdam-Dijkzigt under supervision of Dr F.W.M. de Rooij (Head: Prof. J.H.P. Wilson).

Determinations of the total iron content in liver tissue, the amount of low molecular weight iron in liver tissue and the production of malondialdehyde in liver tissue were performed at the Department of Chemical Pathology, Erasmus University Rotterdam (Head: Prof. Dr H.G. van Eijk)

Routine clinical chemistry laboratory determinations were performed at the Central Clinical Chemistry Laboratory (Head: Dr J. Lindemans).

Serological Hepatitis B virus (HBV) markers and antibodies against Hepatitis C virus (HCV) were determined at the Department of Virology, Academical Hospital Rotterdam-Dijkzigt (Head: Prof. Dr N. Masurel).

### 2.2.1 *Porphyryns in urine*

A 2-ml sample of urine was lyophilized in the dark. The residue was dissolved in 100  $\mu$ l of chloroform. Then, 1 ml H<sub>2</sub>SO<sub>4</sub> (10%) in methanol was added and the mixture was incubated for 60 min in the dark at 37 °C. Then, 2 ml of distilled water and 4 ml of chloroform were added. After shaking for 1 to 2 min, the sample was centrifuged at 1,800 g for 15 min and the (upper) water phase was removed. To neutralize the chloroform phase, 1 ml of NaHCO<sub>3</sub> (5%) was added and gently mixed. After centrifugation, this procedure was repeated if the pH of the water phase was still below 7.0. The final neutralized chloroform layer was washed twice with 2 ml of distilled water. Then, the chloroform phase was evaporated under nitrogen at 40 °C in a Reacti-Therm Heating Module (Pierce, Rockford, USA). The porphyrin methyl-esters produced in this way were dissolved in a small volume of chloroform for separation and applied to a silica gel column (Merckosorb SI 100, 20- $\mu$ m particle size; Merck, Darmstadt, Germany) for high-pressure liquid chromatography. A linear gradient of tetrahydrofuron/heptane (with increasing concentrations from 30% to 60%) was used to elute the porphyrin methyl-esters, which were detected in a fluorescence-spectrophotometer (excitation 400 nm; emission 625 nm; Perkin Elmer LS 40, Beaconsfield, UK). Concentrations were expressed in nmol/mmol creatinine (51,204).

### 2.2.2 *Porphyryns in liver tissue*

Porphyryns in liver tissue were measured using a modification of the method described by Lim et al. (205). Briefly, 300 mg of liver tissue was homogenized in a Potter-Elvehjem homogenizer to yield a 10% homogenate in water, which was centrifuged at 10,000 x g for 4 min. The supernatant was stored at -20 °C until further processing. To a sample of 0.1 ml of the homogenate, 0.1 ml of Tris-HCl (50 mmol/l, pH 8.0) and 0.8 ml of a "mix" were added. This "mix" contained: 25 ml dimethylsulphoxide (100% wt/vol), 10 ml trichloroacetic acid (50% wt/vol), 10 ml HCl (1 mol/l), *p*-Benzoquinon (2.3 mmol/l; Merck-Schuchardt, Hohenbrunn, Germany) and 35 ml of distilled water. This was stirred and centrifuged for 15 min at 1,800 x g. Free porphyryns in the supernatant were separated by reversed-phase liquid chromatography on a Hypersyl Sas C1 5 Micron column (Alltech, Deerfield, USA), using a linear gradient of 95% Eluens A [ammoniumacetate (350 mmol/l), (NH<sub>4</sub>)<sub>2</sub>HPO<sub>4</sub> (9 mmol/l) and acetonitrile (8%, v/v)] to 95% Eluens B [acetonitrile (8%, v/v) in methanol]. The free porphyryns were detected in a fluorescence-spectrophotometer (excitation 400 nm; emission 625 nm; Perkin Elmer LS 40, Beaconsfield, UK). The amount of porphyryns was expressed in pmol/mg protein.

### 2.2.3 *Indirect URO-D activity in erythrocytes*

URO-D activity in erythrocytes was measured indirectly by analyzing the pattern of porphyryns formed during incubation of a fresh hemolysate in the presence of PBG under conditions identical to the PBG-D assay (see paragraph 2.2.5). The reaction was stopped by freezing the mixture, which was subsequently stored at -20 °C. Porphyryns were methylated and the formed methyl-esters were applied to a silica gel column (Merckosorb SI 100, 20 µm particle size; Merck, Darmstadt, Germany) for high-pressure liquid chromatography. The methyl-ester porphyryns were measured in a fluorescence-spectrophotometer (excitation 400 nm; emission 625 nm; Perkin Elmer LS 40, Beaconsfield, UK). Using this method, the uroporphyrin + heptacarboxylporphyrin/coproporphyrin ratio was calculated. This ratio was considered to be consistent with a diagnosis of the familial form of PCT, if >2.80 (51).

### 2.2.4 *URO-D activity in liver tissue*

URO-D activity in liver tissue was measured using a modification of the method

described by Straka et al. (206). To 0.1 ml of a 10% homogenate of liver tissue (as described in paragraph 2.2.2), 0.05 ml of DL-Dithiothreitol (30 mmol/l; Sigma Chemical Co., St. Louis, USA) in Tris-HCl (50 mmol/l, pH 8.0) was added to restore the activity of the enzyme uroporphyrinogen-III-synthase (207) and incubated for 30 min at 4 °C. Then, 0.05 ml of porphobilinogen (0.8 mg) in 5 ml of EDTA (4 mmol/l) in Tris-HCl (50 mmol/l, pH 8.0) was added, which was incubated for 60 min at 37 °C. The reaction was stopped by adding 0.8 ml of the "mix" (as described in paragraph 2.2.2). This was stirred and centrifuged for 15 min at 1,800 x g. The free porphyrins in the supernatant were separated by passage over a reversed-phase high-pressure liquid chromatography column and measured in a fluorescence-spectrophotometer (excitation 408 nm; emission 648 nm; Perkin Elmer LS 5B, Beaconsfield, UK). The amount of formed copro-(4-carboxyl-), 3-carboxyl-, and proto-(2-carboxyl-)porphyrins was expressed in pmol/mg protein/hour.

#### 2.2.5 *PBG-D activity in erythrocytes*

For the PBG-D activity in erythrocytes, hemolysates were diluted 20-fold with Tris-HCl buffer (50 mmol/l, pH 8.0, at room temperature). Two hundred  $\mu$ l of the diluted preparation was added to 400  $\mu$ l of a mixture containing PBG (150  $\mu$ mol/l) in Tris-HCl buffer (50 mmol/l, pH 8.0). This was incubated for 60 min at 37 °C. The reaction was stopped by the addition of 600  $\mu$ l trichloroacetic acid (25%). After centrifugation, the formed porphyrins were measured in the supernatant in a fluorescence-spectrophotometer (excitation 408 nm; emission 648 nm; Perkin Elmer LS 5B, Beaconsfield, UK). Results were expressed as total porphyrins (in pmol/mg protein/hour), using coproporphyrin I as standard (208).

#### 2.2.6 *Immuno-detectable PBG-D/100 units PBG-D activity in erythrocytes*

The amount of immuno-detectable PBG-D per 100 units of PBG-D activity (Ig PBG-D/100 U) in hemolysates was determined using rabbit IgG anti-human PBG-D, which was raised by use of human PBG-D, as described by De Rooij et al. (209). Hemolysates were diluted to a standard PBG-D catalytic activity, and Ig PBG-D/100 U was detected as follows: 50  $\mu$ l of a Protein A-Sepharose suspension (Pharmacia, Woerden, The Netherlands) was placed in 6 x 2 microtiter wells. Then, either 50  $\mu$ l of rabbit anti-human PBG-D antiserum in various dilutions, or 50  $\mu$ l of diluted control serum was added and

incubated for 60 min at room temperature. After 50  $\mu$ l of the hemolysate was added, the mixture was incubated for 60 min at room temperature. The plates were centrifuged and the residual (unbound) PBG-D activity was determined in the supernatant (208,210). Ig PBG-D/100 U was defined as the amount of antibodies needed to bind 100 units of PBG-D (1 unit of PBG-D activity is that producing 1 pmol of uroporphyrinogen per hour at 37 °C) and was calculated using linear-regression analysis of the duplicate PBG-D-binding values found in five different IgG dilutions (208,210).

#### 2.2.7 *Total immuno-detectable PBG-D in erythrocytes*

The total amount of immuno-detectable PBG-D (Ig PBG-D) in erythrocytes, expressed in microliters of IgG per milligram of erythrocyte protein per hour, was calculated as the product of Ig PBG-D/100 U ( $\mu$ l IgG/100 U) and the PBG-D activity (units/mg protein/hour).

#### 2.2.8 *PBG-D activity in liver tissue*

PBG-D activity in liver tissue was not measured separately, but was calculated from the incubation experiment for the URO-D activity in liver tissue (see paragraph 2.2.4), by summation of the total amount of formed porphyrins and expressed in pmol/mg protein/hour.

#### 2.2.9 *Total iron content in liver tissue*

Total liver iron content was measured using a modification of the method described by Harris (211). Liver tissue was dried at 110 °C overnight. The dried liver tissue was weighed. To the dried tissue, 0.5 ml perchloric acid (70% wt/vol) was added and this was heated until the solution was colourless. After cooling, distilled water was added to a final volume of 2.0 ml. From this solution, 0.2 ml was taken and 0.1 ml HCl (1 mol/l), 0.2 ml L-ascorbic acid (0.14 mol/l), 0.1 ml sodium acetate (saturated) and 0.2 ml Ferrozine (10 mmol/l; Sigma Chemical Co., St. Louis, USA) were added. This solution was thoroughly mixed and after 10 minutes the absorbance was measured at 562 nm against three standard iron solutions. The amount of iron was expressed in mmol/100 gm dry weight or in  $\mu$ mol/gm dry weight.

### 2.2.10 *Low molecular weight iron in liver tissue*

Low molecular weight (LMW) iron amounts were measured using a method described by Voogd et al. (212). Some modifications were necessary, due to the limited quantity of liver tissue available for analysis.

A 10% (w/v) liver homogenate in Tris/HCl (100 mmol/l, pH 7.4) was centrifuged for 15 min at 10,000 x g at 0 °C. To 1 ml of the supernatant, 100 µl desferrioxamine (DFx; 22 mmol/l) was added and the samples were incubated for 5, 15, 30 and 60 minutes respectively, at 37 °C. To stop the reaction between the available iron and DFx, samples were passed through a SEPPAK C18 cartridge (Millipore Corp., Milford, USA), immediately after incubation. Prior to use, the cartridges were conditioned by means of pre-elution with 5 ml methanol, followed by 5 ml distilled water. After adding the samples, cartridges were flushed with 5 ml distilled water. In this way, Ferrioxamine (Fx) and DFx were retained, while most other compounds were eluted. Fx and DFx were subsequently eluted from the SEPPAK C18 cartridge with 1 ml methanol and the effluent was applied to a HPLC RP 18 column (250 x 4 mm id; Merck, Darmstadt, Germany). The mobile phase consisted of 88% Na<sub>2</sub>HPO<sub>4</sub>/NaH<sub>2</sub>PO<sub>4</sub> (20 mmol/l), acetonitrile (12%), Na-EDTA (2 mmol/l) and ammoniumacetate (1 mol/l). HPLC analysis was performed on a dual pump LKB-system with automatic sample injector and two variable wavelength detectors to measure Fx (430 nm) and DFx (229 nm) simultaneously in the effluent. The results (duplo samples, fourfold measurements per sample) were compared with three standard amounts of iron, treated in the same manner as the liver samples. The amount of LMW iron was expressed in nmol/gm wet weight liver tissue.

### 2.2.11 *Total protein measurement*

#### In liver tissue:

A small sample of liver tissue was homogenized (Ultrathurax, Janke and Kunkel, Germany), which was followed by stepwise dilution. To 100 µl of the 0.1% (w/v) homogenate, 5 ml of Coomassie Brilliant Blue was added and after 10 min the absorbance was measured at 595 nm. The results were compared with four different standard solutions of Bovine Serum Albumin (Pierce, Rockford, USA) in the range of 100-400 µg/ml. The amount of protein was expressed in µg/gm wet weight liver tissue (213).

### In hemolysates:

The amount of protein in hemolysates was measured using the method described by Lowry et al. (214).

#### *2.2.12 Malondialdehyde content in liver tissue*

Malondialdehyde (MDA) content was measured using a method, described by Kornbrust and Mavis (215). Four aliquots (of 0.25, 0.5, 0.75 and 1.0 ml respectively) of a 10% (w/v) liver tissue homogenate, which was dissolved in Tris-HCl buffer (5 mmol/l, pH 7.8), were filled out to a final volume of 1.0 ml with the same buffer solution. To each of these samples, 0.3 ml trichloroacetic acid (20% v/v), 0.6 ml 2-thiobarbituric acid (0.05 mol/l) and 0.1 ml di(2,6)-tert-butyl-4-methylphenol (0.2% in ethanol, w/v) were added. The solution was mixed and centrifuged (10 min, 2800 x g). The supernatant was heated for 8 min at 100 °C and immediately cooled. Subsequently, the absorbance was measured (535 nm;  $\epsilon = 156,000$ ) and the results were compared with a standard solution of MDA, treated in the same manner.

#### *2.2.13 Serological HBV markers*

Hepatitis B surface antigen (HBsAg) and antibodies against hepatitis B core antigen (anti-HBc) were determined using the IMx system microparticle enzyme immunoassay (Abbott Lab, USA). Antibodies against hepatitis B surface antigen (anti-HBs) were determined by an enzyme-immuno assay employing the AUSAB-EIA (Abbott Lab, USA), according to the instructions of the manufacturer.

#### *2.2.14 Antibodies against HCV*

Antibodies against HCV (anti-HCV) were determined by an enzyme-immuno assay, employing recombinant C100-3 (Abbott Lab, USA). If samples were tested positive, they were subjected to a confirmatory neutralization enzyme-immuno assay (Abbott Lab, USA). A positive result in this assay was required for samples to be regarded as definitively positive.

### **2.3 Histological study (Light microscopy)**

Histological studies were performed at the Department of Pathology, Erasmus

University Rotterdam (Head: Prof.Dr F.T. Bosman) and at the Department of Pathology, Academic Medical Centre, Amsterdam (Head: Prof.Dr F.J.W. ten Kate).

All liver specimens underwent a macroscopical examination. In addition, as soon as the specimens were obtained, they were examined with an ultraviolet lamp for fluorescence.

#### Light microscopy in animals:

A part of the glutaraldehyde-perfusion fixed liver was dehydrated briefly through graded alcohol series, embedded in paraffin, serially sectioned and stained. The staining protocol included Gill's hematoxylin stain (with reduced water contact) (120), the ferric ferricyanide reduction test in Lillie's modification (216) and, Perl's Prussian blue stain for ferric iron (217). Histology, birefringence and fluorescence (excitation filter with a transmission range of 300-420 nm and an absorption filter with a transmission peak above 610 nm) were studied with a Zeiss axioplan microscope.

#### Light microscopy in patients:

The most relevant staining procedures were: the hematoxylin-eosin stain (216), the periodic acid-Schiff stain with and without diastase digestion (216), the ferric ferricyanide reduction test in Lillie's modification (216) and, Perls' Prussian blue stain for iron (217).

Liver biopsy specimens were blindly evaluated for: fibrosis (graded 0: no fibrosis, 1: mild periportal fibrosis, 2: moderate periportal fibrosis with some porto-portal septum formation, 3: marked periportal fibrosis with extensive portoportal septum formation and 4: cirrhosis); portal triad changes; lobular changes; ground glass hepatocytes; steatosis (graded 0: absent, 1: mild, 2: moderate, 3: marked); siderosis (graded according to Scheuer et al. (217); 0: absent, 1: minimal, 2: moderate, 3: abundant and 4: massive); dysplasia, defined by Anthony et al. (218) and hepatocellular carcinoma. Histology was studied with a Zeiss axioplan microscope.

## **2.4 Ultrastructural study (Electron microscopy)**

Ultrastructural studies were performed at the Analytical Electron Microscopical Unit (Head: Dr W.C. de Bruijn) of the Department of Pathology, Erasmus University Rotterdam (Head: Prof.Dr F.T. Bosman).

Because uroporphyrins have been described to be water-soluble (116,120), two procedures were used for the preparation of the liver tissue from C57BL/10 mice:

a) Small blocks were taken randomly from the fixed livers, dehydrated briefly through



graded acetone series and embedded in Epon (direct method).

b) Paraffin-embedded liver blocks, in which uroporphyrin crystals were found with light microscopy, were deparaffined with xylol, followed by acetone-immersion and embedded in Epon (indirect method).

Ultrastructurally, there were no essential differences between liver tissue processed according to either the "direct" or the "indirect" method (results not shown).

For the ultrastructural study of the liver biopsies from patients with PCT, the "direct" method was used.

Ultrathin sections (60 nm) were collected on copper grids and examined with and without conventional staining (uranyl acetate and lead citrate) in a Zeiss EM 902 transmission microscope. This instrument is equipped with an integrated electron spectrometer, which allows:

1. Electron spectroscopic imaging (ESI) for high resolution contrast-sensitive imaging with energy-filtered electrons. For technical details, see Sorber et al. (219,220).
2. Electron energy-loss spectroscopic imaging (EELS) for element-related images, i.e., for the detection of iron in ferritin. For technical details, see Cleton et al. (221).

## 2.5 Morphometrical analysis

Morphometrical studies were performed at the Analytical Electron Microscopical Unit (Head: Dr W.C. de Bruijn) of the Department of Pathology, Erasmus University Rotterdam (Head: Prof. Dr F.T. Bosman).

Unstained Epon sections, 500-750 nm thick, were visualized by way of reflection contrast microscopy with the use of a Zeiss antiflex planneofluar, 63x/1.25, Ph3, oil-immersion objective (222,223). Images were transferred to the image analyzer IBAS 2000 (Kontron/Zeiss, Munich, Germany) with a sensitive camera mounted on a Zeiss Axioplan microscope (Zeiss, Oberkochen, Germany). In sections of livers from each treatment group of mice, 40 hepatocyte cytoplasmic areas of 8,100  $\mu\text{m}^2$  each were randomly selected. In liver biopsies of PCT patients, 25 hepatocyte cytoplasmic areas of 8,100  $\mu\text{m}^2$  each were randomly selected. The area fractions (expressed as percentages of the total measured cytoplasmic frame area) of uroporphyrin crystals and of ferritin iron core particles, present in each area, were calculated. Grey-value frequency histograms were used for objective segmentation and discrimination between ferritin and uroporphyrin

crystals. For further technical details, see Cleton et al. (224) and Sorber et al. (219,220).

## 2.6 Statistical analysis

All measurements were presented as means  $\pm$  standard deviation (SD).

The statistical analysis for Chapters 3,5 and 6, comparing biochemical, morphological and morphometrical parameters of different treatment groups, was performed with Wilcoxon's rank-sum test for ordinal data and with Fisher's exact test for categorial data.

Differences within and between groups in Chapter 4 were evaluated by a oneway analysis of variance. As multiple groups were compared, a oneway analysis procedure was used with a Bonferroni correction option in STATA release 2 (Computing Resource Centre, Los Angeles, USA).

The null hypothesis was rejected when  $p \geq 0.05$ .

**PART A. EXPERIMENTAL UROPORPHYRIA**



## CHAPTER 3

**Ferritin Iron Accumulation and Uroporphyrin Crystal Formation in Hepatocytes of C57BL/10 mice: A Biochemical and Morphological Study**

<b>Contents</b>	<b>page</b>
3.1 Summary	38
3.2 Introduction	38
3.3 Materials & Methods	39
3.4 Results	40
3.5 Discussion	52

This chapter is based on:

Siersema PD, van Helvoirt RP, Ketelaars DAM, Cleton MI, de Bruijn WC, Wilson JHP, van Eijk HG. Iron and uroporphyrin in hepatocytes of inbred mice in experimental porphyria: a biochemical and morphological study. *Hepatology* 1991; 14: 1179-1188.

Siersema PD, van Helvoirt RP, Cleton-Soeteman MI, de Bruijn WC, Wilson JHP, van Eijk HG. The role of iron in experimental porphyria and porphyria cutanea tarda. *Biol Trace Elem Res* 1992; 35: 65-72.

Siersema PD, Cleton-Soeteman MI, de Bruijn WC, ten Kate FJW, van Eijk HG, Wilson JHP. Ferritin accumulation and uroporphyrin crystal formation in hepatocytes of C57BL/10 mice: a time-course study. *Cell Tissue Res* 1993, in press.

### 3.1 Summary

Hexachlorobenzene-induced porphyria is iron-dependent and characterized by a decreased activity of uroporphyrinogen decarboxylase and the accumulation of porphyrins in the liver. To establish the time-sequence relationship between iron accumulation and uroporphyrin crystal formation in livers of C57BL/10 mice, a biochemical, morphological and morphometrical study was performed in livers of these mice, which were treated with hexachlorobenzene (HCB), iron dextran (IMF) or the combination of HCB plus IMF.

An increased total iron content and an accumulation of porphyrins were found in livers of mice treated with HCB plus IMF, but also in mice treated with IMF alone. In contrast, the amount of porphyrins was only slightly increased in livers of mice treated with HCB alone. Uroporphyrin crystal formation started in hepatocytes of mice treated with HCB plus IMF at 2 weeks and in mice treated with IMF alone at 9 weeks. In the course of time, uroporphyrin crystals gradually increased in size. Uroporphyrin crystals were initially formed in hepatocytes located in the periportal areas of the liver, in which also ferric iron staining was first detected. The amount and the distribution of the main storage form of iron in hepatocytes, ferritin, did not differ between the two treatment groups. Ferritin iron accumulation preceded the formation of uroporphyrin crystals in hepatocytes of both treatment groups. Moreover, uroporphyrin crystals were nearly always found close to ferritin iron. Only a few uroporphyrin crystals, surrounded by ferritin iron, were observed in hepatocytes of mice treated with HCB alone.

Conclusions: In C57BL/10 mice, uroporphyrinemia can be induced by iron-overload alone; HCB accelerates the effects of iron in porphyrin metabolism, but does not influence the accumulation of iron into the liver; uroporphyrin crystals are only formed in hepatocytes, in which also iron accumulates; and the morphological co-occurrence of uroporphyrin crystals and ferritin-iron in hepatocytes suggests a role for iron in the pathogenesis of uroporphyrinemia.

### 3.2 Introduction

Several polyhalogenated aromatic hydrocarbons (PAH's), including hexachlorobenzene (HCB), produce in humans and animals uroporphyrinemia closely resembling human porphyria cutanea tarda (PCT) (66,68). Both experimental uroporphyrinemia and PCT are characterized by a decreased activity of uroporphyrinogen decarboxylase (URO-D) and the

accumulation of uroporphyrins and heptacarboxylporphyrins in the liver (1,46).

The exact mechanism of experimental uroporphyria is not clear, however, any proposed mechanism has to take into account the role played by iron (97,146-153,174). It has been demonstrated that HCB, or other PAH's, cause the induction of cytochrome P-4501A2 (CYP1A2) in hepatocytes (166,167). Because HCB is a poor substrate for the cytochrome P-450 (Cyt P-450) isoenzyme (169), a recently favoured theory proposed that induction of CYP1A2 by HCB leads to uncoupling of the microsomal system (191). If "free" iron is present in hepatocytes, highly reactive oxygen-related free radicals could be produced by the Haber-Weiss reaction (151,152,181,191-198,225). These processes could, under certain circumstances, initiate the formation of a specific inhibitor of URO-D (183-186,200).

In PCT, earlier histological and ultrastructural [light microscopy (LM) and electron microscopy (EM)] studies revealed needle-like structures, representing uroporphyrin crystals (73), in hepatocytes (73,116-123). In HCB-induced uroporphyria four morphological studies have also been published (142-145), of which only one study reported the presence of uroporphyrin crystals in hepatocytes (143). Both in PCT and in experimental uroporphyria, the nature of the endogenous iron pool involved and its correlation with the site within the liver where uroporphyrin production takes place are not clear. In PCT, one LM study investigated the histological relation between porphyrins and iron, reporting that there was no correlation between areas of porphyrinogen fluorescence and areas of stainable iron (226). Regarding HCB-induced porphyria, no study on the morphological relationship between porphyrins and iron has been published.

We therefore performed a biochemical, morphological (both LM and EM) and morphometrical study in livers of C57BL/10 mice, which were treated with HCB, iron-dextran or the combination of HCB plus IMF. We aimed to establish the time-sequence relationship between the accumulation of iron and the formation of uroporphyrin crystals in these livers at regular intervals from 1 week to 52 weeks. In addition, we tried to establish the nature of the iron pool involved.

### 3.3 Materials & Methods

The mice were divided into five groups: Group 1 (HCB plus IMF, 55 mice), Group 2 (IMF alone, 55 mice), Group 3 (HCB alone, 25 mice), Group 4 (non-treated control

mice, 19 mice) and Group 5 (corn oil alone, 10 mice). Biochemical measurements in livers of mice treated with HCB plus IMF and with IMF alone were performed at weeks 10, 20, 30, 40 and 52. Morphological and morphometrical observations in livers of mice treated with HCB plus IMF and with IMF alone were performed at weekly intervals until week 15 and thereafter at weeks 20, 25, 30, 40 and 52. Biochemical measurements and morphological observations in livers of mice treated with HCB alone, with corn oil alone, and in livers of control mice were performed at weeks 10, 20, 30, 40 and 52. Two mice were sacrificed for the morphological and morphometrical studies and 3 mice were sacrificed for the biochemical measurements.

The methods of the biochemical measurements and the morphological and morphometrical observations have been described in Chapter 2, paragraphs 2.2.2, 2.2.9, 2.3, 2.4 and 2.5.

### 3.4 Results

#### 3.4.1 *Biochemistry*

The results of the biochemical determinations at the different time intervals are given in Table 1.

#### 3.4.2 *Light microscopy*

The lobular architecture of the livers from mice treated with HCB plus IMF, HCB alone and IMF alone remained intact during the experimental period, i.e., the portal tracts did not show inflammatory infiltration or fibrosis. Starting from week 3, the nuclei of the hepatocytes from mice treated with HCB plus IMF and with IMF alone appeared somewhat enlarged and some nuclei contained up to three nucleoli. This was more pronounced in livers of mice treated with HCB plus IMF than in livers of mice treated with IMF alone. In livers of mice treated with HCB, which was dissolved in corn oil, and in livers of mice treated with corn oil alone, there was a patchy, but similar distribution of lipid droplets in the hepatocytes (results not shown).

During the whole period of the study, the pattern of (ferric) iron deposition was not different between livers of mice treated with HCB plus IMF and with IMF alone. Livers of mice treated with HCB alone did not accumulate iron. Immediately after the administration of IMF, iron-positive granules were observed in Kupffer's cells. Thereafter,



**Table 1.**  
**Biochemical results in liver tissue of control mice and in liver tissue of mice treated with HCB alone, with HCB plus IMF and with IMF alone.**

Parameter	Duration of study (weeks)	Treatment groups			
		Controls	HCB	HCB+IMF	IMF
Porphyrin content <sup>a</sup>	0	2.3 ± 0.5	n.d.	n.d.	n.d.
	10	n.d.	1.81 ± 0.4 <sup>c</sup>	398 ± 61 <sup>d</sup>	90 ± 11
	20	2.1 ± 0.4	2.66 ± 0.6 <sup>c</sup>	891 ± 92 <sup>d</sup>	212 ± 42
	30	n.d.	3.02 ± 0.7 <sup>c</sup>	1298 ± 105 <sup>d</sup>	745 ± 98
	40	n.d.	3.58 ± 0.7 <sup>c</sup>	1343 ± 101 <sup>e</sup>	1159 ± 98
	52	2.4 ± 0.5	3.84 ± 0.9 <sup>c</sup>	1469 ± 122 <sup>c</sup>	1324 ± 112
Iron content <sup>b</sup>	0	0.3 ± 0.2	n.d.	n.d.	n.d.
	10	n.d.	n.d.	4.9 ± 0.6 <sup>c</sup>	4.7 ± 0.7
	20	0.4 ± 0.2	0.5 ± 0.2 <sup>c</sup>	11.2 ± 0.9 <sup>c</sup>	11.6 ± 1.1
	30	n.d.	n.d.	12.9 ± 1.2 <sup>c</sup>	13.3 ± 1.4
	40	n.d.	0.4 ± 0.1 <sup>c</sup>	10.5 ± 1.1 <sup>c</sup>	9.9 ± 1.3
	52	0.4 ± 0.2	0.4 ± 0.2 <sup>c</sup>	9.2 ± 1.0 <sup>c</sup>	9.4 ± 1.2

HCB, hexachlorobenzene; IMF, iron dextran; n.d., not determined;

<sup>a</sup> mean (± SD) in pmol per mg protein;

<sup>b</sup> mean (± SD) in mmol/100 gm dry weight;

<sup>c</sup> HCB group not different from control group;

<sup>d</sup> p < 0.05 compared with IMF group;

<sup>e</sup> HCB+IMF group not different from IMF group

the amount of iron-positive granules in Kupffer's cells increased and many of these cells became enlarged. In addition, aggregates of iron-loaded macrophages ("siderophages") were formed. By the 2nd week, iron-loaded Kupffer's cells were observed to accumulate in the portal and periportal areas, but already spreading to the midzonal areas of the liver lobule as well (Figure 1). By the 5th week, both iron-containing Kupffer's cells and siderophages, occurring singly or in small groups, were also noted in the centrilobular areas of the liver (Figure 2). By the 2nd week, iron-positive granules were noted in hepatocytes,

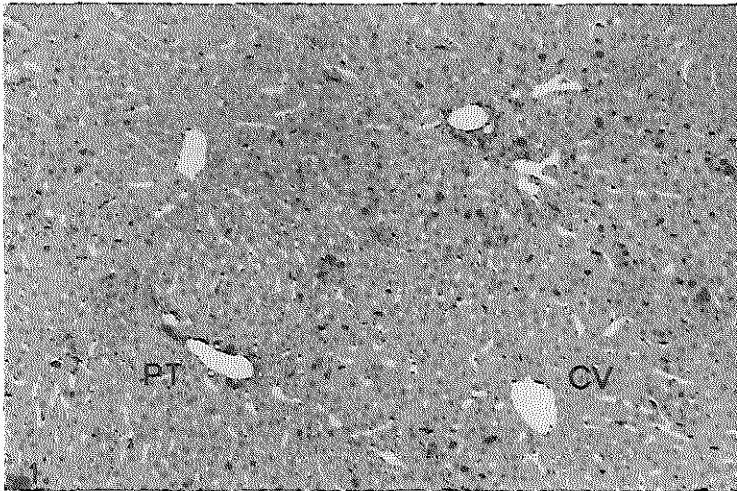


**Figure 1.**

Light micrograph (Perls' Prussian blue stain; x 25) of mouse liver tissue, 2 weeks after treatment with hexachlorobenzene and iron dextran. Note the staining (indicating ferric iron) in the (peri-)portal and midzonal areas of the liver.

PT, Portal Tract; CV, Central Vein

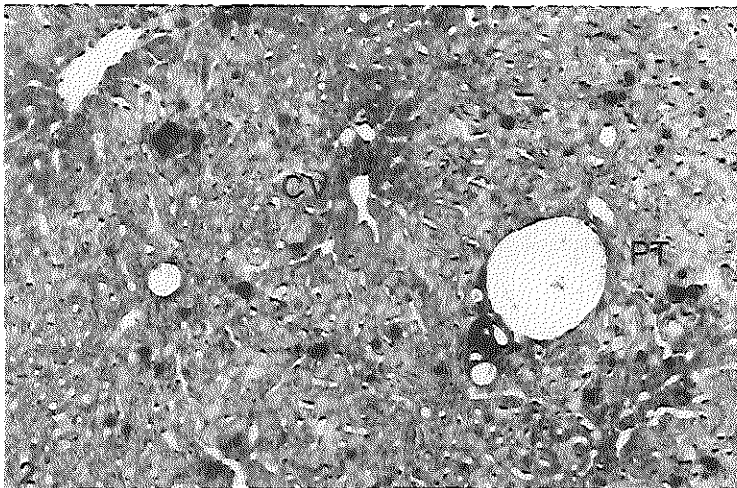


**Figure 2.**

Light micrograph (Perls' Prussian blue stain; x 50) of mouse liver tissue, 5 weeks after treatment with hexachlorobenzene and iron dextran. Note the staining (indicating ferric iron) in the (peri-)portal, midzonal and centrilobular areas of the liver.

PT, Portal Tract; CV, Central Vein

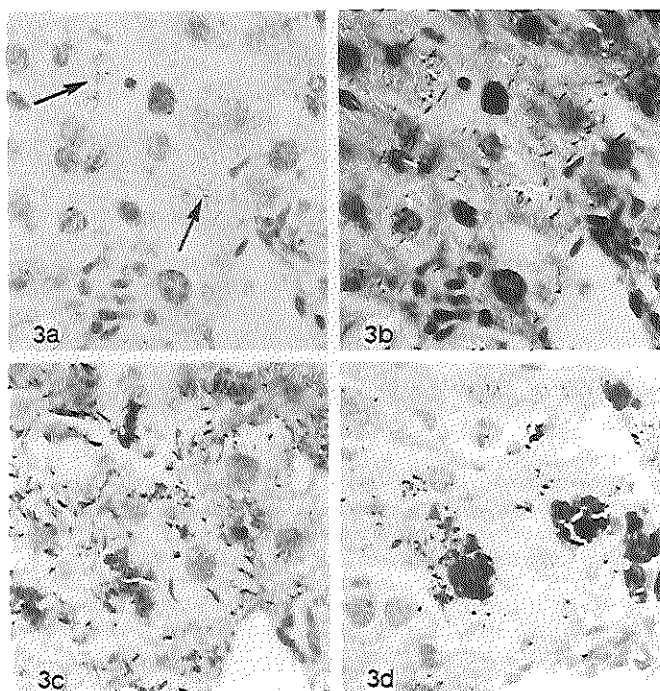


**Figure 3.**

Light micrographs (x 650) of the same field in four sequential sections of a liver from a mouse treated with hexachlorobenzene and iron dextran. (a) Gill's hematoxylin stain. Uroporphyrin crystals in hepatocytes (*arrows*). (b) Polarized light. Uroporphyrin crystals display birefringence. (c) Ferric ferricyanide reduction test in Lillie's modification. Uroporphyrin crystals stain dark. (d) Perls' Prussian blue stain. Staining in hepatocytes and in Kupffer's cells indicates ferric iron.

mainly located close to the portal areas of the liver lobule, but soon spreading to the midzonal areas of the liver lobule (Figure 1). In the course of time, iron-positive staining in hepatocytes was spreading diffusely through the liver, across to the centrilobular areas of the liver lobule (Figure 2). At week 6, siderosis of the liver was graded massive [grade 4 according to Scheuer et al. (217)]. After 52 weeks, Kupffer's cells and siderophages, but also hepatocytes in the liver lobule, were still staining iron-positive. At this time, the highest concentration of iron-positive granules seemed to be present in the periportal areas.

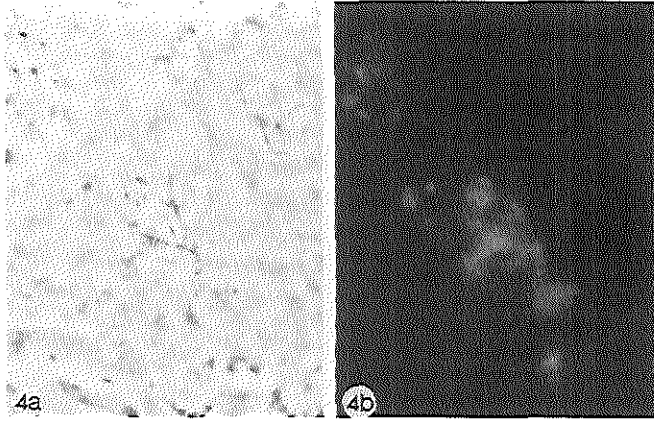


**Figure 4.**

(a) Light micrograph (Phase contrast; x 1,000) of a frozen section of liver tissue of a mouse treated with iron dextran, showing uroporphyrin crystals. (b) Light micrograph (x 1,000) of the same field, showing the fluorescence in areas with uroporphyrin crystals of Figure 4a. Note that the fluorescence was more widespread and not limited to the uroporphyrin crystals.

Needle-like structures, representing uroporphyrin crystals (Figure 3), were first noted in hepatocytes of mice treated with HCB plus IMF by the 2nd week. The first uroporphyrin crystals were observed in those hepatocytes in which the first iron depositions were also detected, i.e., in the periportal areas of the liver. In hepatocytes of mice treated with IMF alone, the first uroporphyrin crystals were observed by the 9th week. Both in livers of mice treated with HCB plus IMF and with IMF alone, uroporphyrin crystals were not regularly distributed, but were usually found in those hepatocytes, in which also the highest concentration of iron-positive granules seemed present, i.e., in the periportal areas and later, although to a lesser degree, in the centrilobular areas of the liver. Only at weeks 40 and 52, a few uroporphyrin crystals were observed in hepatocytes of mice treated with HCB alone.

Fluorescence of liver tissue could only be demonstrated in frozen sections of liver tissue (Figure 4). In livers of mice treated with HCB plus IMF and treated with IMF alone, it was noticed that areas with uroporphyrin crystals (Figure 4a) displayed fluorescence (Figure 4b); however, fluorescence seemed more widespread and not limited to uroporphyrin crystals alone.

### 3.4.3 Electron microscopy

Iron overload in hepatocytes of mice treated with HCB plus IMF and with IMF alone was initially seen as an increase and a clustering of cytoplasmic ferritin. From 2 weeks onwards, ferritin was also found in siderosomes (iron-containing lysosomes) in hepatocytes of mice treated with HCB plus IMF and with IMF alone (Figures 5,6). At week 6, the cellular organelles showed the characteristic signs of iron overload: swollen endoplasmic reticulum, flattened microvilli in the bile canalicular region, widened spaces

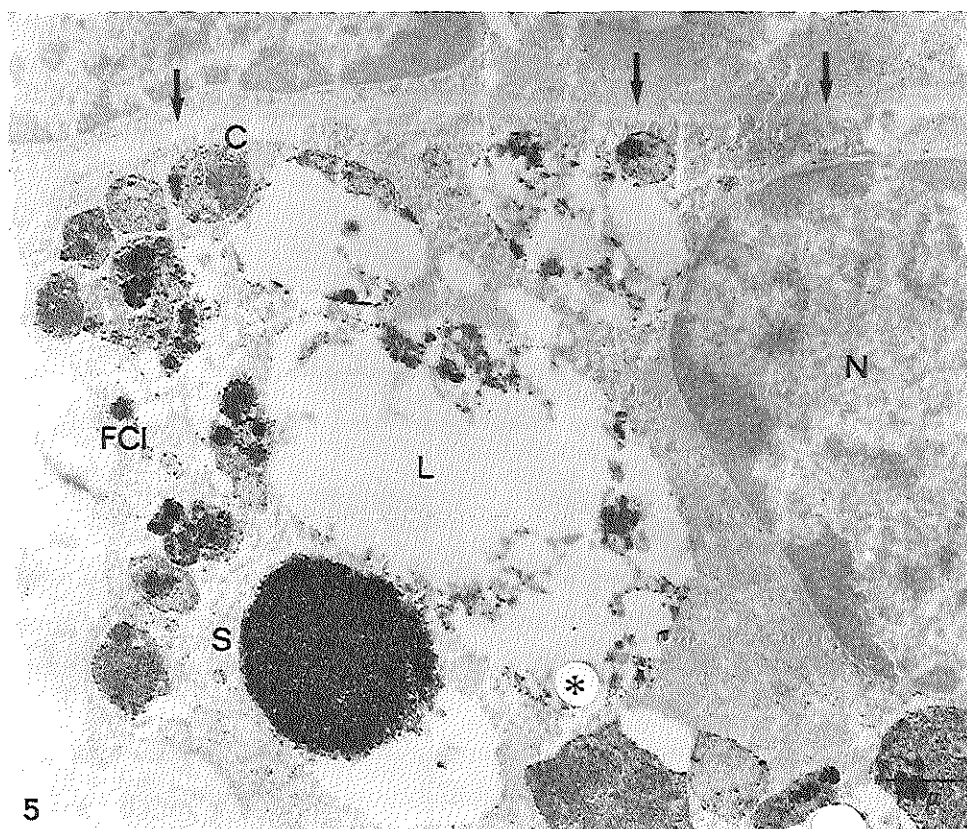


**Figure 5.** Electron micrograph (electron spectroscopic image (ESI) of a stained section; bar= 1.1  $\mu\text{m}$ ) of a mouse hepatic parenchymal cell, 6 weeks after treatment with hexachlorobenzene and iron dextran. Note the interdigitation of the lateral cell membrane (*arrows*). S, siderosome (iron-containing lysosome); FCI, Ferritin Cluster; C, Collagen fibres; L, lipid droplet; N, Nucleus; \*, hole in section

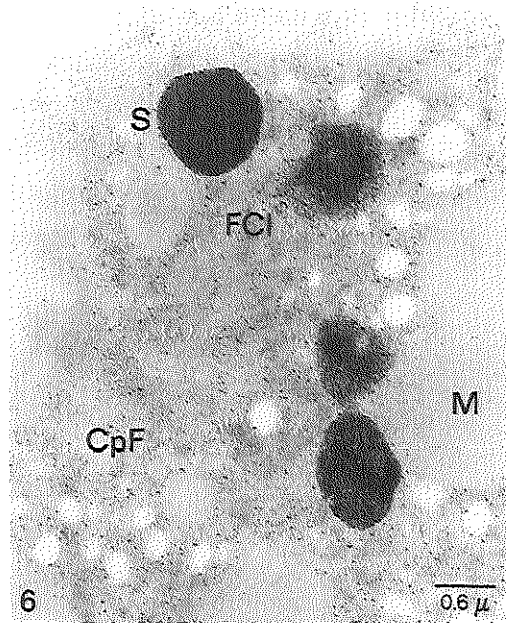


**Figure 6.**

Electron micrograph (electron spectroscopic image (ESI) of an unstained section; bar = 0.6  $\mu\text{m}$ ) of a mouse hepatic parenchymal cell, 6 weeks after treatment iron dextran.

S, Siderosome (iron-containing lysosome); FCI, Ferritin Cluster; CpF, Cytoplasmic Ferritin; M, Mitochondrion

between cells sometimes containing collagen fibres and indented heterochromatic nuclei (Figure 5). The pattern of distribution and the storage forms of iron were not different between hepatocytes of mice treated with HCB plus IMF (Figure 5) and with IMF alone (Figure 6).

Apart from an increased amount of lipid droplets in hepatocytes of mice treated with HCB (which was dissolved in corn oil), no other ultrastructural alterations were observed in hepatocytes of mice treated with HCB during the experimental period.

Uroporphyrin crystals in hepatocytes could be examined best in unstained Epon sections. Uroporphyrin crystals were randomly located in hepatocytes, often close to ferritin. Throughout the study period, it appeared that uroporphyrin crystals gradually increased in size (Figure 7a,b).

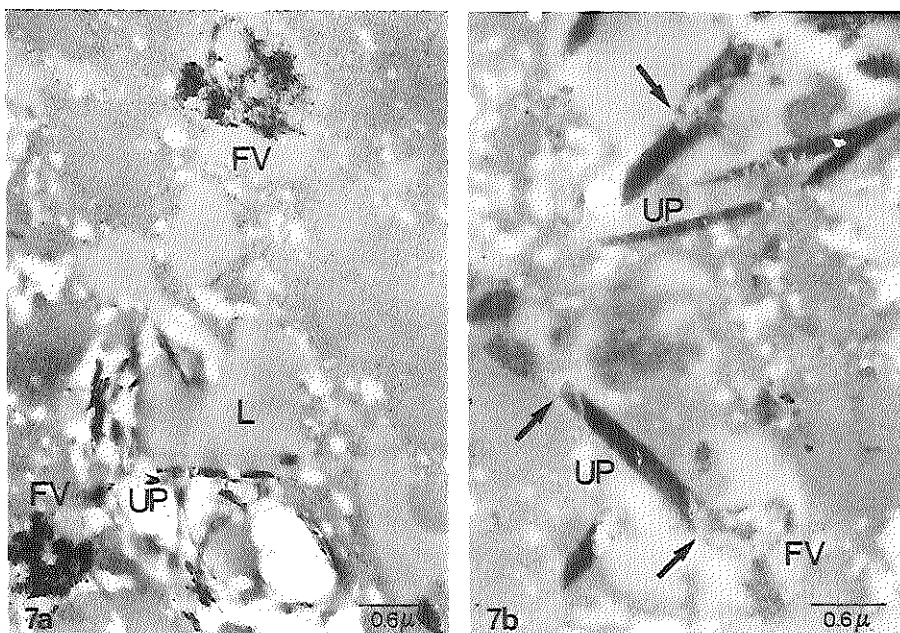


**Figure 7.**

Electron micrographs (electron spectroscopic images (ESI) of unstained sections; bar= 0.6  $\mu\text{m}$ ) of hepatic parenchymal cells of (a) a mouse, 6 weeks after treatment with hexachlorobenzene (HCB) plus iron dextran (IMF) and (b) a mouse, 20 weeks after treatment with HCB plus IMF. Note the close association between the uroporphyrin crystal (UP) and ferritin in Figure 7b (arrows).

FV, Ferritin-containing Vacuole; L, Lipid droplet

In hepatocytes of mice treated with HCB alone, very little ferritin iron was present. Starting from week 30, a few uroporphyrin crystals were detected. However, if a crystal was observed in a hepatocyte, then it was always surrounded by ferritin (Figure 8).

#### 3.4.4 Morphometrical analysis

##### At 20 weeks:

Morphometrical analysis was performed by reflection contrast microscopy. An example of a reflection contrast microscopical view is given in Figure 9.

The results of the morphometrical analysis in livers of mice treated with HCB plus IMF

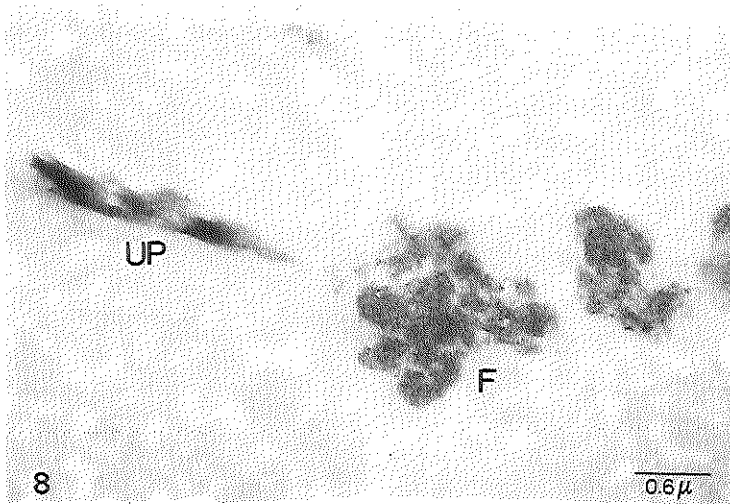


**Figure 8.**

Electron micrograph (electron spectroscopic image (ESI) of an unstained section; bar=  $0.6 \mu\text{m}$ ) of a hepatic parenchymal cell of a mouse, 52 weeks after treatment with hexachlorobenzene. Note the association between the uroporphyrin crystal (UP) and ferritin (F).

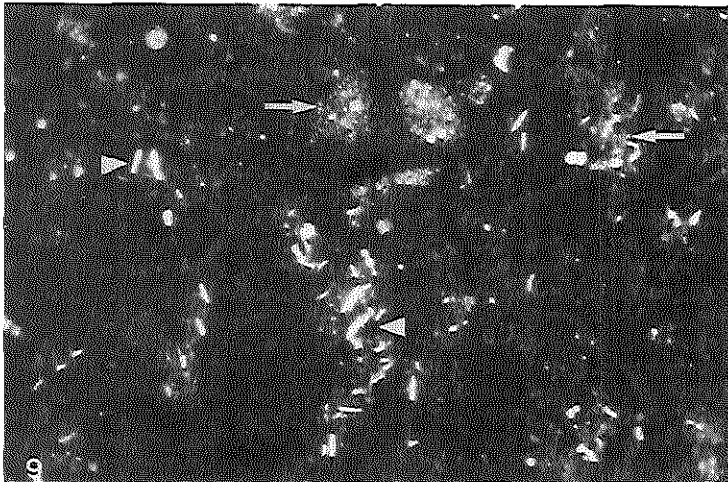


**Figure 9.**

Reflection contrast micrograph (x 500) of an unstained Epon section of liver tissue of a mouse, 20 weeks after treatment with iron dextran, showing uroporphyrin crystals (*arrowheads*) and ferritin iron cores (*arrows*).



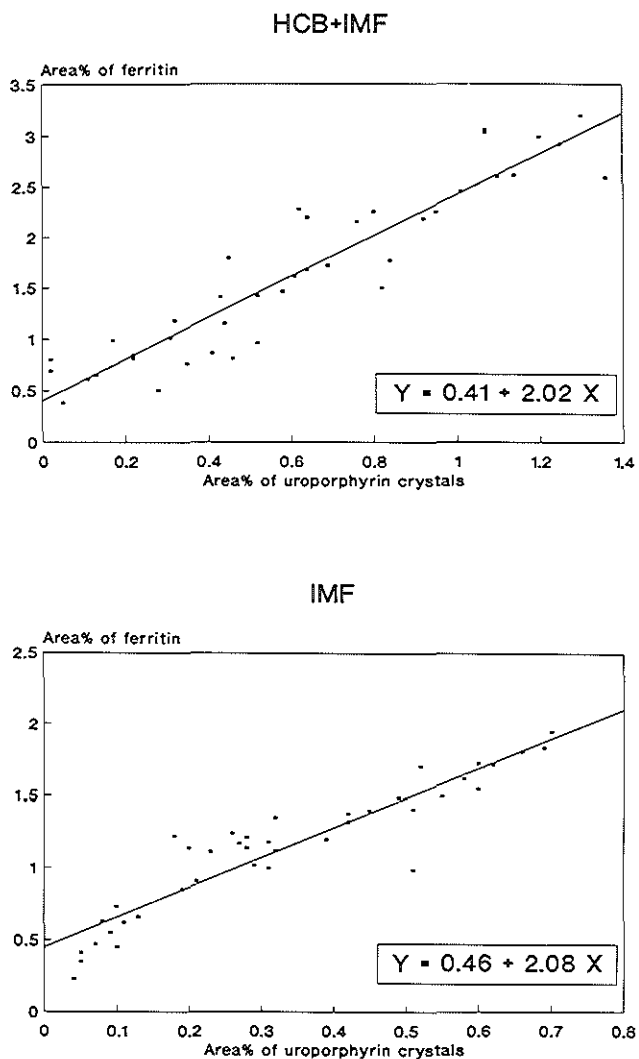


**Figure 10.**

Morphometrical analysis by reflection contrast microscopy of unstained, thin Epon sections, showing the linear relationship between area fractions of uroporphyrin crystals and area fractions of ferritin iron cores. The area fractions are expressed as percentages (%) of the total measured hepatocyte cytoplasmic frame area (40 areas of  $8,100 \mu\text{m}^2$ ). (a) Mice treated with hexachlorobenzene and iron dextran (HCB+IMF). (b) Mice treated with iron dextran (IMF) alone. The calculated regression lines are indicated.

and in livers of mice treated with IMF alone, at week 20, are given in Figure 10. As can be seen from this figure, an increased hepatocyte area fraction (expressed as a percentage of the total measured cytoplasmic frame area) of uroporphyrin crystals, present in each area, was associated with an increased hepatocyte area fraction of ferritin iron. The difference between the two treatment groups was the increased area fraction of uroporphyrin crystals in livers of mice treated with HCB plus IMF compared with livers of mice treated with IMF alone. However, the ratio between uroporphyrin crystals and ferritin iron was the same in both treatment groups (HCB+IMF:  $Y = 0.41 + 2.02X$  and IMF:  $Y = 0.46 + 2.08X$ ).

Time-sequence:

The results of the morphometrical analysis in hepatocytes of mice treated with HCB plus IMF and with IMF alone in the course of time are shown in Figure 11. As can be seen from these figure, the mean ( $\pm$  SD) area fractions of ferritin iron in hepatocytes at the various time intervals were not different between mice treated with HCB plus IMF or with IMF alone. Up to 20 weeks, there was a steep increase in the mean area fractions of ferritin iron (HCB+IMF:  $Y = 0.13X + 0.07$ ; IMF:  $Y = 0.13X + 0.05$ ). Thereafter, the mean area fractions of ferritin iron gradually decreased in both treatment groups. In the course of time, the mean ( $\pm$  SD) area fractions of uroporphyrin crystals in hepatocytes gradually increased in both treatment groups. Up to 30 weeks, the mean area fractions of uroporphyrin crystals were significantly different between livers of mice treated with HCB plus IMF and with IMF alone. At weeks 40 and 52 however, the mean area fractions of uroporphyrin crystals were not different between the two treatment groups.

In Figure 12 the mean ( $\pm$  SD) ratios between the hepatocyte area fractions of uroporphyrin crystals and the area fractions of ferritin iron core particles at different time intervals are presented, this has been called the porphyrins per ferritin area fraction ratio. As can be seen from this figure, from 2 weeks up to 20 weeks in hepatocytes of mice treated with HCB plus IMF, these ratios were relatively constant, i.e., between 0.2 and 0.3. In contrast, by the 9th week, in hepatocytes of mice treated with IMF alone, the porphyrins per ferritin area fraction ratios became positive at a lower level and increased in the course of time. By the 20th week, there was a similar and sustained increase in the porphyrins per ferritin area fraction ratios in both treatment groups in the course of time (HCB+IMF:  $Y = 0.004X + 0.208$ ; IMF:  $Y = 0.004X + 0.118$ ).

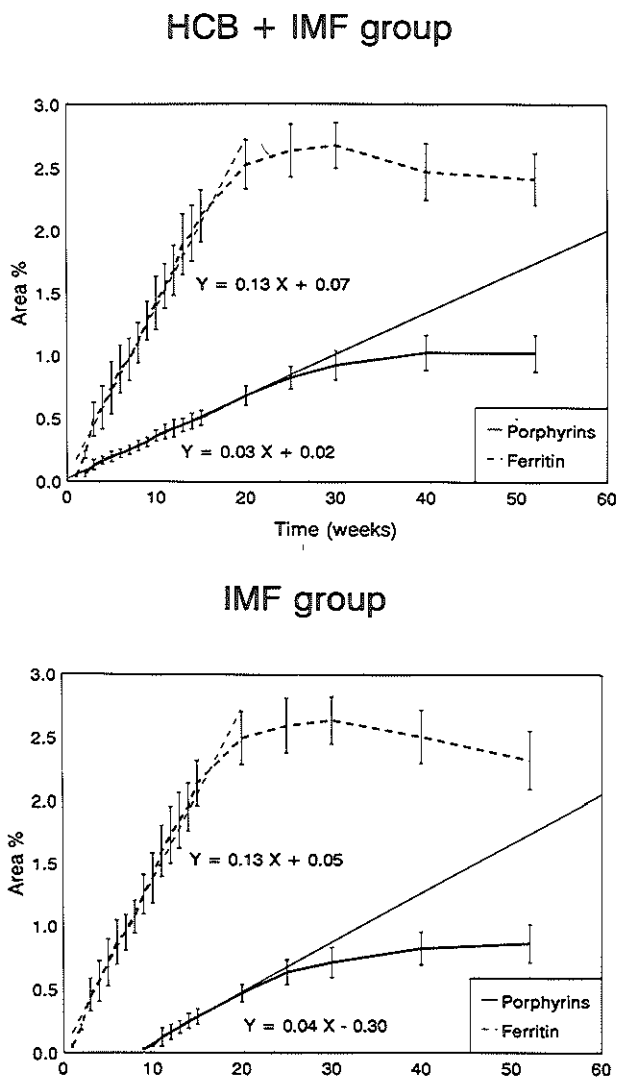


**Figure 11.**

Morphometrical analysis by reflection contrast microscopy of unstained Epon sections, showing the mean ( $\pm$  SD) area fractions of uroporphyrin crystals (Porphyrins) and of ferritin particles (Ferritin) at different time intervals in livers of mice treated with hexachlorobenzene plus iron dextran (HCB+IMF group) and in livers of mice treated with iron dextran alone (IMF group). The calculated regression lines are indicated.

## Porphyrins/Ferritin ratios

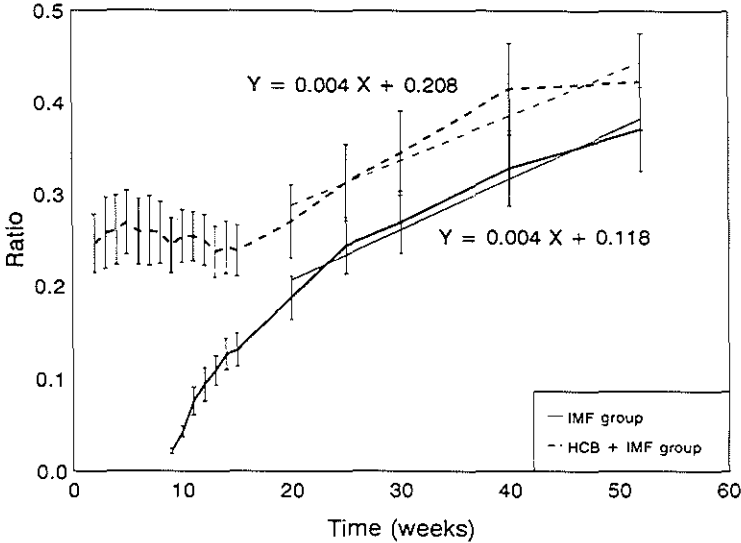


**Figure 12**

Morphometrical analysis by reflection contrast microscopy of unstained Epon sections, showing the mean ( $\pm$  SD) ratios of porphyrins per ferritin area fractions at different time intervals in livers of mice after treatment with iron dextran (IMF group) and after treatment with hexachlorobenzene plus iron dextran (HCB+IMF group). For the period from 20 weeks up to 52 weeks, the calculated regression lines in both treatment groups are indicated.

### 3.5 Discussion

A biochemically increased amount of hepatic porphyrins (Table 1) was found to coincide, histologically (Figures 3,4) and ultrastructurally (Figure 7a,b), with the presence of needle-like structures in liver parenchymal cells of C57BL/10 mice. It has been shown that needle-like structures represent uroporphyrin crystals, since uroporphyrin I and III, crystallized *in vitro*, display the same ultrastructural characteristics (73). Uroporphyrin crystals were presumably synthesized *in vivo* in the liver, since they were found in frozen sections (Figure 4a). In the course of time, uroporphyrin crystals gradually increased in

size in both treatment groups (Figure 7a,b). In areas where uroporphyrin crystals were found, fluorescence could be detected as well (Figure 4b). The fluorescence was not limited to uroporphyrin crystals, but more widespread in the surrounding cytoplasm (Figure 4a,b). Therefore, it seems likely that the enlargement of uroporphyrin crystals in the course of time is caused by the synthesis and apposition from surrounding porphyrinogens.

Our data on iron distribution in livers after administration of IMF were in agreement with observations by others, in that iron-positive staining initially was detected in Kupffer's cells and siderophages, followed by the presence of ferric iron in hepatocytes in both treatment groups (Figure 1) (227-233). The main storage form of iron in both treatment groups was ferritin (Figures 5-7) (227,231-233). Morphometrically, no difference in the amount of ferritin was observed between hepatocytes of mice treated with HCB plus IMF and with IMF alone (Figures 10,11). In addition, at the ultrastructural level, the distribution pattern of ferritin was not different between the two treatment groups (Figures 5-7). Therefore, it can be concluded that HCB by itself does not influence the accumulation of iron into the liver.

A time-dependent accumulation of uroporphyrin crystals (Figure 11) was found in livers of mice treated with HCB plus IMF, but also in livers of mice treated with IMF alone. The only difference was that uroporphyrin crystal formation developed more rapidly in livers of mice treated with HCB plus IMF than in livers of mice treated with IMF alone. Moreover, the morphometrical analysis revealed that for the formation of uroporphyrin crystals in hepatocytes of mice treated with IMF alone (as compared with mice treated with HCB plus IMF) much more iron (as ferritin) needed to be accumulated before uroporphyrin crystal formation was initiated (Figure 12). In livers of mice treated with HCB alone, without concomitant administration of iron dextran, the amount of porphyrins was only slightly increased (Table 1).

Evidence on the role of HCB in experimental porphyria proposes that HCB induces CYP1A2 (166,167), leading to the uncoupling of the system (191). If "free" iron is present, highly reactive oxygen-related free radicals could be produced by the Haber-Weiss reaction (151,152,181,191-198,225). Induction of the Cyt P-450 system appears to depend on binding of the chemical to a receptor protein (*Ah* phenotype) (164,165). Greig et al. (173) found that 2,3,7,8-tetrachlorodibenzo-*p*-dioxin (TCDD), another PAH,

induced uroporphyrin both in C57BL/10 mice (*Ah*-responsive) and in AKR mice (*Ah*-non-responsive). TCDD did not induce porphyria in DBA/2 mice (also *Ah*-non-responsive), even with concomitant iron administration. These and our results suggest that induction of the Cyt P-450 system is not an absolute requirement for uroporphyrin to develop. As a possible explanation for this observation, Cheeseman et al. (234) reported that NADPH/ADP-iron-dependent lipid peroxidation in microsomes of C57BL/6 mice (*Ah*-responsive) and AKR mice was two-fold increased compared with microsomes of DBA/2 mice, suggesting that iron-catalyzed free radical-mediated processes are important in inducing uroporphyrin. This difference in lipid peroxidation was also found in microsomes of C57BL/10 mice compared with microsomes of DBA/2 mice (194). The role of iron is further illustrated by findings of Smith et al. (146), who described the development of uroporphyrin in rats, which were treated with HCB alone, to depend on the endogenous iron content of the liver.

Petryka et al. (226) were not able to demonstrate iron and porphyrinogen fluorescence in the same hepatocyte in livers of patients with PCT. They concluded that certain cells preferentially accumulate either porphyrins or iron. In contrast to their findings, we observed in hepatocytes of C57BL/10 mice that uroporphyrin crystals and ferritin-iron were located in the same hepatocyte (Figure 7a,b). Moreover, an increased hepatocyte area fraction of uroporphyrin crystals was associated with an increased hepatocyte area fraction of ferritin iron in each cytoplasmic area (Figure 10). Another finding was that the single uroporphyrin crystal, found in a hepatocyte of a mouse treated with HCB alone, was also surrounded by ferritin aggregates (Figure 8), which was remarkable in the light of the scarcity of (ferritin) iron present in these livers. Our results suggest a role for iron (as ferritin) in the pathogenesis of (experimental) uroporphyrin. Ferric iron however, is sequestered in ferritin as a non-toxic oxyhydroxide, complexed with phosphate; oxidation and storage of iron appear to be related processes and release of iron from ferritin requires reduction (235). Although *in vitro* release of ferrous iron from ferritin by liver microsomes has been described (174,225,236-238), it is not clear whether this also occurs *in vivo*.

On the basis of these results, we postulate that in hepatocytes of C57BL/10 mice, either as a result of CYP1A2 induction (after administration of HCB) (166,167) and/or as a result of a genetically-determined mechanism, as suggested by Smith and de Matteis

(191), an active oxidative metabolism exists. Above a certain level of iron accumulation in hepatocytes (Figures 10-12), toxic species could be produced (151,152,181,191-198,225), which could react with uroporphyrinogen or another substance to form an inhibitor of URO-D (183-186,200), thus explaining the accumulation of uroporphyrin crystals in hepatocytes (191). Alternatively, damage to URO-D, either by a direct action of iron or by a free radical-mediated mechanism, has been postulated (95,96).

In this Chapter, we proposed a role for iron (as ferritin) in the pathogenesis of uroporphyria. However, it has been suggested that a small fraction of intracellular iron is bound to a variety of molecules of low molecular weight (LMW) (239-242). This pool of LMW iron is thought to be more readily available for a catalytic role in the Haber-Weiss cycle. Moreover, a role for LMW iron has been demonstrated in the process of free radical formation in iron-loaded cells (212,243,244). Therefore in Chapter 4, we will investigate the possible role of this pool of LMW iron in the pathogenetic mechanism of uroporphyria.





**CHAPTER 4****The Effect of Desferrioxamine on Iron Metabolism, Lipid Peroxidation and Porphyrin Metabolism in Hepatocytes of C57BL/10 Mice with Uroporphyrin**

<b>Contents</b>	<b>page</b>
4.1 Summary	58
4.2 Introduction	58
4.3 Materials & Methods	60
4.4 Results	60
4.5 Discussion	67

Parts of this chapter are based on:

Van Gelder W, Siersema PD, Voogd A, de Jeu-Jaspars NCM, van Eijk HG, Koster JF, de Rooij FWM, Wilson JHP.  
The effect of desferrioxamine on iron metabolism and lipid peroxidation in hepatocytes of C57BL/10 mice in experimental uroporphyrin.  
Biochem Pharmacol 1993; 46: 221-228.

#### 4.1 Summary

The effects of the iron chelator, desferrioxamine (DFx), on iron accumulation, malondialdehyde (MDA) production (as a marker of lipid peroxidation), porphyrin accumulation, uroporphyrinogen decarboxylase (URO-D) activity and porphobilinogen deaminase (PBG-D) activity were investigated over a period of 14 weeks in livers of C57BL/10 mice, which were treated with hexachlorobenzene (HCB), iron dextran (IMF) or the combination of HCB plus IMF. In addition, the amount of low molecular weight (LMW) iron was measured in these livers to determine a possible correlation with MDA production.

Treatment with HCB plus IMF and with IMF alone, resulted in an increased production of MDA and porphyrin accumulation, a reduced URO-D activity and an increased PBG-D activity, whereas treatment with HCB alone had no effect. DFx caused a reduction in MDA production and hepatic porphyrins, this reduction being more pronounced in livers of mice treated with IMF alone than in livers of mice treated with HCB plus IMF. The effects of DFx on URO-D activity were in agreement with the results on porphyrin accumulation. LMW iron measurements at 11 weeks correlated well with data on MDA production in all treated groups in the same period ( $R^2 = 0.84$ ), suggesting that both variables were interdependent.

Conclusions: Iron plays an important role in porphyrin accumulation and decreased URO-D activity in livers of C57BL/10 mice; DFx is effective in reducing porphyrin accumulation, probably due to a reduction of the LMW pool of iron, thus diminishing the amount of iron available for a catalytic role in the generation of oxygen-related free radicals; the finding of an increased PBG-D activity could provide an additional explanation for the marked uroporphyrin accumulation.

#### 4.2 Introduction

Human porphyria cutanea tarda (PCT) is characterized by a partial block in the heme biosynthetic pathway at the level of uroporphyrinogen decarboxylase (URO-D) and the accumulation of uroporphyrins and heptacarboxylporphyrins in the liver (1,46). Uroporphyrin can be induced in rodents and humans by the administration of hexachlorobenzene (HCB), a polyhalogenated aromatic hydrocarbon (PAH) (66,68).

Iron plays an important role in PAH-induced uroporphyrin (97,146-153,174). Moreover,

it was shown in Chapter 3, that in livers of C57BL/10 mice, uroporphyrin can be induced by iron-overload alone.

The effect of iron in experimental uroporphyrin has been explained by its ability to participate in iron-catalyzed free radical-mediated processes. It has been suggested that there is a highly active oxidative metabolism in hepatocytes of C57BL/10 mice, either as a result of cytochrome P-4501A2 (CYP1A2) induction by PAH's (166,167), or genetically-determined in these mice, as suggested by Smith and de Matteis (191). If "free" iron is present, highly reactive oxygen-related free radicals could be formed by the Haber-Weiss reaction (151,152,181,191-198,225). In addition, the intracellular presence of free ferrous iron by itself can induce the formation of  $O_2^-$  (superoxide) (243,245), and thus initiate the chain of reactions leading to the formation of oxygen-related free radicals.

In the presence of oxygen-related free radicals, a variety of reactions can be initiated, such as peroxidation of membrane lipids (199). Recently, it has been suggested that the process of lipid peroxidation is involved in the pathogenesis of experimental uroporphyrin (152,196).

Since the effect of the iron chelator desferrioxamine (DFx) on liver iron accumulation, malondialdehyde (MDA) production (as a marker of lipid peroxidation), porphyrin accumulation and URO-D activity in the course of time has not been studied extensively, we decided to investigate these effects of DFx in livers of C57BL/10 mice, which were treated with HCB, iron-dextran (IMF), or the combination of HCB plus IMF. In addition, we studied the activity of porphobilinogen deaminase (PBG-D), one of the preceding enzymes of URO-D in the heme biosynthetic pathway. An increased PBG-D activity has been reported in livers of patients with PCT (48,52) and an increased PBG-D activity could provide an additional explanation for uroporphyrin accumulation in experimental uroporphyrin.

The nature of the iron pool involved in experimental uroporphyrin is not clear. On the basis of the finding in Chapter 3, of a morphological co-occurrence of uroporphyrin crystals and ferritin iron in hepatocytes of porphyric C57BL/10 mice, a role for ferritin-bound iron in the pathogenesis of experimental uroporphyrin has been suggested. However, ferric iron is sequestered in ferritin as a non-toxic oxyhydroxide, complexed with phosphate. The release of iron from ferritin requires reduction (235). Although *in vitro* release of ferrous iron from ferritin by liver microsomes has been described

(174,225,236-238), it is not clear whether this also occurs *in vivo*. An alternative possibility could be an intracellular pool of low molecular weight (LMW) iron (239-242). A role for this LMW pool of iron has been demonstrated in free radical formation in iron-loaded cells (212,243,244). A recently developed technique (212; see also paragraph 2.2.10) to measure the amount of LMW iron in tissue homogenates was used to further elucidate this problem.

### 4.3 Materials & Methods

At weeks 4, 7, and 14, measurements were performed in livers of mice treated with HCB plus IMF (HCB+IMF group, 25 mice), HCB alone (HCB group, 20 mice), IMF alone (IMF group, 25 mice), and in control mice (20 mice). In addition, subgroups of mice treated with HCB plus IMF and with IMF alone were treated with daily DFX injections. Daily DFX injections started either from the beginning of the experiment (HCB+IMF+DFX group: 25 mice and IMF+DFX group: 25 mice) or started from week 7 (HCB+IMF+DFX7 group: 15 mice and IMF+DFX7 group: 15 mice). In livers of mice in which DFX injections started at week 7, measurements were performed at weeks 7, 11 and 14.

The amount of liver tissue in each mouse (average weight  $\pm$  2.1 gm) was too small to perform LMW iron measurements in combination with the other measurements at all time intervals. We therefore chose to carry out these incubations at week 11, as sufficient time should have elapsed for the biochemical discrimination of the different treatment groups.

The methods of the biochemical determinations have been described in Chapter 2, paragraphs 2.2.2, 2.2.4, 2.2.8, 2.2.9, 2.2.10 and 2.2.12.

### 4.4 Results

#### 4.4.1 Total iron content in liver tissue

The results of mean ( $\pm$  SD) iron content in liver tissue at the different time intervals are given in Figure 1. Measurements were performed in duplo samples of liver tissue.

Liver iron content in the IMF group was increased at week 4, but even in the following 10 weeks a distinct rise could be measured. Liver iron content in the IMF+DFX group was lower at all times compared with the IMF group ( $p < 0.001$ ). In the IMF+DFX7 group, liver iron content decreased after starting DFX administration at week 7, resulting

in about a 50% liver iron content reduction at week 14. The increase in liver iron content in the HCB+IMF group was equal to that in the IMF group. However, in the HCB+IMF+DFx group, liver iron contents were elevated at all times compared with the iron results in the IMF+DFx group ( $p = 0.008$ ). In contrast, iron contents in livers of non-treated control mice and in livers of mice treated with HCB alone were low, with a mean of  $3 \mu\text{mol/gm}$  dry weight liver tissue.

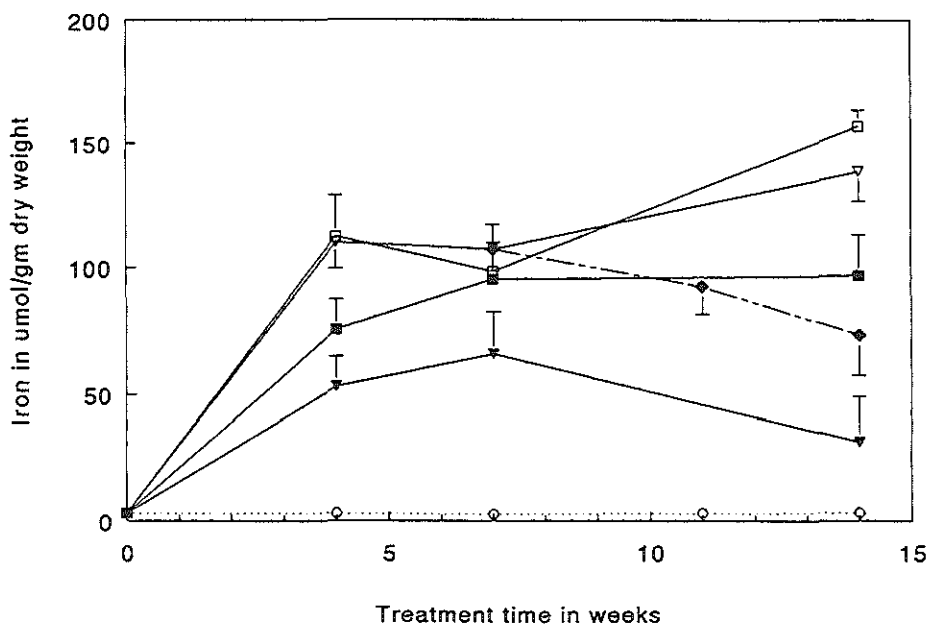


Figure 1.

Total liver iron content during the experimental period in liver tissue of C57BL/10 mice.

Open circles: Control group; Open triangles: Mice treated with iron dextran (IMF group); Closed triangles: Mice treated with IMF and desferrioxamine from the beginning of the experiment (IMF+DFx group); Open squares: Mice treated with hexachlorobenzene and IMF (HCB+IMF group); Closed squares: HCB+IMF+DFx group; Closed diamonds: Mice treated with IMF and DFX from week 7 (IMF+DFx7 group);

Values shown represent the means  $\pm$  SD.

#### 4.4.2 Malondialdehyde content in liver tissue

Results of mean ( $\pm$  SD) MDA production in liver tissue at the different time intervals are given in Figure 2. Measurements were performed in 4-fold in samples of liver tissue.

All DFX-treated groups showed a distinct reduction in MDA production compared with the groups receiving the same treatment without DFX. In the IMF+DFX group, MDA production at week 14 was even lower than that in the control groups. Treatment with HCB+IMF resulted in higher MDA concentrations than treatment with IMF alone. MDA production in mice treated with HCB alone did not differ from the non-treated control group of mice.

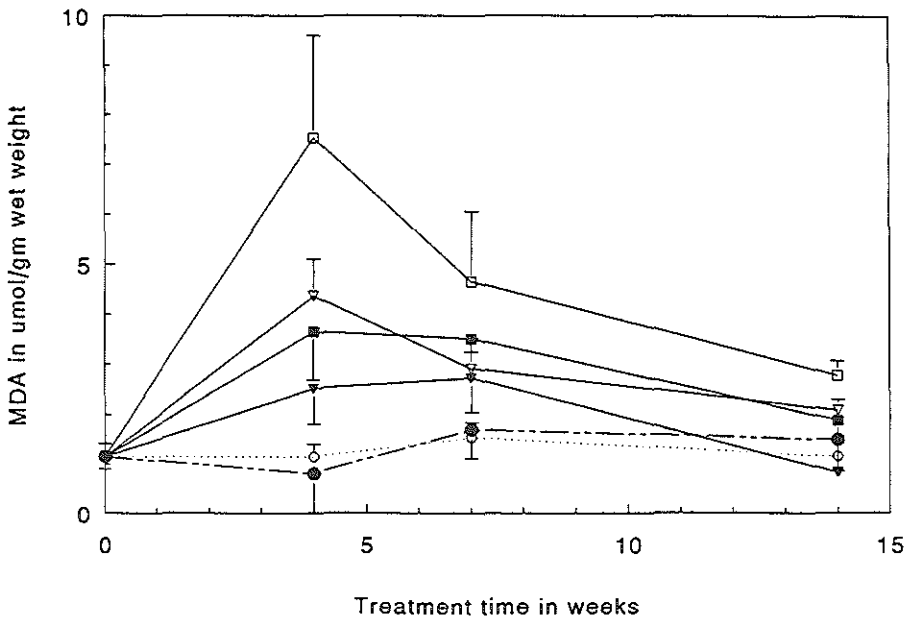


Figure 2.

Malondialdehyde (MDA) content during the experimental period in liver tissue of C57BL/10 mice.

Open circles: Control group; Closed circles: Mice treated with hexachlorobenzene (HCB group); Open triangles: Mice treated with iron dextran (IMF group). Closed triangles: Mice treated with IMF and desferrioxamine from the beginning of the experiment (IMF+DFX group); Open squares: HCB+IMF group; Closed squares: HCB+IMF+DFX group;

Values shown represent the means  $\pm$  SD.

#### 4.4.3 Porphyrins in liver tissue

Results of mean ( $\pm$  SD) porphyrin content in liver tissue at the different time intervals are given in Figure 3. Measurements were performed in duplo samples of liver tissue.

Both in the HCB+IMF group and in the IMF group, but not in the HCB group, an increase in hepatic porphyrin accumulation was observed during the 14 weeks. Apart from the results at week 14, hepatic porphyrin contents were higher in the HCB+IMF group than in the IMF group ( $p < 0.001$ ). The reduction in porphyrin accumulation was more pronounced in livers of the IMF+DFx group than in the HCB+IMF+DFx group.

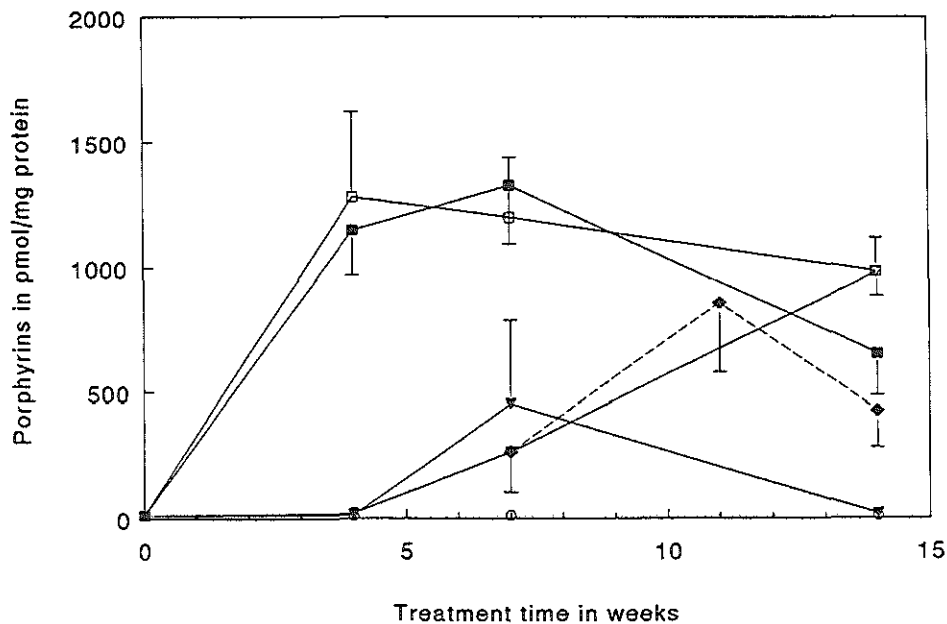


**Figure 3.**

Porphyrin content during the experimental period in liver tissue of C57BL/10 mice.

Open circles: Control group; Open triangles: Mice treated with iron dextran (IMF group); Closed triangles: Mice treated with IMF and desferrioxamine from the beginning of the experiment (IMF+DFx group); Open squares: Mice treated with hexachlorobenzene and IMF (HCB+IMF group); Closed squares: HCB+IMF+DFx group; Closed diamonds: Mice treated with IMF and DFX from week 7 (IMF+DFx7 group);

Values shown represent the means  $\pm$  SD.

#### 4.4.4 URO-D activity in liver tissue

Results of mean ( $\pm$  SD) URO-D activity (in percentages of values found in the control group) in liver tissue at the different time intervals are given in Figure 4.

At week 4, URO-D activity in the HCB+IMF group and in the HCB+IMF+DFx groups diminished to  $\pm$  15% of control group values. URO-D activity in livers of mice in the IMF+DFx and IMF+DFx7 groups showed an increase at week 14. A strong negative correlation, varying between -0.80 and -0.92, was found between liver porphyrin accumulation and liver URO-D activity data in all treatment groups.

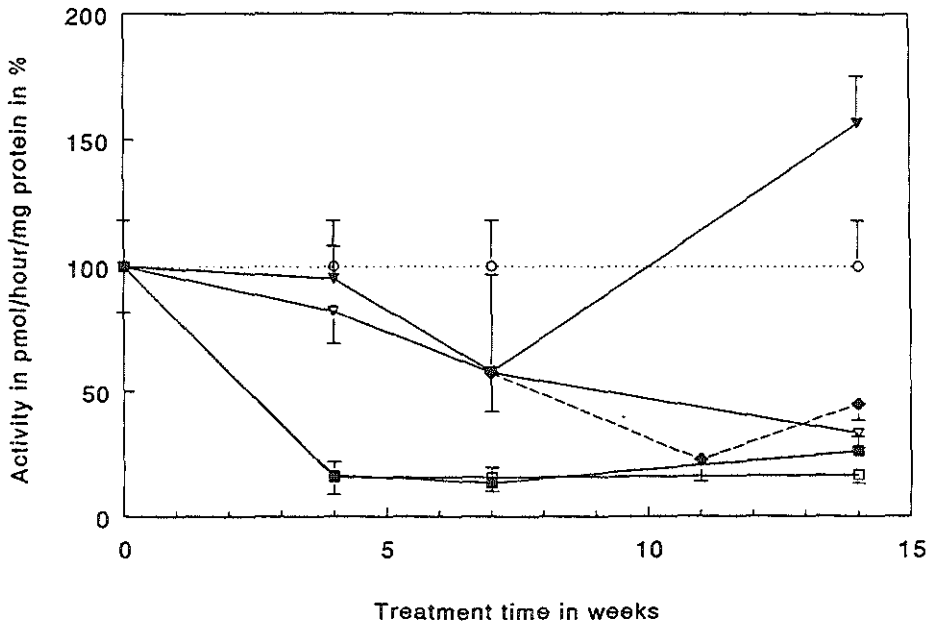


Figure 4.

Uroporphyrinogen decarboxylase activities (in percentages of values found in the control group) during the experimental period in liver tissue of C57BL/10 mice (100%:  $161 \pm 25$  pmol/mg protein/hour).

Open circles: Control group; Open triangles: Mice treated with iron dextran (IMF group); Closed triangles: Mice treated with IMF and desferrioxamine from the beginning of the experiment (IMF+DFx group); Open squares: Mice treated with IMF and hexachlorobenzene (HCB+IMF group); Closed squares: HCB+IMF+DFx group; Closed diamonds: Mice treated with IMF and DFX from week 7 (IMF+DFx7 group);

Values shown represent the means  $\pm$  SD.



#### 4.4.5 PBG-D activity in liver tissue

Results of mean ( $\pm$  SD) PBG-D activity (in percentages of values found in the control group) in liver tissue at the different time intervals are given in Figure 5.

PBG-D activities in the HCB+IMF group and in the HCB+IMF+DFx group, and to a lesser degree in the IMF group and in the IMF+DFx group, were increased over the 14-weeks observation period. At week 14, PBG-D activity was lower in the HCB+IMF+DFx group than in the HCB+IMF group ( $p < 0.01$ ), however, PBG-D activities in all treatment groups were still increased at that time.

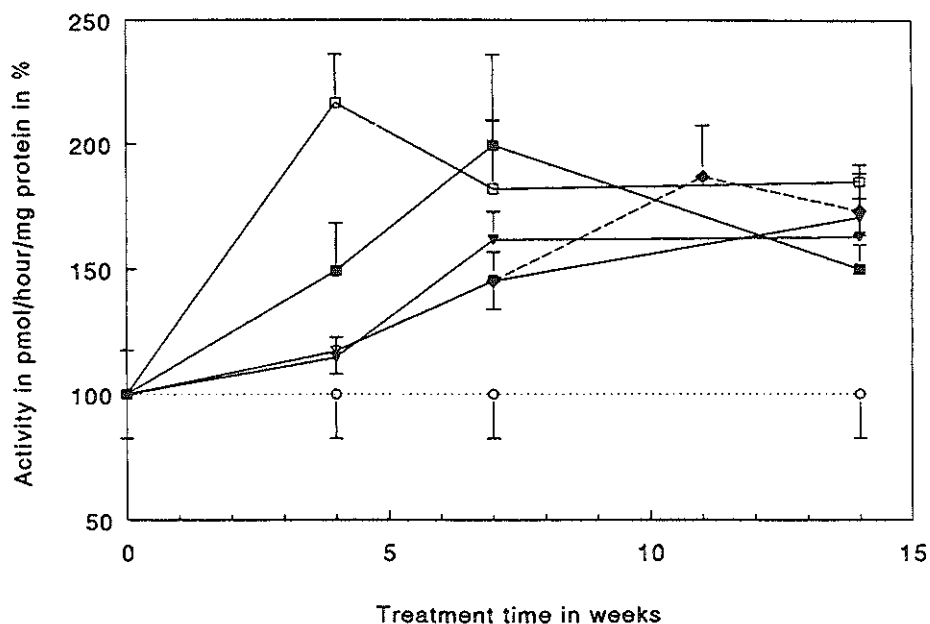


Figure 5.

Porphobilinogen deaminase activities (in percentages of values found in the control group) during the experimental period in liver tissue of C57BL/10 mice (100%:  $215 \pm 36$  pmol/mg protein/hour).

Open circles: Control group; Open triangles: Mice treated with iron dextran (IMF group); Closed triangles: Mice treated with IMF and desferrioxamine from the beginning of the experiment (IMF+DFx group); Open squares: Mice treated with hexachlorobenzene and IMF (HCB+IMF group); Closed squares: HCB+IMF+DFx group; Closed diamonds: Mice treated with IMF and DFx from week 7 (IMF+DFx7 group);

Values shown represent the means  $\pm$  SD.

#### 4.4.6 Low molecular weight iron in liver tissue

Results of mean ( $\pm$  SD) LMW iron measurements in liver tissue are given in Table 1. LMW iron measurements were performed in duplo samples, with 4-fold measurements per sample.

Both in the HCB+IMF group and in the IMF group, treatment with DFX resulted in a decreased amount of LMW iron in the liver. When treatment with DFX started at week 7, DFX reduced the amount of LMW iron also in livers of mice treated with HCB plus IMF (as compared with the non-DFX-treated mice) and in livers of mice treated with IMF alone (as compared with the non-DFX-treated mice). Results of LMW iron measurements in the HCB group were not different from the control group of mice.

In Figure 6, the results of the LMW iron measurements at week 11 were compared with data on MDA production at the same time. Calculations yielded a correlation coefficient of 0.84, thus indicating that both variables were interdependent.

**Table 1.**  
Low Molecular Weight iron measurements in liver tissue of C57BL/10 mice at 11 weeks.

Treatment group	Low molecular weight iron (in nmol/gm wet weight liver tissue)
Controls	86 $\pm$ 9
HCB	99 $\pm$ 22 <sup>a</sup>
HCB+IMF	190 $\pm$ 15 <sup>b</sup>
HCB+IMF+DFx	136 $\pm$ 9
HCB+IMF+DFx7	139 $\pm$ 26
IMF	121 $\pm$ 15 <sup>c</sup>
IMF+DFx	55 $\pm$ 13
IMF+DFx7	81 $\pm$ 17

HCB, hexachlorobenzene; IMF, iron dextran; DFX, desferrioxamine from the beginning of the experiment; DFX7, desferrioxamine from week 7;

<sup>a</sup> HCB group not different from control group;

<sup>b</sup>  $p < 0.005$  compared with all other groups;

<sup>c</sup>  $p < 0.01$  compared with the control group, the IMF+DFx group and the IMF+DFx7 group

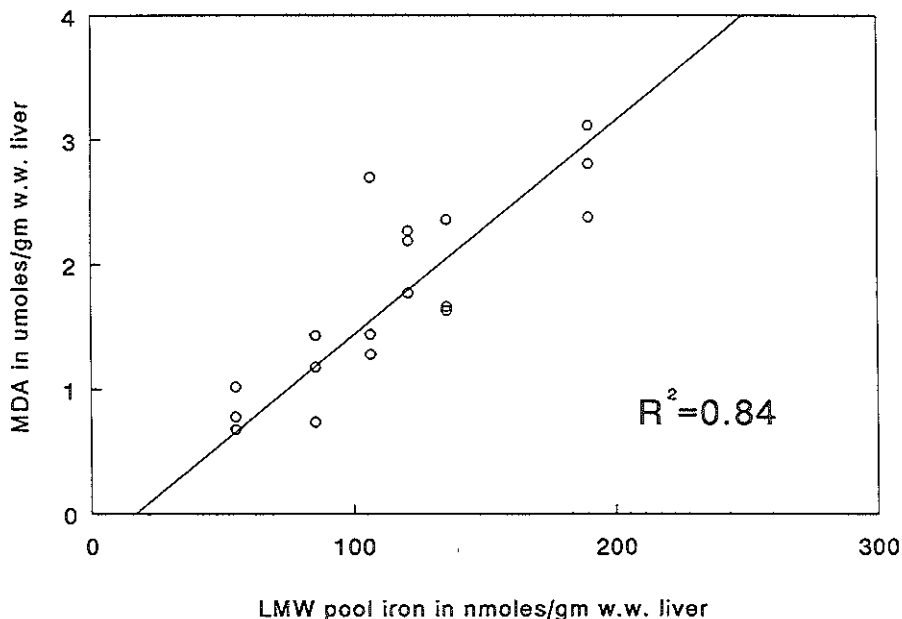


**Figure 6.**

Low molecular weight (LMW) iron concentrations in liver tissue compared with malondialdehyde (MDA) concentrations in liver tissue at 11 weeks.

Open circles represent individual results. Calculations yielded a correlation coefficient of 0.84.

#### 4.5 Discussion

We confirmed that treatment of C57BL/10 mice with HCB plus IMF, but also with IMF alone, resulted in the accumulation of (uro)porphyrins in the liver. Moreover, in this strain of mice, HCB alone did not produce uroporphyrin. These results point to an important role of iron in the pathogenesis of experimental uroporphyrin.

Two mechanisms for the role of iron in experimental uroporphyrin have been proposed.

(i) An oxygen-independent inhibition by direct interaction of iron ( $\text{Fe}^{2+}$ ) with essential sulphhydryl group(s) at the catalytic site(s) of the enzyme (95,96), and/or an oxygen-dependent inhibition, where iron (in the presence of an electron donor) is generating free

radicals, thereby (directly) damaging the URO-D enzyme (95).

(ii) An iron-mediated mechanism with the production of highly reactive oxygen-related free radicals by the Haber-Weiss reaction (151,152,181,191-198,225), which could react with uroporphyrinogen or another susceptible target to form an inhibitor of URO-D (183-186,200), thus explaining the accumulation of uroporphyrins in livers of C57BL/10 mice (191).

In addition, an iron-independent oxidation of uroporphyrinogen to uroporphyrin has been proposed (166,167,180-182,187). Because uroporphyrin is not a substrate for URO-D, accumulation of uroporphyrin results (188). However, this mechanism of uroporphyrinogen oxidation does not explain the inhibition of URO-D, that can be measured at the same time.

Experimental evidence for a direct (oxygen-independent) inhibitory effect of iron on URO-D activity has been obtained *in vitro*. Mukerji et al. (95,96) found that  $Fe^{2+}$  concentrations in the range of 0.1 - 1.0 mM reduced the activity of partially purified URO-D. Since Kozlov et al. (203) recently have demonstrated that it is unlikely that these  $Fe^{2+}$  concentrations can be met *in vivo*, it is not clear whether a direct interaction of ferrous iron with URO-D also occurs *in vivo*.

Oxygen-related free radicals can initiate a variety of reactions, such as the peroxidation of membrane lipids (199). The process of lipid peroxidation has been suggested to play a role in the pathogenesis of experimental uroporphyrinemia (152,196). In our experiments, treatment with HCB plus IMF, but also with IMF alone, resulted in an increased MDA production (as a marker of lipid peroxidation), which was maximal at 4 weeks, but was still significantly increased at 14 weeks (Figure 2).

Both treatment with HCB plus IMF and with IMF alone, resulted in porphyrin accumulation (Figure 3) and a decreased URO-D activity (Figure 4). The differences between the HCB+IMF group and IMF group in MDA production (Figure 2), porphyrin accumulation and URO-D activity were statistically significant for all results, except for those at 14 weeks ( $p < 0.004$ ). In contrast, liver iron accumulation (Figure 1) showed more or less equal results in both groups. These findings on iron accumulation and porphyrin accumulation in the HCB+IMF group and the IMF group were also found in the morphological and morphometrical study reported in Chapter 3.

The results support the suggestion that HCB stimulates the production of free radicals in

the presence of iron. In hepatocytes of C57Bl/10 mice, as a result of induction of CYP1A2 by PAH's (166,167), but also in mice treated with IMF alone on the basis of a genetically-determined mechanism, as suggested by Smith and de Matteis (191), an active oxidative metabolism has been proposed. If "free" iron is present, highly reactive oxygen-related free radicals could be formed by the Haber-Weiss reaction (151,152,181,191-198,225). HCB alone did not induce porphyrin accumulation in livers of C57Bl/10 mice (see also Chapter 3), neither did it affect the production of MDA (Figure 2). This might be due to the very low levels of total liver iron in non-treated animals (146,149,150).

Our results suggest that DFX reduced the amount of iron available for a catalytic role in the generation of free radicals. This is clearly demonstrated by the finding that MDA production at 14 weeks in the IMF+DFX group was significantly lower than in the IMF group ( $p < 0.001$ ), which could explain why URO-D activity was restored, despite the presence of an iron excess in the liver at that time (Figures 1,2,4). In the HCB+IMF+DFX group, it appeared that URO-D activity was slightly (however, not statistically significant) increased at 14 weeks compared with the non-DFX-treated mice at that time, but measurements over a longer period will be necessary to confirm this trend. Moreover, the LMW iron results (mean  $\pm$  SD in nmol/gm liver tissue) in the HCB+IMF+DFX group ( $136 \pm 9$ ) and in the IMF+DFX group ( $55 \pm 13$ ) were lower than those in the HCB+IMF group ( $190 \pm 15$ ) and IMF group ( $121 \pm 15$ ) respectively, and correlated closely with the data on MDA production (Figure 6). The discrepancy in LMW iron between the HCB+IMF group and the IMF group could be the result of a reductive release of iron from ferritin (the main storage form of iron in hepatocytes), due to the generation of reactive oxygen species by HCB (174,181,237).

There seemed to be a discrepancy between the results on MDA production and iron accumulation (Figures 1,2). After 4 weeks, MDA production decreased, while iron was still accumulating in the liver. It has been demonstrated in Chapter 3, that the transport of iron dextran from the injection site to the hepatocytes takes a considerable amount of time. However, once iron reaches the hepatocyte, ferritin synthesis is stimulated. It is reasonable to assume that ferritin synthesis will not be able to immediately accommodate this iron excess, since ferritin synthesis is a slow process, regulated by iron at the mRNA level (246). Iron storage in ferritin reduces the availability of catalytic iron for the generation of free radicals (235). Eventually, most iron will be stored in ferritin, but in

the meantime the amount of "free" iron (LMW iron) will probably be elevated, enhancing the generation of free radicals.

It was remarkable to find an increased PBG-D activity in livers of mice treated with HCB plus IMF and IMF alone (Figure 5). An increased PBG-D activity has also been reported in livers of patients with PCT (48,52). The mechanism of an increased PBG-D activity in experimental uroporphyrin (Figure 5) and in PCT (48,52) is not clear. Both HCB (247) and iron (248) have been demonstrated to increase the activity of the rate-limiting enzyme in the heme biosynthetic pathway, 5-aminolevulinic acid (ALA) synthase. This could result in an increased supply of ALA and porphobilinogen (PBG) (1,46). The enzyme PBG-D has been reported to be protected from degradation when the enzyme is bound to its substrate, PBG (249). An increased PBG-D activity could explain the absence of acute attacks in PCT. Moreover, an increased PBG-D activity could also provide an additional explanation for the marked uroporphyrin accumulation in experimental and human uroporphyrin.

These results support a mechanism of URO-D inactivation and uroporphyrin accumulation as a result of a free radical-mediated process. It is not clear whether this occurs directly by damage to URO-D itself (95,96), or indirectly, by the formation of an inhibitor of URO-D (due to free radical-mediated oxidation of uroporphyrinogen or another susceptible target) (183-186,200). However, the results on porphyrin accumulation, URO-D activity and PBG-D activity in the HCB+IMF+DFx group by 14 weeks could be indicative of the presence of an inhibitor of URO-D, for both the amount of porphyrins and the PBG-D activity were already significantly diminished ( $p < 0.001$ ), whereas URO-D activity was still markedly decreased at that time (compare Figures 3-5).

It is concluded that iron is an important factor, both in porphyrin accumulation and for a decreased URO-D activity, in livers of C57BL/10 mice. The effectiveness of DFx in reducing porphyrin accumulation is most likely the result of a reduction of LMW iron, thus diminishing the amount of iron available for a catalytic role in the generation of oxygen-related free radicals. An increased hepatic PBG-D activity could provide an additional explanation for the marked uroporphyrin accumulation. In the presence of free radicals, uroporphyrinogen or another compound, could be oxidated to an inhibitor of URO-D.

**PART B. PORPHYRIA CUTANEA TARDA**





## CHAPTER 5

### The Liver in Porphyria Cutanea Tarda: A Morphological and Morphometrical Study

Contents	page
5.1 Summary	74
5.2 Introduction	75
5.3 Materials & Methods	76
5.4 Results	77
5.5 Discussion	87

This chapter is based on:

Siersema PD, ten Kate FJW, Mulder PGH, Wilson JHP.  
Hepatocellular carcinoma in porphyria cutanea tarda: frequency and factors related to its occurrence.  
*Liver* 1992; 12: 56-61.

Siersema PD, van Helvoirt RP, Cleton-Soeteman MI, de Bruijn WC, Wilson JHP, van Eijk HG.  
The role of iron in experimental porphyria and porphyria cutanea tarda.  
*Biol Trace Elem Res* 1992; 35: 65-72.

Siersema PD, Cleton-Soeteman MI, Rademakers LHPM, ten Kate FJW, Marx JJM, de Bruijn WC,  
van Eijk HG, Wilson JHP.  
The liver in porphyria cutanea tarda: a morphological and morphometrical study.  
In preparation.

## 5.1 Summary

We collected follow-up data on 49 patients with porphyria cutanea tarda (PCT), who had been seen over a period of 20 years. Five of these patients (10%) developed a hepatocellular carcinoma (HCC) during this follow-up period. In this study, we analyzed the differences in clinical, laboratory and liver morphological findings obtained at presentation, between patients who developed HCC during follow-up (HCC-group, n=5) and those who did not (PCT-group, n=44). In addition, in 45 liver biopsies, the histology was re-examined. In livers of 8 patients, of whom 3 had familial PCT (F-PCT) and 5 had sporadic PCT (S-PCT), ultrastructural findings were compared and in livers of 13 patients, of whom 5 had F-PCT and 8 had S-PCT, a morphometrical analysis was performed to study the relationship between porphyrins and iron in hepatocytes.

Patients in the HCC-group had skin-symptoms for a longer period (mean:  $10.4 \pm 1.1$  years) than patients in the PCT-group (mean:  $1.8 \pm 1.2$  years) ( $p < 0.001$ ). No differences in routine laboratory findings were found. Although 15/49 (31%) patients had serologic evidence of a past hepatitis B virus infection and 9/49 (18%) patients had antibodies against hepatitis C virus, no differences in these parameters were found between the PCT-group and the HCC-group. Only piecemeal necrosis ( $p < 0.01$ ) and advanced fibrosis or cirrhosis ( $p < 0.001$ ) were more common in liver biopsies of the HCC-group.

Uroporphyrin crystals were detected in 15/45 (33%) liver biopsies. All patients had a variable degree of siderosis of the liver (PCT-group vs. HCC-group: NS; F-PCT patients vs. S-PCT patients: NS). The storage form of iron in hepatocytes was cytoplasmic ferritin and ferritin-like particles in lysosomal bodies. The amount and distribution of iron was not different between livers of F-PCT and S-PCT patients. Uroporphyrin crystals and ferritin iron were located in the same hepatocyte, often close to each other. The mean amount of uroporphyrin crystals to the mean amount of ferritin iron was increased in the F-PCT group compared with the S-PCT group of patients ( $p = 0.008$ ).

Conclusions: Liver biopsies of patients with PCT reveal a broad spectrum of lesions, ranging from minimal changes to HCC; factors related to an increased risk of HCC in PCT are a long symptomatic period before start of treatment and the presence of chronic-active hepatitis and/or advanced fibrosis or cirrhosis in liver biopsies; uroporphyrin crystals are formed in hepatocytes of PCT patients (either with F-PCT or S-PCT), in

which also iron accumulates; F-PCT increases the susceptibility to the effects of iron in comparison with S-PCT; these results suggest an important role for iron in the pathogenesis of familial and sporadic forms of PCT.

## 5.2 Introduction

Porphyria cutanea tarda (PCT) is a disorder of porphyrin metabolism, characterized by a decreased activity of uroporphyrinogen decarboxylase (URO-D) and an overproduction of porphyrinogens, primarily uroporphyrinogens and heptacarboxylporphyrinogens, in the liver (1,46). Familial and sporadic forms of PCT have been described. In familial PCT (F-PCT), liver and extrahepatic URO-D activities are about 50% of normal (2,4,24). The enzymatic defect is inherited as an autosomal-dominant trait. In the sporadic form of PCT (S-PCT), the enzyme defect is restricted to the liver and a decreased URO-D activity is only detected in the symptomatic phase (3,24).

Possession of the enzyme defect in F-PCT is not enough to produce clinically-overt porphyria. Inheritance of the enzyme defect leads to clinical expression in only a minority of affected individuals (2,4,24). Similarly in S-PCT, URO-D activity in livers may remain low during clinical remission (3,24). Therefore, interaction between the hepatic enzyme defect and other factors seems necessary for PCT to become clinically-manifest. The most frequently incriminated agents are: ethanol (54,55,58), estrogens (63,64) and iron. Of these factors, iron has attracted most attention. Most PCT patients have increased hepatic iron stores: a variable degree of hepatic siderosis has been reported in 72-100% of patients with PCT (54,70-76).

Histological and ultrastructural [light microscopy (LM) and electron microscopy (EM)] studies of liver tissue in PCT have revealed a broad spectrum of lesions ranging from minimal changes to cirrhosis (54,70,73,74,76,116-119). An increased frequency of hepatocellular carcinoma (HCC) has been described in PCT (126,127,130-132), but this has not been confirmed in all series (54,70,74,76,123,133). Of the morphological findings, only the presence of needle-like structures in hepatocytes, representing uroporphyrin crystals (73), is characteristic (73,116-123). In PCT, one LM study investigated the histological relationship between porphyrins and iron in livers, reporting that there was no correlation between areas with porphyrin fluorescence and areas with stainable iron (226).

Clinical features and laboratory findings, obtained at presentation, were available in 49 patients with PCT, seen during the previous 20 years. In 45 patients, a liver biopsy was performed. When 5/49 (10%) patients developed a HCC during follow-up, we analyzed whether there were differences in the parameters, obtained at presentation, between patients who developed HCC during follow-up, and those who did not.

In addition, in the liver biopsies, the histology was re-examined systematically, the ultrastructural findings were compared and a morphometrical analysis was performed to study the relationship between iron and uroporphyrins in hepatocytes of PCT patients, either with F-PCT and S-PCT.

### 5.3 Materials & Methods

From 1973 to 1992, 49 patients were seen with symptomatic PCT in the Academical Hospitals of Rotterdam and Utrecht, of whom 44 developed no HCC (PCT-group, n=44) and 5 developed HCC (HCC-group, n=5) during this follow-up period. In 24/44 patients of the PCT-group and in 2/5 patients of the HCC-group, indirect erythrocyte URO-D activity was measured. Of these 26 patients, 7/26 (27%) had F-PCT and 19/26 (73%) had S-PCT. Both of the 2 tested HCC patients were found to have S-PCT. A diagnosis of F-PCT was based on a positive family history and an indirect URO-D activity >2.80. A diagnosis of S-PCT was based on a negative family history and an indirect URO-D activity comparable to controls (51). All patients presented with characteristic skin-symptoms (bullae, skin fragility, hypertrichosis and pigmentary changes). At presentation, routine clinical chemistry laboratory results were obtained and serum from all patients was stored at -70 °C. Since assays for hepatitis B virus (HBV) and hepatitis C virus (HCV) only became available in recent years, stored serum samples were used for these determinations. In 45 patients, a percutaneous liver biopsy was performed at presentation. In these 45 liver biopsies, the histology was re-examined systematically. In liver biopsies of 8 patients, of whom 3 had F-PCT and 5 had S-PCT, ultrastructural findings were compared and in liver biopsies of 13 patients, of whom 5 had F-PCT and 8 had S-PCT, a morphometrical analysis was performed. Treatment resulted in a clinical remission in all patients. Therefore, liver biopsies were not repeated. Only in 4 of the 5 patients, who developed HCC during the follow-up period, the diagnosis of HCC was confirmed with a repeated liver biopsy. In the 5th patient a diagnosis of HCC was suspected, which was

based on: a) increasing levels of  $\alpha$ -fetoprotein; b) a space occupying lesion in the liver at abdominal ultrasound and computerized axial tomography, and c) the histology of a vertebral tumour, consistent with a metastasis of HCC.

The methods of the biochemical measurements and the morphological observations have been described in Chapter 2, paragraphs 2.2.3, 2.2.13, 2.2.14, 2.3, 2.4 and 2.5.

## 5.4 Results

### 5.4.1 Clinical findings

The clinical findings of all patients are summarized in Table 1.

The follow-up time in all patients ranged from 1 to 19 years (mean:  $8.0 \pm 5.9$  years). HCC was detected after 1.5, 5.5, 7, 8 and 9 years, respectively.

Of the clinical findings, only the symptomatic period was longer in patients of the HCC-group ( $n=5$ ) than in patients of the PCT-group ( $n=44$ ). The clinical findings were not different between F-PCT ( $n=7$ ) and S-PCT ( $n=19$ ) patients (results not shown).

Table 1.

Clinical findings at presentation in patients with porphyria cutanea tarda, who developed no hepatocellular carcinoma (HCC) (PCT-group;  $n=44$ ) and in patients who developed HCC (HCC-group;  $n=5$ ) during follow-up.

Clinical finding	PCT-group (%)	HCC-group (%)	p-value*
Sex (Male/Female)	27/17	4/1	NS
Age (mean years $\pm$ SD)	$49.2 \pm 14.1$	$53.8 \pm 4.3$	NS
Symptomatic period (mean years $\pm$ SD)	$1.8 \pm 1.2$	$10.4 \pm 1.1$	<0.001
Symptom-provoking factors:			
Ethanol (>60 g/day)	30/44 (69%)	5/5 (100%)	NS
Estrogens	5/44 (11%)		
Ethanol + Estrogens	5/44 (11%)		
No factor identified	4/44 (9%)		
Therapy:			
Phlebotomy	26/44 (60%)	5/5 (100%)	NS
Phlebotomy + Chloroquine	8/44 (18%)		
Chloroquine	5/44 (11%)		
Other	5/44 (11%)		

\* p-value: comparing PCT-group with HCC-group

### 5.4.2 Biochemistry

Table 2 shows the amount and percentage of abnormal results of the excretion of urinary porphyrins and the routine clinical chemistry results.

Serum levels of ferritin were increased in 41/49 (84%) patients with PCT [in 6/7 (86%) F-PCT patients and in 16/19 (84%) S-PCT patients]. Of all patients with PCT, 11/49 (22%) had serum ferritin levels of >500 ng/ml and 8/49 (16%) had serum ferritin levels of >1000 ng/ml.

Treatment succeeded in normalization of the biochemical features in all patients. When HCC was detected,  $\alpha$ -fetoprotein levels were found to be increased in 4 of the 5 patients in the HCC-group.

Statistical analysis (with the absolute values) did not show a difference in any of these

**Table 2.**  
Biochemical features at presentation in patients with porphyria cutanea tarda who developed no hepatocellular carcinoma (HCC) (PCT-group; n=44) and in patients who developed HCC (HCC-group; n=5) during follow-up.

Laboratory test	PCT-group (%)	HCC-group (%)	p-value <sup>a</sup>
Urinary porphyrins †	44/44 (100%)	5/5 (100%)	NS
Bilirubin †	13/44 (30%)	1/5 (20%)	NS
AST †	28/44 (64%)	3/5 (60%)	NS
ALT †	28/44 (64%)	3/5 (60%)	NS
gamma-GT †	32/44 (73%)	4/5 (80%)	NS
AP †	13/44 (30%)	1/5 (20%)	NS
Iron †	31/44 (70%)	4/5 (80%)	NS
Tf sat †	24/44 (55%)	3/5 (60%)	NS
Ferritin †	37/44 (84%)	4/5 (80%)	NS
AFP †	0/44 (0%)	0/5 (0%)	NS

†, increased serum levels; AST, aspartate transferase; ALT, alanine transferase; gamma-GT, gamma-glutamyl transpeptidase; AP, alkaline phosphatase; Tf sat, transferrin saturation; AFP,  $\alpha$ -fetoprotein;

<sup>a</sup> p-value: comparing (absolute) values in PCT-group with HCC-group

Table 3.

Serologic markers of hepatitis B virus and of hepatitis C virus infection at presentation in patients with porphyria cutanea tarda who developed no hepatocellular carcinoma (HCC) (PCT-group; n=44) and in patients who developed HCC (HCC-group; n=5) during follow-up.

Serologic marker	PCT-group (%)	HCC-group (%)	p-value <sup>a</sup>
HBsAg positive	0/44 (0%)	0/5 (0%)	NS
anti-HBs positive <sup>b</sup>	12/44 (27%)	1/5 (20%)	NS
anti-HBc positive	13/44 (30%)	2/5 (40%)	NS
anti-HCV positive <sup>c</sup>	8/44 (18%)	1/5 (20%)	NS

HBsAg, hepatitis B surface antigen; anti-HBs, antibodies against HBsAg; anti-HBc, antibodies against hepatitis B core antigen; anti-HCV, antibodies against hepatitis C virus;

<sup>a</sup> p-value: comparing PCT-group with HCC-group;

<sup>b</sup> Patients who were anti-HBs positive, were also anti-HBc positive;

<sup>c</sup> Patients who were anti-HCV positive, were also anti-HBs and anti-HBc positive

laboratory findings between the PCT-group and the HCC-group and between F-PCT and S-PCT patients (results of F-PCT and S-PCT patients not shown).

Table 3 shows the presence of serologic markers of HBV (HBsAg, anti-HBs, anti-HBc) and HCV (anti-HCV) infection.

Patients who had antibodies against HCV, had also serological evidence of a past HBV infection. In none of the patients was evidence found of a persistent HBV infection.

With respect to the serological markers, no differences were found between the PCT-group and the HCC-group and between patients with F-PCT and S-PCT (results of F-PCT and S-PCT patients not shown).

#### 5.4.3 Light microscopy

Table 4 summarizes the histological findings in the 45 biopsies, obtained at presentation. Uroporphyrin crystals could be detected in 15/45 (33%) biopsies (Figure 1). Piecemeal necrosis was found in 11/40 (27%) biopsies of the PCT-group (to a mild degree in all biopsies) and in all 5 biopsies of the HCC-group (in 1 biopsy to a marked degree and in the other 4 to a mild degree) ( $p < 0.01$ ). The presence of advanced fibrosis or cirrhosis correlated with the presence of piecemeal necrosis ( $p < 0.05$ ), as well as with a long symptomatic period ( $p < 0.005$ ). Histological evidence of a chronic HBV infection (ground

Table 4.

Histologic findings at presentation in patients with porphyria cutanea tarda who developed no hepatocellular carcinoma (PCT-group; n=40) and in patients who developed HCC (HCC-group; n=5) during follow-up.

Histologic finding	PCT-group (%)	HCC-group (%)	p-value*
Liver fluorescence	40/40 (100%)	5/5 (100%)	NS
Uroporphyrin crystals	14/40 (35%)	1/5 (20%)	NS
Fibrosis grade 0	13/40 (32%)	0/5 (0%)	<0.001
grade 1	17/40 (44%)	0/5 (0%)	
grade 2	7/40 (17%)	0/5 (0%)	
grade 3	3/40 (7%)	2/5 (40%)	
grade 4 (cirrhosis)	0/40 (0%)	3/5 (60%)	
<i>Portal tract:</i>			
Portal inflammation:			
-absent	9/40 (23%)	0/5 (0%)	NS
-mainly lymphocytes	28/40 (70%)	3/5 (60%)	
-mainly PMN's	3/40 (7%)	2/5 (40%)	
Piecemeal necrosis	11/40 (27%)	5/5 (100%)	<0.01
Lymph follicle formation	5/40 (13%)	1/5 (20%)	NS
Bile duct abnormalities	7/40 (17%)	1/5 (20%)	NS
<i>Lobular area:</i>			
Liver cell necrosis	13/40 (32%)	3/5 (60%)	NS
Kupffer's cell proliferation	19/40 (48%)	3/5 (60%)	NS
Ceroid pigment in Kupffer's cells	11/40 (28%)	2/5 (40%)	NS
Mallory's hyaline bodies	6/40 (15%)	1/5 (20%)	NS
Steatosis grade 0	10/40 (25%)	0/5 (0%)	NS
grade 1	13/40 (32%)	3/5 (60%)	
grade 2	16/40 (40%)	2/5 (40%)	
grade 3	1/40 (3%)	0/5 (0%)	
Siderosis grade 0	0/40 (0%)	0/5 (0%)	NS
grade 1	8/40 (20%)	1/5 (20%)	
grade 2	20/40 (50%)	3/5 (60%)	
grade 3	9/40 (23%)	0/5 (0%)	
grade 4	3/40 (7%)	1/5 (20%)	
Dysplasia	6/40 (15%)	2/5 (40%)	NS

PMN's, polymorphonuclear leucocytes;

\* p-value: comparing PCT-group with HCC-group

glass hepatocytes) was not found in any of the 45 biopsies. Antibodies against HCV correlated with the presence of follicular lymphocytic aggregates ( $p < 0.001$ ) and with bile duct abnormalities in the portal tracts ( $p < 0.01$ ). The amount and distribution of the



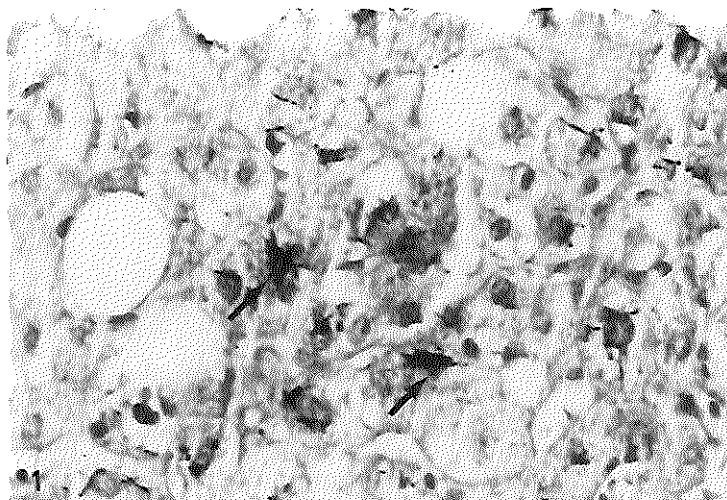


**Figure 1.**

Light micrograph (ferric ferricyanide reduction test in Lillie's modification; x 560) of liver biopsy material of a patient with sporadic porphyria cutanea tarda. Note the presence of uroporphyrin crystals (*arrows*).

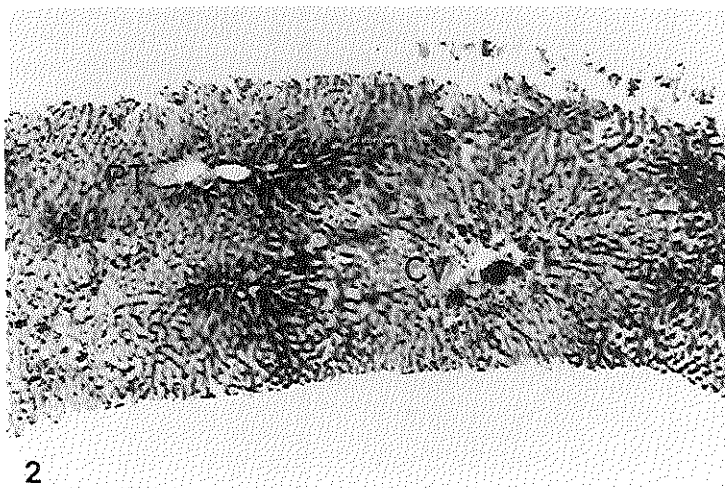


**Figure 2.**

Light micrograph (Perls' Prussian blue stain; x 50) of liver biopsy material of a patient with familial porphyria cutanea tarda. Note the staining (indicating ferric iron) in the (peri-)portal, midzonal and centrilobular areas of the liver.

PT, Portal Tract; CV, Central Vein

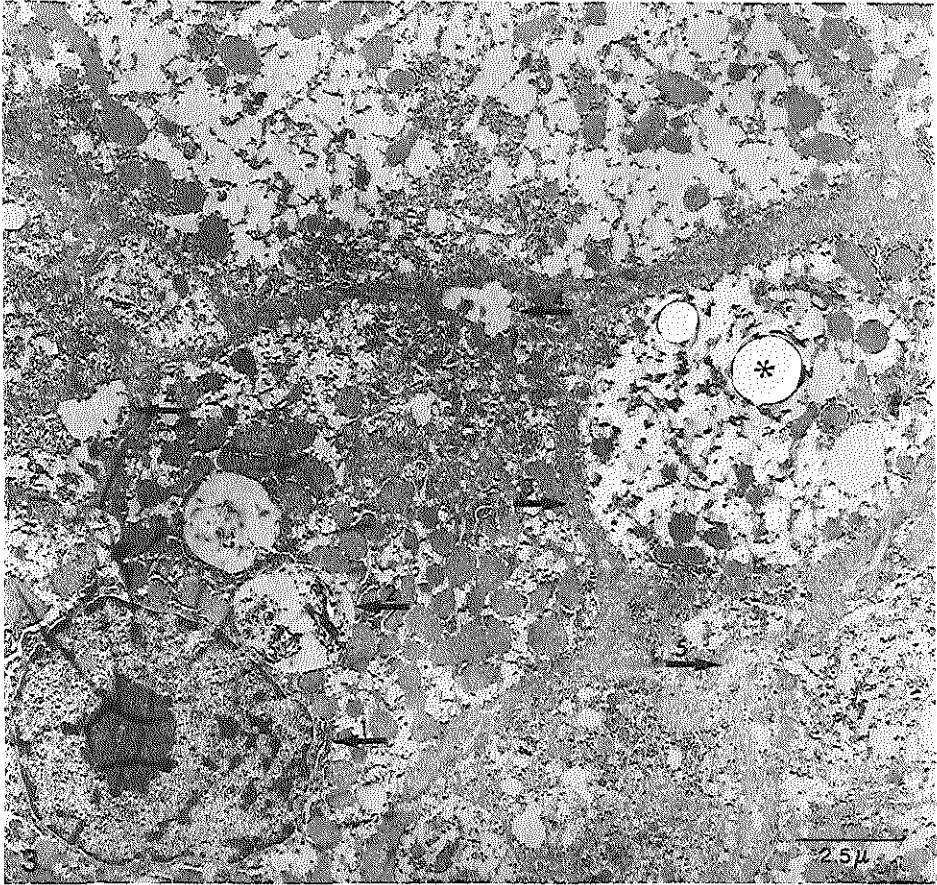


**Figure 3.**

Electron micrograph (electron spectroscopic image (ESI) of a stained section; bar= 2.5  $\mu$ m) of hepatic parenchymal cells of a patient with sporadic porphyria cutanea tarda. Note the following ultrastructural changes: 1. a heterochromatic nucleus; 2. lipid droplets; 3. the thickening of lateral cell membranes; 4. the loss of microvilli in the bile canaliculi; and 5. the presence of collagen fibres.

\*, hole in section

steatosis was not different between biopsies of the PCT-group and the HCC-group. Siderosis was present in all liver biopsies (Figure 2), however, there was no difference in the localization and distribution of the siderosis between biopsies of the PCT-group and the HCC-group. In the 41 biopsies, in which it could be determined, the distribution of

the siderosis was mainly periportal in 22 (siderosis grade 1 and 2 in all biopsies) and diffuse in 19 biopsies (siderosis grade 2 in 6 biopsies and siderosis grade 3 or 4 in the remainder of biopsies). The localization of the siderosis in all 45 biopsies was mainly hepatocellular in 30, mainly in Kupffer's cells in 5, and both hepatocellular and in Kupffer's cells in 10 biopsies. Increased serum ferritin levels correlated with the grade of siderosis in liver biopsies ( $p < 0.05$ ).

In 4 of the 5 patients of the HCC-group, a diagnosis of HCC was confirmed with a repeated liver biopsy. In 3 of these biopsies, "normal" and "malignant" liver tissue was evaluable. Neither in "normal", nor in "malignant" liver tissue was fluorescence or siderosis found.

The histologic findings were not different between livers of patients with F-PCT and with S-PCT (results of F-PCT and S-PCT patients not shown).

#### 5.4.4 *Electron microscopy*

Ultrastructural findings were studied in liver biopsies of 3 F-PCT patients and 5 S-PCT patients.

In sections of all 8 liver biopsies, different degrees of ultrastructural alterations were detected (Figures 3-5), such as: indented heterochromatic nuclei, mitochondria with paracrystalline inclusions, swollen rough endoplasmic reticulum, vesicular smooth endoplasmic reticulum, interdigitation of lateral cell membranes, widened intercellular spaces sometimes containing collagen fibres, flattened microvilli in the bile canalicular region, lipofuscin pigment and an increased amount of glycogen rosettes. In hepatocytes of all 8 liver biopsies, an increased amount of lipid droplets was present.

Iron in hepatocytes of all 8 liver biopsies was seen as cytoplasmic ferritin and as clustered ferritin particles. In hepatocytes of most patients, iron was also present in lysosomes. Moreover, some lysosomes contained less tightly-packed ferritin-like particles and amorphous non-iron electron-dense material without recognizable structure (Figures 4,5). The iron or non-iron nature of this material in lysosomes was confirmed by electron energy-loss spectroscopic imaging (see paragraph 2.4).

Uroporphyrin crystals were located in hepatocytes, either "free" in the cytoplasm or in vacuoles. In conventionally-prepared sections, "ghosts" of uroporphyrin crystals were found. Ferritin clusters were found close to uroporphyrin crystals in all patients (Figure 5).

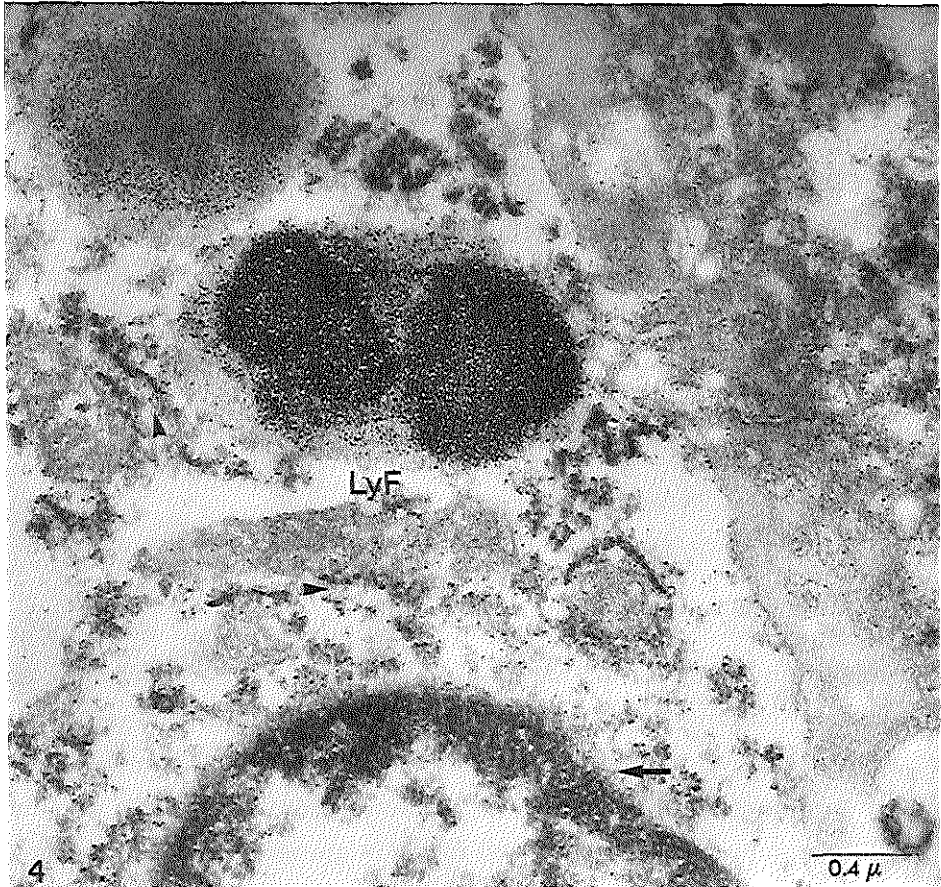


**Figure 4.**

Electron micrograph (electron spectroscopic image (ESI) of a stained section; bar= 0.4  $\mu\text{m}$ ) of a hepatic parenchymal cell of a patient with familial porphyria cutanea tarda, showing a heterochromatic nucleus (*arrow*) and dilatation of the endoplasmic reticulum (*arrowheads*). Note the difference in density of lysosomal ferritin accumulation (LyF).

In conclusion, although our results showed different degrees of alterations in the hepatocyte cellular ultrastructure, no differences were observed between liver biopsies of F-PCT and S-PCT patients.

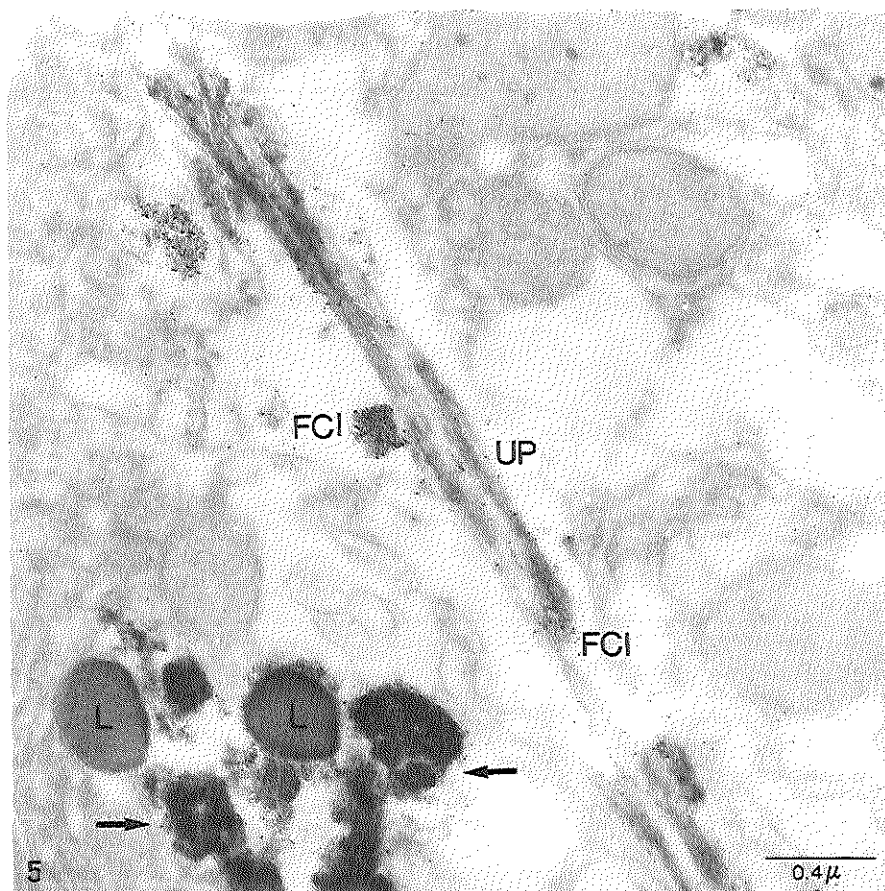


**Figure 5.**

Electron micrograph (electron spectroscopic image (ESI) of an unstained section; bar =  $0.4 \mu\text{m}$ ) of a hepatic parenchymal cell of a patient with sporadic porphyria cutanea tarda, showing a uroporphyrin crystal (UP) surrounded by ferritin clusters (FCI). Note the presence of lysosomal ferritin-like material (*arrows*) and lipid droplets (L).

#### 5.4.5 Morphometrical analysis

The results of the morphometrical analysis in liver tissue of 5 patients with F-PCT and 8 patients with S-PCT are shown in Figure 6. As can be seen from this figure, an increased mean ( $\pm$  SD) area fraction (expressed as percentages of the total measured

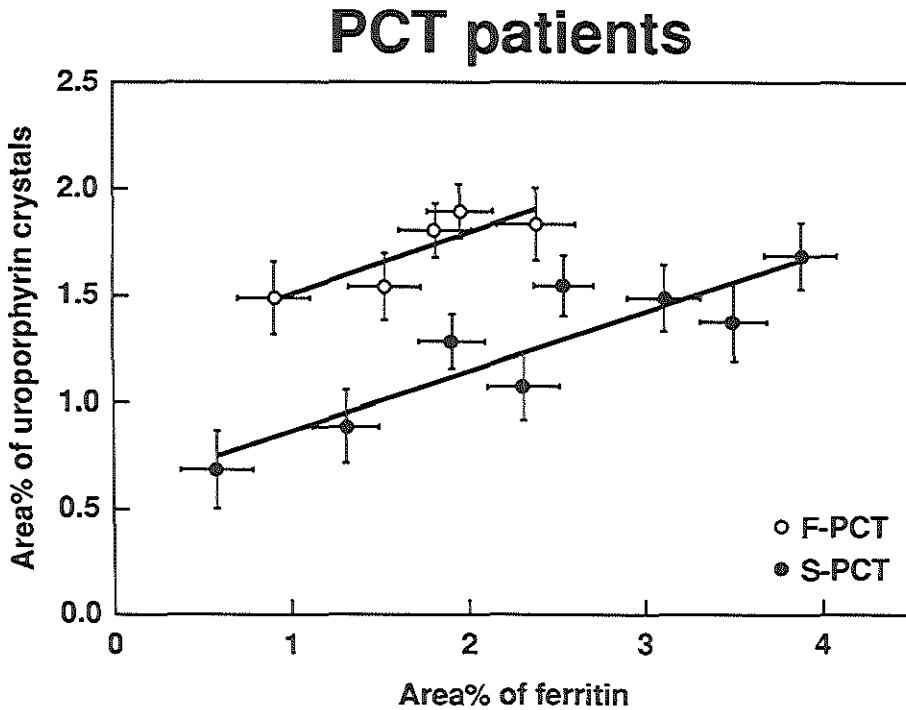


Figure 6.

Morphometrical analysis by reflection contrast microscopy of unstained, thin Epon sections, showing the relationship between mean ( $\pm$  SD) area fractions of ferritin iron and mean ( $\pm$  SD) area fractions of uroporphyrin crystals. The mean area fractions are expressed as percentages (%) of the total measured hepatocyte cytoplasmic frame area (25 areas of  $8,100 \mu\text{m}^2$ ) in patients with familial (F-PCT) and sporadic (S-PCT) forms of porphyria cutanea tarda.

hepatocyte cytoplasmic frame area) of ferritin iron was associated with an increased mean ( $\pm$  SD) area fraction of uroporphyrin crystals in both groups of PCT patients. Mean area fractions of ferritin iron were not different between livers of F-PCT patients and S-PCT patients. However, mean area fractions of uroporphyrin crystals were higher in livers of patients with F-PCT ( $1.62 \pm 0.28$ ) than in livers of patients with S-PCT ( $0.98 \pm 0.23$ ) ( $p = 0.008$ ).

## 5.5 Discussion

Five of the 49 (10%) patients with PCT developed HCC. This is in accordance with findings of Salata et al. (126), who described the development of HCC in 16% of PCT patients. In other studies (130,131), the risk of HCC in PCT patients varied between 39% and 47%, however, in these studies, risks were calculated on the basis of autopsies, which were performed in only a minority of PCT patients.

Much emphasis has been laid on the importance of different causes of liver disease on the development of HCC. Since histological evidence of cirrhosis is found in up to 90% of cases of HCC, it has become clear that cirrhosis *per se*, rather than the causative agent of cirrhosis is an important risk factor for HCC (250). In this study, in all biopsies of the HCC-group (obtained before evidence of HCC was present), advanced fibrosis or cirrhosis was found, while at most advanced fibrosis was found in only 3/40 (7%) biopsies of the PCT-group ( $p < 0.001$ ). Moreover, all biopsies of the HCC-group showed piecemeal necrosis, while this was present in only 11/40 (27%) biopsies of the PCT-group ( $p < 0.01$ ).

Piecemeal necrosis is the hallmark for a diagnosis of chronic-active hepatitis, whatever its cause. Cirrhosis is usually the end-stage of chronic-active hepatitis, particularly, if the causative agent persists (251). In PCT, several causes probably contributed to the presence of chronic-active hepatitis in livers of these patients, including ethanol, HBV, HCV, siderosis and perhaps porphyrinogens themselves. However, in our study, no correlation was found between any of these causes and histological (Table 4) or ultrastructural changes (Figures 3-5) in liver biopsies. Only the symptomatic period was longer in the group of patients that developed a HCC than in the group of patients that did not ( $p < 0.001$ ). A long symptomatic period correlated with the presence of advanced fibrosis or cirrhosis in liver biopsies. Therefore, it is speculated that a combination of causes, being present over a long period, caused advanced fibrosis or cirrhosis in livers of PCT patients with HCC. This could have resulted in the development of HCC.

Serologic markers of a past infection with HBV were found in 15/49 (31%) PCT patients. This has been described before in PCT (54,124-127), however, in some of these studies, patients were also positive for HBsAg. In this study, none of the patients had serological or histological evidence of a persistent HBV infection. Antibodies against HCV were detected in 9/49 (18%) patients. The reason for the high percentages of past

HBV infection (31%) and antibodies against HCV (18%) in our patients with PCT is not clear and needs further elucidation.

All liver biopsies, examined directly after biopsy with ultraviolet light, showed fluorescence, consistent with the presence of porphyrinogens. It has been described that prolonged contact of liver biopsy material with water should be avoided to preserve uroporphyrin crystals in liver tissue (116,120). This could explain why uroporphyrin crystals were detected by LM in only 15/45 (33%) liver biopsies. Morphologically, uroporphyrin crystals were randomly distributed in hepatocytes of patients with F-PCT and S-PCT. All patients in this study had a variable degree of liver siderosis. In other studies, siderosis of the liver in PCT varied between 72% and 100% (54-70-76). In iron-storage disorders, independent of the etiology, siderosis is found predominantly in hepatocytes, and to a lesser degree in Kupffer's cells. Moreover, with advanced stages of iron-overload, stainable iron-deposits in parenchymal cells are deposited progressively in the periportal, the midzonal, and centrilobular areas of the liver lobulus (252,253). These findings are in agreement with our results on localization and distribution of siderosis in PCT. The storage form of iron in hepatocytes was cytoplasmic ferritin and ferritin-like particles in lysosomal bodies (Figures 4,5) (253,254). The amount and distribution of iron was not different between livers of F-PCT and S-PCT patients.

Petryka et al. (225) were not able to demonstrate iron staining and porphyrinogen fluorescence in the same hepatocyte in livers of patients with PCT. They concluded that certain cells preferentially accumulate either porphyrinogens or iron. In contrast to their findings, we observed in hepatocytes of PCT patients that uroporphyrin crystals and ferritin iron were located in the same hepatocyte. Moreover, uroporphyrin crystals were often found close to ferritin iron (Figure 5). An increased mean area fraction of ferritin iron was associated with an increased mean area fraction of uroporphyrin crystals in each cytoplasmic area. A striking finding was that the mean area fractions of uroporphyrin crystals were significantly higher in livers of F-PCT patients ( $1.62 \pm 0.28$ ) than in livers of S-PCT patients ( $0.98 \pm 0.23$ ) ( $p = 0.008$ ) (Figure 6). These results suggest an important role for iron in the pathogenesis of PCT. Investigations on the interactions of ferrous or ferric iron with preparations of URO-D from human and other mammalian tissues have shown inhibition (93-97), activation (98) or no effect (35,99,100). Elder et al. (101) measured URO-D activities and URO-D enzyme concentrations in liver tissue of



S-PCT and F-PCT patients. In S-PCT, patients in remission following phlebotomy had normal URO-D activities and URO-D protein concentrations, whereas in symptomatic patients before phlebotomy, URO-D activities were decreased and URO-D protein concentrations increased. In F-PCT, patients in remission following phlebotomy had 50% reduced URO-D activities and URO-D protein concentrations, with a further fall in activities of URO-D and a slight increase in URO-D protein concentrations in symptomatic patients. An inherited defect of URO-D, as in F-PCT, is clearly an important factor in determining susceptibility, but is not sufficient by itself to produce overt PCT. In S-PCT, genetic factors may also play a role, but these are not clearly defined (29,101). However, in both forms, clinically-overt PCT is possibly precipitated by an iron-dependent process, which inactivates the active site(s) of URO-D molecule(s) in the liver (102). Whether this is a direct effect of iron on URO-D is not clear. The increased mean amount of uroporphyrin crystals to the mean amount of ferritin iron in livers of F-PCT patients compared with that found in livers of S-PCT patients (Figure 6), is a good example of the interaction between genetic susceptibility and another factor (in this case iron). Moreover, the fact that iron overload by itself does not lead to uroporphyrin in all humans (1,92) and the findings of the morphometrical analysis (Figure 6) suggest that even in F-PCT an extra factor, in addition to iron, might be involved.

The exact mechanism involved in the development of cirrhosis in PCT patients has not yet been elucidated. However, it seems feasible that iron plays an important role in this process. In addition, treatment should start before irreversible liver damage (i.e., cirrhosis) has occurred. Similar findings have been described in hemochromatosis in which iron by itself is not the cause of HCC, however, once cirrhosis has developed, phlebotomy does not reduce the risk of HCC (255). The most important therapeutic option in PCT is phlebotomy or treatment with desferrioxamine, which leads to clinical and biochemical remission (5,71,75,77-80).



**CHAPTER 6****Porphobilinogen Deaminase Activity in Erythrocytes of Patients with Porphyria Cutanea Tarda**

<b>Contents</b>	<b>page</b>
6.1 Summary	92
6.2 Introduction	92
6.3 Materials & Methods	95
6.4 Results	95
6.5 Discussion	97

This chapter is based on:

Siersema PD, de Rooij FWM, Edixhoven-Bosdijk A, Wilson JHP.  
Erythrocyte porphobilinogen deaminase activity in porphyria cutanea tarda.  
*Clin Chem* 1990; 36: 1779-1783.

Siersema PD, de Rooij FWM, Edixhoven-Bosdijk A, Wilson JHP.  
The activity of erythrocyte porphobilinogen deaminase in familial and sporadic forms of porphyria cutanea tarda.  
In: Vermeer BJ, Wuepper KD, van Vloten WA, Baart de la Faille H, van der Schroeff JG (eds):  
Metabolic disorders and nutrition correlated with the skin.  
*Curr Probl Dermatol* 1991; 20: 116-122.

## 6.1 Summary

Porphyria Cutanea Tarda (PCT) is due to a metabolic block in the biosynthesis of heme at the level of uroporphyrinogen decarboxylase (URO-D), leading to the urinary excretion of uroporphyrins and heptacarboxylporphyrins. To determine whether an increased production of uroporphyrinogens, in addition to the reduced conversion of uroporphyrinogens to coproporphyrinogens by URO-D, contributes to these high levels, the activity of one of the preceding enzymes in the heme pathway, porphobilinogen deaminase (PBG-D), was measured in erythrocytes of 23 patients with the familial form of PCT (F-PCT) and 24 patients with the sporadic form of PCT (S-PCT), either symptomatic or asymptomatic.

Erythrocyte PBG-D activity was increased in all four patient groups compared with controls. To study the mechanism of this increased PBG-D activity, the amount of immuno-detectable PBG-D per 100 units standard PBG-D activity (Ig PBG-D/100 U) and the total amount of immuno-detectable PBG-D (Ig PBG-D) in erythrocytes, using polyclonal antibodies, were determined in all patients and in controls. Both in F-PCT and S-PCT patients, the Ig PBG-D/100 U was decreased ( $p < 0.05$ ). Especially in asymptomatic patients of the F-PCT group, there was an inverse correlation between increasing PBG-D activity and Ig PBG-D/100 U ( $R^2 = -0.90$ ). In F-PCT patients, and to a minor degree in S-PCT patients, the increase in PBG-D activity was accompanied by an increase in Ig PBG-D (F-PCT:  $p < 0.001$ ; S-PCT:  $p < 0.05$ ).

Conclusions: In patients with F-PCT and S-PCT, an increased erythrocyte PBG-D activity can, at least partly, be explained by a diminished degradation of PBG-D; in patients with F-PCT, in symptomatic more than in asymptomatic patients, and to a minor degree in patients with S-PCT, there is in addition an increase in the absolute amount of PBG-D enzyme.

## 6.2 Introduction

Porphyria cutanea tarda (PCT) is a disorder of porphyrin metabolism which usually presents in adult life with photosensitivity. The disease is characterized by the excretion of uroporphyrins and heptacarboxylporphyrins in the urine and by a decreased activity of the enzyme catalyzing the conversion of uroporphyrinogen to coproporphyrinogen, uroporphyrinogen decarboxylase (URO-D), in the liver (1,46). Sporadic and familial

forms of PCT have been distinguished. In sporadic PCT (S-PCT), a decreased URO-D activity is restricted to the liver and is not detectable in erythrocytes. There is no family history of PCT (3,24). Familial PCT (F-PCT) is transmitted as an autosomal-dominant disorder and the enzymatic defect is apparently present in all tissues (2,4,24). Clinical disease is produced when hepatic siderosis (54,70-76) and/or another disease-precipitating factor such as high ethanol-intake (54,55,58), estrogen-use (63,64) or ingestion with polyhalogenated aromatic hydrocarbons (66,68,69) is present.

Normally, the sequence of enzymatic reactions in the heme biosynthetic pathway proceeds with little or no accumulation of enzyme substrates (Figure 1). However, reduced activity at any enzyme step can lead to accumulation of that enzyme's substrate,

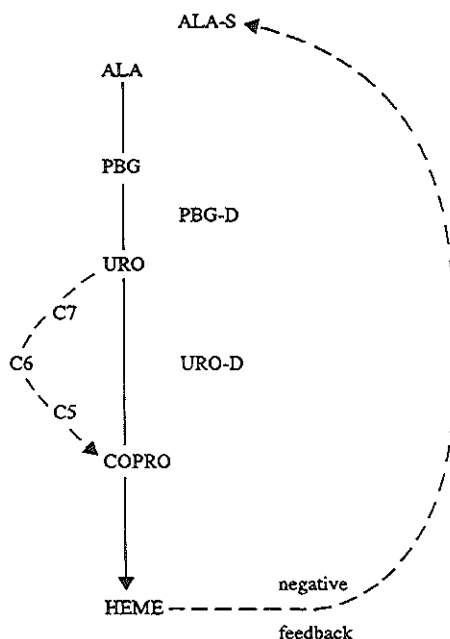


**Figure 1.**

The heme biosynthetic pathway with special reference to porphyria cutanea tarda.

ALA-S, 5-aminolevulinic acid synthase; PBG-D, porphobilinogen deaminase; URO-D, uroporphyrinogen decarboxylase; ALA, 5-aminolevulinic acid; PBG, porphobilinogen; URO, uroporphyrinogen; C7, heptacarboxylporphyrinogen; C6, hexacarboxylporphyrinogen; C5, pentacarboxylporphyrinogen; COPRO, coproporphyrinogen

because decreased production and concentration of the end-product heme, will lead to the induction of the first enzyme, 5-aminolevulinic acid synthase (ALA-S), and an increased production of porphyrin precursors (1).

Two enzymes in the heme pathway, ALA-S and porphobilinogen deaminase (PBG-D), have low activities compared to the remaining enzymes (Figure 1) (1). In all porphyrias, the rate-limiting enzyme ALA-S is increased (1,47). In patients with forms of porphyria associated with an acute attack (acute intermittent porphyria, hereditary coproporphyria, variegate porphyria and 5-aminolevulinic acid (ALA) dehydratase deficiency), induction of ALA-S is associated with an increased excretion of ALA and porphobilinogen (PBG); i.e., PBG-D forms a partial metabolic block (1). In PCT, however, plasma ALA and PBG levels are slightly increased (1,48) and PCT is not associated with acute attacks of neurological dysfunction.

Some authors have reported an increased PBG-D activity in erythrocytes (49-52) and in livers (48,52) of patients with PCT. However, most of these studies did not discriminate between patients with F-PCT or S-PCT or between symptomatic and asymptomatic uroporphyria. In addition, in Chapter 4, an increased PBG-D activity was demonstrated in livers of porphyric C57BL/10 mice. An increased PBG-D activity in PCT and in experimental uroporphyria could provide an additional explanation for the marked uroporphyrin accumulation observed in these disorders.

For this reason, we studied erythrocyte PBG-D activity in F-PCT and S-PCT patients, both in the symptomatic (before phlebotomy) and asymptomatic (following phlebotomy) phase. When we found an increased erythrocyte PBG-D activity in both F-PCT and S-PCT patients, we extended the study to examine the mechanism of this increase in enzyme activity.

In erythrocytes, PBG-D is still active even after long storage at -20 °C. Under normal conditions during the lifetime of an erythrocyte, a part of this PBG-D is degraded and is no longer catalytically-active, although it is still immuno-detectable. In this study, this has been called "Ig PBG-D/100 U", which is the amount of immuno-detectable PBG-D per 100 units of standard PBG-D activity. In other publications (208,210,256), this has been called "cross-reacting immune material". Conditions which result in a relatively diminished PBG-D degradation result in higher levels of catalytically active PBG-D, and therefore a decrease in the Ig PBG-D/100 U in erythrocytes.

To study whether a change in erythrocyte PBG-D activity is somehow related to changes in PBG-D degradation, Ig PBG-D/100 U was determined in both groups of PCT patients and in control subjects. Apart from this, we also determined the total amount of immunodetectable PBG-D (Ig PBG-D) in all four patient groups and in controls.

### 6.3 Materials & Methods

Observations were made in 23 patients with F-PCT (based on a positive family history, skin-symptoms and a characteristic pattern of porphyrins produced from PBG by hemolysates (indirect URO-D activity) (51), 12 with characteristic skin-symptoms and an increased urinary excretion of uroporphyrins and heptacarboxylporphyrins before phlebotomy (Fsym), and 11 symptom-free following phlebotomy and a normal urinary excretion of porphyrins (Fasym). In addition, 24 patients with S-PCT (based on a negative family history, skin-symptoms and an indirect URO-D activity comparable to controls) were studied, 12 with characteristic skin-symptoms before phlebotomy (SPsym) and an increased urinary excretion of uroporphyrins and heptacarboxylporphyrins, and 12 symptom-free following phlebotomy and a normal urinary excretion of porphyrins (SPasym). Sixty individuals without liver disease served as controls.

The methods of the biochemical determinations have been described in Chapter 2, paragraphs 2.2.1, 2.2.3, 2.2.5, 2.2.6 and 2.2.7.

### 6.4 Results

Male/female ratios and mean ( $\pm$  SD) ages in the different patient groups and in the control subjects were as follows: Fsym: 7/5,  $49 \pm 16$ ; Fasym: 8/3,  $52 \pm 17$ ; SPsym: 8/4,  $60 \pm 10$ ; SPasym: 8/4,  $64 \pm 14$ ; and controls: 49/21,  $41 \pm 21$ . These parameters were not different between the different group of patients and controls.

#### 6.4.1 *Porphyrins in urine*

The results of the urinary porphyrin measurements are given in Table 1.

The urine analysis of both F-PCT and S-PCT patients with symptoms (before phlebotomy) showed the pattern of PCT with a predominant increase in urinary uroporphyrins and heptacarboxylporphyrins. Patients, who were treated by phlebotomy and without symptoms, showed a normal rate of urinary excretion of porphyrins.

Table 1.

Uroporphyrins and heptacarboxylporphyrins in urine and the corresponding erythrocyte indirect uroporphyrinogen decarboxylase activity in porphyria cutanea tarda (PCT).

Group	URINARY <sup>a</sup>			ERYTHROCYTE <sup>b</sup>		
	C7	URO	URO	C7	COPRO	URO+C7/ COPRO
Fsym	27	58	34.9 ± 9.8	14.4 ± 5.6	14.2 ± 5.9	>2.80
Fasym	0.9	3.1	27.0 ± 4.2	11.2 ± 1.4	10.5 ± 1.8	>2.80
SPsym	43	88	20.2 ± 4.0	9.1 ± 2.1	14.2 ± 3.7	<2.80
SPasym	0.6	2.6	20.6 ± 5.3	9.3 ± 2.3	15.3 ± 3.8	<2.80
Controls	<3.2	<4.0				<2.80

Fsym, familial PCT with symptoms; Fasym, familial PCT without symptoms; SPsym, sporadic PCT with symptoms; SPasym, sporadic PCT without symptoms; C7, heptacarboxylporphyrin; URO, uroporphyrin; URO+C7/COPRO, uroporphyrin + heptacarboxylporphyrin/ coproporphyrin;

<sup>a</sup> mean values in nmol/mmol creatinine

<sup>b</sup> mean values (± SD) in pmol/mg protein/hour

#### 6.4.2 Indirect URO-D activity in erythrocytes

The indirect URO-D activity of patients with F-PCT showed an increased erythrocyte uroporphyrin + heptacarboxylporphyrin/ coproporphyrin ratio of >2.80, whereas in patients with S-PCT this ratio was <2.80 (51) (Table 1).

#### 6.4.3 PBG-D activity in erythrocytes

The results of mean (± SD) PBG-D activity in erythrocytes of patients with F-PCT and S-PCT and in the controls were as follows: Fsym: 136 ± 12, Fasym: 111 ± 16, SPsym: 99 ± 17, SPasym: 97 ± 18 and controls: 80 ± 14. PBG-D activity was higher in all PCT patients than in controls (Fsym, Fasym and SPsym: p <0.001, SPasym: p <0.005). PBG-D activity was higher in the Fsym group of patients than in both groups of S-PCT patients (p <0.005) (Figure 2).

#### 6.4.4 Immuno-detectable PBG-D/100 units PBG-D activity in erythrocytes

Figure 2 illustrates PBG-D activity, Ig PBG-D/100 U and Ig PBG-D in the patients with F-PCT and with S-PCT and in controls. In both groups of F-PCT and S-PCT patients,



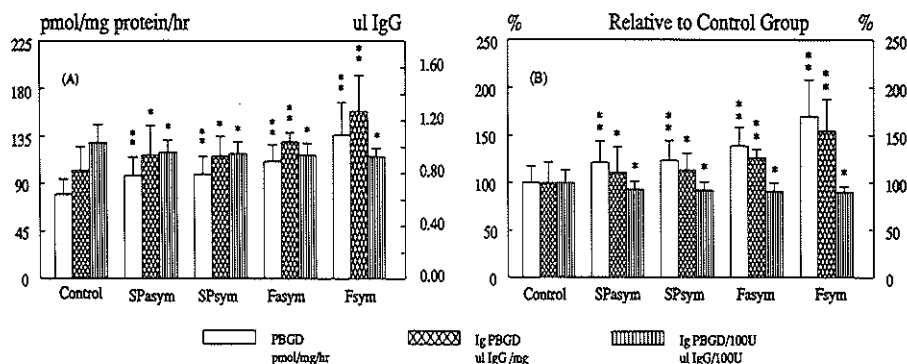


**Figure 2.**

The bars (left to right) depict porphobilinogen deaminase (PBGD) activity in pmol/mg protein/hr, the total amount of immuno-detectable PBG-D per mg protein (Ig PBGD) in  $\mu\text{l}$  IgG/mg protein and the amount of immuno-detectable PBG-D per 100 units of PBG-D activity (Ig PBGD/ 100 U) in  $\mu\text{l}$  IgG/100 U in erythrocytes of controls and in patients with sporadic (SPasym and SPsym) and familial (Fasym and Fsym) porphyria cutanea tarda; (a) in absolute amounts and (b) relative to the control group.

\*  $p < 0.05$ ; \*\*  $p < 0.001$

Ig PBG-D/100 U was less than in controls ( $p < 0.05$ ).

Figure 3 illustrates the individual relation between PBG-D activity and Ig PBG-D/100 U in all four groups of PCT patients and in controls. Especially in the Fasym group, there was a strong inverse correlation ( $R^2 = -0.90$ ) between individual increasing PBG-D activity and decreasing Ig PBG-D/100 U.

#### 6.4.5 Total immuno-detectable PBG-D in erythrocytes

Ig PBG-D was found to be increased in patients with F-PCT ( $p < 0.001$ ). In S-PCT patients, Ig PBG-D was only slightly increased ( $p < 0.05$ ). In Fsym patients, Ig PBG-D was more increased than in Fasym patients ( $p < 0.01$ ) (Figure 2).

## 6.5 Discussion

After the initial enzyme of the heme biosynthetic pathway, ALA-S, PBG-D has the next lowest endogenous activity of all eight enzymes in the heme pathway of the liver and some

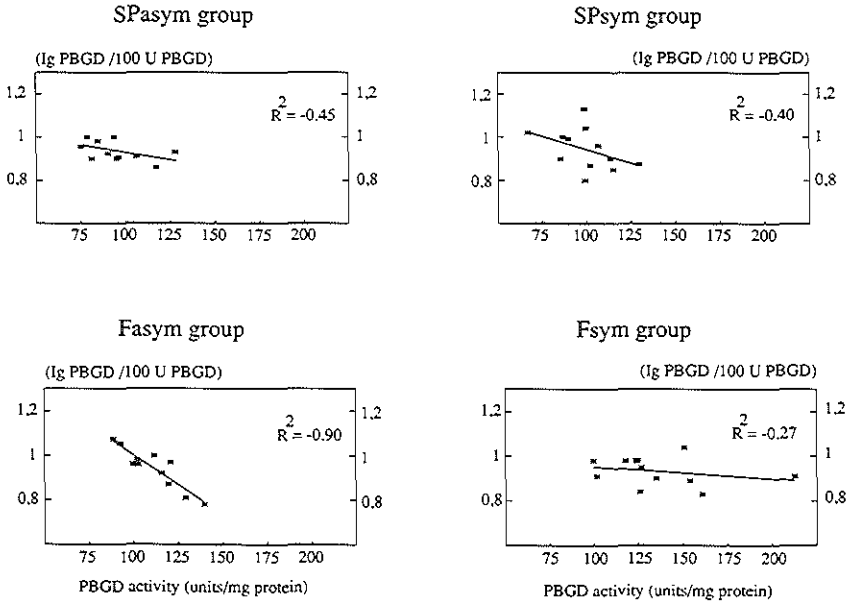


**Figure 3.** Relation between porphobilinogen deaminase (PBGD) activity in pmol/mg per hour and the amount of immuno-detectable PBG-D per 100 units of PBG-D activity (Ig PBGD/100 U PBGD) in  $\mu$ l of IgG/100 U in individuals with sporadic (SPasym and SPsym) and familial (Fasym and Fsym) PCT. In all four patient groups, the correlation coefficient ( $R^2$ ) is indicated.

other tissues (Figure 1) (1). This makes PBG-D a possible second control point in the heme biosynthetic pathway (50).

This study demonstrated an increased erythrocyte PBG-D activity in F-PCT and S-PCT patients, both symptomatic and asymptomatic, compared with controls (Figure 2). Apart from an increased erythrocyte PBG-D activity (49-52), an increased PBG-D activity in liver cells has been described in PCT (48,52). Moreover, in Chapter 4, an increased PBG-D activity was demonstrated in livers of porphyric C57BL/10 mice. An increased

PBG-D activity could provide an explanation for the absence of acute attacks in PCT, but also for the marked uroporphyrin accumulation observed in this disorder.

An increased erythrocyte PBG-D activity has been found in patients with liver cirrhosis (257), in patients with lymphoreticular malignancies (258) and also in reticulocytosis (259). Results of liver function tests (bilirubin, alkaline phosphatase and aminotransferases) were, however, within normal limits in our asymptomatic patients (results not shown). In addition, reticulocytosis has not been described in PCT and reticulocyte counts were normal in our patients.

To our surprise, we found an increased erythrocyte PBG-D activity, both in symptomatic and asymptomatic patients with PCT, but also in S-PCT patients. S-PCT has been described to be confined to the liver, and a 50% reduction of URO-D activity in the liver has been reported only in the symptomatic phase of the disorder (3,24). An increased PBG-D activity in erythrocytes can either be due to decreased rates of inactivation of PBG-D enzyme, or to an increased amount of PBG-D enzyme protein.

Results of Ig PBG-D/100 U were found to be slightly decreased in both groups of patients with sporadic PCT ( $p < 0.05$ ) (Figure 2); especially in the Fasym group, there was a strong inverse correlation between an increasing activity of PBG-D and a decreasing Ig PBG-D/100 U in individual patients ( $R^2 = -0.90$ ) (Figure 3). These findings suggest that both in S-PCT and in F-PCT patients, an increased erythrocyte PBG-D activity can be explained, at least partly, by diminished degradation of PBG-D enzyme.

The mechanism of this proposed diminished degradation is not clear, however, it can be speculated that in erythroid cells of PCT patients there is a small but increased production of the substrate of PBG-D, i.e., PBG. This seems likely because the rate-limiting enzyme, ALA-S, is increased in erythroid (1) and liver (47) cells of patients with PCT. Also, plasma ALA and PBG have been found to be slightly increased in PCT (1,48). These observations suggest an increased supply of PBG in erythroid cells, initiated by diffusion of ALA from plasma. PBG-D reportedly is protected from degradation when the enzyme is bound to its substrate, PBG (249). Therefore, it is proposed that in PCT an increased amount of PBG is bound to PBG-D, protecting the enzyme from degradation, which leads to a diminished Ig PBG-D/100 U.

Apart from a diminished degradation of PBG-D enzyme in PCT, there was, in addition in F-PCT patients, and to a minor degree in S-PCT patients, an increased total amount of

immuno-detectable PBG-D in erythrocytes present (Figure 2). At the molecular level, there is a single PBG-D gene, which has two promoters, one housekeeping and one erythroid-specific, which yield two different exons by virtue of different splicing. The raised levels found both in erythrocytes (49-52, this study) and in livers (48,52) of patients with PCT suggest that, whatever mechanism is responsible for increased PBG-D activity in PCT, it might operate on both the erythroid and housekeeping gene products and could therefore be a post-translational phenomenon (260). However, the precise mechanism of the increase in enzyme protein is not clear and needs further elucidation.

**CHAPTER 7****General Discussion and Summary**

<b>Contents</b>	<b>page</b>
7.0 Introduction	102
7.1 Experimental uroporphyrin	102
7.2 Porphyria cutanea tarda	106
7.3 Conclusions	108
7.4 Future research	109

## 7.0 Introduction

Porphyria cutanea tarda (PCT) is the most common form of all porphyrias and is characterized by photosensitivity of the skin. The underlying disorder is an overproduction of uroporphyrins and heptacarboxylporphyrins due to a reduced activity of the enzyme which converts uroporphyrinogen to coproporphyrinogen, uroporphyrinogen decarboxylase (URO-D), in the liver (2-4,24). Familial and sporadic forms of PCT have been described. In familial PCT (F-PCT), liver and extrahepatic URO-D activities are about 50% of normal (2,4,24). The enzymatic defect is inherited as an autosomal-dominant trait. In sporadic PCT (S-PCT), the enzyme defect is restricted to the liver and a decreased URO-D activity is only detected in the symptomatic phase (3,24).

Following an outbreak of human uroporphyrin in Turkey, the fungicidal agent hexachlorobenzene (HCB), a polyhalogenated aromatic hydrocarbon (PAH), was shown to induce hepatic uroporphyrin in rodents (68). HCB-induced uroporphyrin is associated with a low hepatic URO-D activity and the accumulation of uroporphyrins and heptacarboxylporphyrins in the liver (140). The biochemical and clinical manifestations are similar to those of sporadic forms of PCT (3,24). Different species and strains vary remarkably in their susceptibility to the porphyrinogenic effects of PAH's (46), and a genetic predisposition of some kind has also been suspected in S-PCT (29). Both in HCB-induced uroporphyrin (97,146-153) and in S-PCT (5,54,70-83), the condition is aggravated by iron overload, while iron deficiency (whether induced by phlebotomy or by treatment with desferrioxamine) prevents the overproduction of porphyrinogens in both conditions. In view of the similarities between experimental HCB-induced uroporphyrin and human S-PCT, HCB-induced uroporphyrin has been used as an appropriate experimental model for the human condition.

### 7.1 Experimental uroporphyrin

C57BL/10 mice have been described to be susceptible to the porphyrinogenic effects of HCB (164). To examine the interactions between treatment with HCB, iron overload and porphyrin accumulation, the rates of accumulation of ferritin iron and of formation of uroporphyrin crystals were examined in livers of C57BL/10 mice, which were treated with HCB, iron dextran (IMF) or the combination of HCB plus IMF, over a period of 52 weeks. A time-dependent increase in total iron content and in the formation of

uroporphyrin crystals was observed in hepatocytes of mice treated with HCB plus IMF, but also in hepatocytes of mice treated with IMF alone. However, uroporphyrin crystal formation started more rapidly in livers of mice treated with HCB plus IMF than in livers of mice treated with IMF alone. In contrast, only a few uroporphyrin crystals were observed in hepatocytes of mice treated with HCB alone. Ferritin iron accumulation preceded the formation of uroporphyrin crystals in hepatocytes of mice treated with HCB plus IMF and with IMF alone. Moreover, uroporphyrin crystals were nearly always found close to ferritin iron in all treatment groups.

Evidence on the role of HCB in experimental uroporphyrin suggests that the drug acts as an inducer of cytochrome P-450IA2 (CYP1A2) (166,167). Subsequently, it interacts with the induced cytochrome to produce an active oxidative metabolism (191). The results in Chapters 3 and 4 clearly demonstrated that uroporphyrin in livers of C57BL/10 mice can also be induced by iron-overload alone. Therefore, induction of the cytochrome P-450 system by HCB, or another PAH, is not an absolute requirement for the development of uroporphyrin.

The effect of iron in experimental uroporphyrin has been explained by its ability to participate in iron-catalyzed free radical-mediated processes. It has been suggested that there is a highly active oxidative metabolism in hepatocytes of C57BL/10 mice, either as a result of cytochrome P-450IA2 (CYP1A2) induction by PAH's (166,167), or genetically-determined in these mice, as suggested by Smith and de Matteis (191). If "free" iron is present, highly reactive oxygen-related free radicals could be formed by the Haber-Weiss reaction (151,152,181,191-198,225). It has been proposed that these free radicals could cause uroporphyrin accumulation and inhibition of URO-D by one of the following mechanisms (Figure 1):

- (i) Direct damage to URO-D by free radicals, generated in the presence of iron (95,96).
- (ii) The reaction of these reactive radicals with uroporphyrinogen or another (related) compound to form an inhibitor of URO-D (183-186,200).

In addition, an iron-independent oxidation of uroporphyrinogen to uroporphyrin has been proposed (166,167,180-182,187). Because uroporphyrin, in contrast to uroporphyrinogen, is not a substrate for URO-D, accumulation of uroporphyrin results (188). However, this mechanism does not explain the inhibition of URO-D, that can be measured at the same time (182-186).

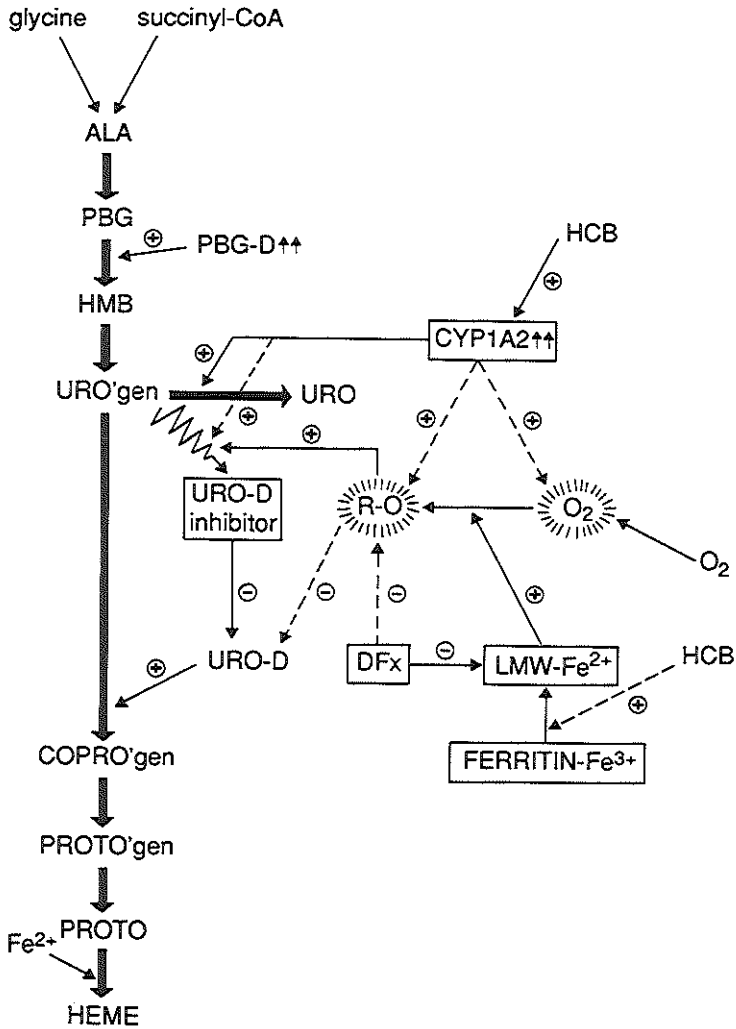


**Figure 1.** Hypothetical scheme of the different proposed mechanisms to explain the induction of experimental uroporphyrin.

—→, mechanism, for which firm experimental evidence has been obtained; - - -→, mechanism, for which no firm experimental evidence has been obtained; +, stimulation; -, inhibition; †, increased; ALA, 5-Aminolevulinic acid; PBG, Porphobilinogen; PBG-D, Porphobilinogen deaminase; HMB, Hydroxymethylbilane; URO'gen, Uroporphyrinogen; URO, Uroporphyrin; URO-D, Uroporphyrinogen decarboxylase; COPRO'gen, Coproporphyrinogen; PROTO'gen, Protoporphyrinogen; PROTO, Protoporphyrin; HCB, Hexachlorobenzene; CYP1A2, Cytochrome P-4501A2; R-O, Oxygen-related free radicals; DFX, Desferrioxamine; LMW, Low molecular weight



Of the postulated mechanisms, explaining uroporphyrin accumulation and URO-D inhibition in the liver, the iron-mediated oxidative mechanism (ii) has attracted most attention. Moreover, most experimental evidence is in favour of this mechanism (see paragraph 1.4.4.2).

Oxygen-related free radicals can initiate a variety of reactions, such as the peroxidation of membrane lipids (199). In a study over a period of 14 weeks, in which C57BL/10 mice were treated with HCB plus IMF and with IMF alone, an increased malondialdehyde (MDA) production (as a marker of lipid peroxidation), with concomitant porphyrin accumulation and a decreased URO-D activity, were measured in livers of these mice. Following treatment with desferrioxamine (DFx), an iron chelator, MDA production was significantly lower in livers of mice treated with DFx than in livers of mice that were not treated with DFx. This suggests that DFx probably complexed with the iron fraction available for the production of free radicals, thus restoring URO-D activity and reducing uroporphyrin accumulation in livers of mice treated with IMF alone and to a lesser degree in livers of mice treated with HCB and IMF, despite the presence of excess liver iron stores at that time.

The nature of the iron pool involved in experimental uroporphyrin is not clear. On the basis of the finding in Chapter 3 of a morphological co-occurrence of uroporphyrin crystals and ferritin iron in hepatocytes of porphyric C57BL/10 mice, a role for ferritin-bound iron seemed possible. However, ferric iron is sequestered in ferritin as a non-toxic oxyhydroxide, complexed with phosphate (235). Although liver microsomes, *in vitro*, promote the release of ferrous iron from ferritin (174,224,236-238), it is not clear whether this also occurs *in vivo*. An alternative to ferritin iron could be an intracellular pool of low molecular weight (LMW) iron (239-242). This LMW pool of iron has been shown to play a role in free radical formation in iron-loaded cells (212,243,244). In our study, LMW iron results were found to be increased in livers of mice treated with HCB plus IMF and with IMF alone. Treatment with DFx reduced the amount of LMW iron in both groups. Moreover, LMW iron measurements correlated well with MDA concentrations in all treatment groups ( $R^2 = 0.84$ ), suggesting that both variables were interdependent.

Porphobilinogen deaminase (PBG-D) is one of the enzymes which precedes URO-D in the heme biosynthetic pathway. PBG-D activity was found to be increased in livers of

mice treated with HCB plus IMF and in livers of mice treated with IMF alone. An increased hepatic PBG-D activity could provide an additional explanation for the marked uroporphyrin accumulation seen in experimental uroporphyrin, separate from the inhibition of URO-D.

Our studies support a free radical-mediated mechanism of URO-D inactivation and uroporphyrin accumulation. It is not clear whether this occurs directly by damage to URO-D itself (95,96), or indirectly, by the formation of an inhibitor of URO-D (183-186,200). However, our results on porphyrin accumulation, URO-D activity and PBG-D activity in livers of mice treated with HCB plus IMF and with DFX at week 14 could be indicative of the presence of an inhibitor of URO-D, for treatment with DFX resulted in a lowering of the PBG-D activity and the amount of porphyrins in the liver, at a time that URO-D activity was still markedly decreased (Figure 1).

Iron is an important factor in porphyrin accumulation and a decreased URO-D activity in C57BL/10 mice. Desferrioxamine's effectiveness in reducing porphyrin accumulation is most likely the result of a reduction of the LMW pool of iron, which is proposed to be the iron pool with a catalytic role in the generation of free radicals. Increased PBG-D activity provides an additional explanation for the marked uroporphyrin accumulation (Figure 1).

## 7.2 Porphyrin cutanea tarda

Histological examination of 45 liver biopsies of patients with PCT (either with F-PCT or with S-PCT) revealed a broad spectrum of lesions, ranging from minimal changes to liver cirrhosis. Moreover, 5 of the 49 patients (10%) developed a hepatocellular carcinoma (HCC) during the follow-up period. Factors related to an increased risk of HCC in PCT were a long symptomatic period before start of treatment and the presence of chronic-active hepatitis and/or advanced fibrosis or cirrhosis in liver biopsies.

Several causes probably contributed to the presence of chronic-active hepatitis in livers, including hepatitis B virus (HBV) infection, hepatitis C virus (HCV) infection, ethanol, siderosis and perhaps porphyrins themselves. Fifteen of the 49 (31%) patients had serologic evidence of a past HBV infection and 9/49 (18%) patients had antibodies against HCV. However, no correlation was found between any of these causes and histological and ultrastructural changes in liver biopsies.

In the 45 liver biopsies, the histology was re-examined. In addition, an ultrastructural study was performed in 8 liver biopsies of patients with PCT, of whom 3 had F-PCT and 5 had S-PCT and a morphometrical analysis was performed in 13 liver biopsies of patients with PCT, of whom 5 had F-PCT and 8 had S-PCT. Uroporphyrin crystals were detected in 15/45 (33%) liver biopsies. All patients in this study had a variable degree of liver siderosis (PCT-group vs. HCC-group: NS; F-PCT patients vs. S-PCT patients: NS). The storage form of iron in hepatocytes was cytoplasmic ferritin and ferritin-like particles in lysosomal bodies. The amount and distribution of iron was not different between livers of F-PCT and S-PCT patients. Uroporphyrin crystals and ferritin iron were located in the same hepatocyte, with uroporphyrin crystals often close to ferritin. Strikingly, mean area fractions of uroporphyrin crystals were significantly higher in livers of F-PCT patients than in livers of S-PCT patients ( $p = 0.008$ ).

Erythrocyte PBG-D activity was significantly increased in patients with F-PCT and with S-PCT, either symptomatic or asymptomatic. This increased erythrocyte PBG-D activity could be explained, partly by a diminished degradation of PBG-D and, partly by an increase in the absolute amount of PBG-D enzyme. Apart from an increased erythrocyte PBG-D activity, other investigators (48,52) have described an increased PBG-D activity in livers of PCT patients.

The results in Chapters 5 and 6 suggest an important role for iron and an increased PBG-D activity in the pathogenesis of the human form of uroporphyrin, PCT. Investigations on the interactions of ferrous or ferric iron with preparations of URO-D from human and other mammalian tissues have shown inhibition (93-97), activation (98) or no effect (35,99,100). Elder et al. (101) measured URO-D activities and URO-D enzyme concentrations in liver tissue of patients with S-PCT and F-PCT. In S-PCT, patients in remission following phlebotomy had normal URO-D activities and URO-D enzyme concentrations, whereas in symptomatic patients before phlebotomy, URO-D activities were decreased and URO-D enzyme concentrations increased. In F-PCT, patients in remission following phlebotomy had 50% reduced URO-D activities and URO-D enzyme concentrations, with a further fall in URO-D activities and a slight increase in URO-D enzyme concentrations in symptomatic patients. An inherited defect of URO-D, as in F-PCT, is clearly an important factor in determining susceptibility but is not sufficient by itself to produce overt PCT. In S-PCT, genetic factors may also play a role,

but these are not clearly defined (29,101). However, in both forms, clinically-overt PCT seems to be precipitated by an iron-dependent process which results in the inactivation of the active site(s) of the URO-D enzyme in the liver (102). In addition, it is likely that an increased PBG-D activity contributes to the uroporphyrin accumulation seen in PCT.

### 7.3 Conclusions

In this thesis, some important similarities in the biochemical manifestations of experimental and human uroporphyrin (PCT) were described. This was illustrated by the following observations:

(i) Both in experimental uroporphyrin and in PCT (either F-PCT or S-PCT), uroporphyrin was precipitated by an iron-dependent process.

a) A morphological co-occurrence of uroporphyrin crystals and ferritin iron was found in hepatocytes of porphyric C57BL/10 mice (Chapter 3) and in hepatocytes of patients with F-PCT and S-PCT (Chapter 5).

b) HCB has been described to induce uroporphyrin, as a result of induction of CYP1A2 (166,167), however, iron was an absolute requirement for uroporphyrin to develop. Moreover, uroporphyrin could also be induced by iron-overload alone in this strain of mice (Chapters 3 and 4). Similarly in PCT, an inherited defect of URO-D enzyme in F-PCT is an important factor in determining susceptibility, but clinically-overt PCT was caused by an iron-dependent process in livers of these patients (Chapter 5).

c) The role of iron in experimental uroporphyrin was further illustrated by the effectiveness of desferrioxamine to reduce porphyrin accumulation, probably by reducing the LMW pool of iron, thus diminishing the amount of iron available for a catalytic role (Chapter 4). In liver biopsies of PCT patients, advanced fibrosis or cirrhosis and the presence of HCC were only found in patients with a long symptomatic period before start of treatment, which suggested that treatment with phlebotomy or with DFX should start before irreversible liver damage has occurred (Chapter 5).

(ii) Both in livers of mice with experimental uroporphyrin (Chapter 4) and in erythrocytes of F-PCT and S-PCT patients (Chapter 6), the activity of one of the preceding enzymes in the heme biosynthetic pathway, PBG-D, was increased. An increased PBG-D activity could provide an additional explanation for the marked uroporphyrin accumulation observed in experimental uroporphyrin and in PCT.

## 7.4 Future research

On the basis of the results described in this thesis, two important issues remained unsolved:

### 1. Use of isolated hepatocyte cultures

a) In experimental uroporphyrin, accumulation of porphyrins and a reduced URO-D activity could be detected at the same time. However, whether URO-D inhibition was due to a direct interaction of iron with URO-D, or to the formation of an (iron-mediated) inhibitor of URO-D, is still not completely clear (Figure 1).

b) An increased PBG-D activity in PCT and in experimental uroporphyrin could provide an (additional) explanation for uroporphyrin accumulation in these disorders. It was found that this increased PBG-D activity could be explained by a diminished degradation of PBG-D enzyme and by an increase in the absolute amount of PBG-D enzyme. However, the precise mechanism of the increase in PBG-D activity is not clear. In addition, the role played by the rate-limiting enzyme of the heme pathway, 5-aminolevulinic acid synthase (ALA-S) and the other heme biosynthetic enzymes in PCT, needs further elucidation.

It has been suggested that an approach to investigate the mechanism of uroporphyrin in more detail, is to use cultures of isolated hepatocytes of C57BL/10 mice (261,262). Recently, Sinclair et al. (261) reported that hepatocytes of this strain of mice can be maintained in culture for a longer period if matrigel is used, which is a tumour biomatrix prepared from the Engelbroth-Holm-Swarm mouse tumour (263).

### 2. Antioxidants in uroporphyrin

In Chapter 4, an important role for oxygen-related free radicals in the pathogenesis of experimental (and human) uroporphyrin was suggested. If radical formation does play a role in the pathogenesis of uroporphyrin, antioxidants could, theoretically, modulate the disease process. Debets et al. (155) found, in *in vitro* experiments with chick embryo hepatocyte cultures, that antioxidants, such as DL- $\alpha$ -tocopherol and ascorbic acid, completely prevented HCB-induced porphyrin accumulation. However, vitamin E, given orally, did not prevent toxicity in rats (264). Further work is needed to determine whether hepatic injury in uroporphyrin can be prevented by oral antioxidants (152).



## CHAPTER 8

### Samenvatting (Summary in Dutch)

In deze dissertatie wordt een aantal experimentele en klinische studies beschreven, die de rol van ijzer en het enzym porfobilinogeen deaminase bij experimentele uroporfyrurie en porfyruria cutanea tarda beschrijven.

In *Hoofdstuk 1* werd een overzicht gegeven van de acht opéénvolgende enzymstappen, die nodig zijn voor de synthese van heem. Ook werden de verschillende vormen van porfyrurie besproken, die ontstaan als gevolg van een deficiëntie van één van deze enzymstappen. Vervolgens werd ingegaan op porfyruria cutanea tarda (PCT), een vorm van porfyrurie die gepaard gaat met huidsymptomen en ontstaat als gevolg van een deficiëntie van het enzym uroporfyrinogeen decarboxylase (URO-D). Hierdoor treedt in eerste instantie accumulatie van uroporfyrines en heptacarboxylporfyrines in de lever op, en vervolgens ook in de huid. In de urine kan de uitscheiding van deze porfyrines gemeten worden. PCT kan worden ingedeeld in een sporadische (verworven) en een familiale vorm. In de sporadische vorm van PCT (S-PCT) is een deficiëntie van URO-D slechts aanwezig in de lever en kan een deficiëntie van het enzym alleen worden aangetoond in de symptomatische fase van de aandoening. Daarnaast is er een autosomaal-dominant overervende vorm, familiale PCT (F-PCT), waarbij het enzymdefekt aanwezig is in alle weefsels, zowel in de periode mét als zonder huidsymptomen. Tenslotte werd ingegaan op een vergelijkbare metabole stoornis, n.l. uroporfyrurie dat door het insecticide hexachloorbenzeen (HCB) wordt geïnduceerd. Deze experimentele vorm van uroporfyrurie wordt gebruikt als een diermodel voor PCT om inzicht te krijgen in de pathogenese van PCT. Aan de hand van het overzicht in Hoofdstuk 1 werden de vraagstellingen van deze dissertatie besproken, n.l. de rol van ijzer en het enzym porfobilinogeen deaminase bij het ontstaan en klinisch manifest worden van experimentele uroporfyrurie en PCT.

In *Hoofdstuk 2* werden de patienten en de behandeling van de gebruikte proefdieren, n.l. C57BL/10 muizen, beschreven. Ook werden de methoden weergegeven, die bij deze studies gebruikt zijn.

In *Hoofdstuk 3* werden muizen behandeld met HCB, met ijzer-dextraan of met de

combinatie van HCB en ijzer-dextraan. Met behulp van licht-microscopie (LM), electronen-microscopie (EM) en morfometrisch onderzoek werd over een periode van 52 weken het verband vastgesteld tussen enerzijds de opname van ijzer en anderzijds het ontstaan van uroporfyrine kristallen in hepatocyten van C57BL/10 muizen. De voornaamste conclusies waren dat experimentele porphyrie eveneens kan worden geïnduceerd door een overmaat aan ijzer in levers van C57BL/10 muizen. Indien, behalve ijzer-dextraan, ook HCB werd toegediend, werden de effecten van ijzer op het ontstaan van experimentele uroporfyrine versterkt, terwijl toediening van HCB, zonder ijzer-dextraan, geen effect had. Uroporfyrine kristallen werden alleen aangetroffen in hepatocyten, waarin ook reeds ijzer, voornamelijk in de vorm van ferritine, aanwezig was. Dit leidde tot de conclusie dat ijzer een belangrijke rol speelt in de pathogenese van experimentele uroporfyrine.

In *Hoofdstuk 4* werden C57BL/10 muizen op dezelfde manier behandeld als beschreven in *Hoofdstuk 3*. Een deel van de proefdieren werd tevens behandeld met desferrioxamine (DFx), een chelator van ijzer. De effecten van DFx op de ijzer-opname, de productie van malondialdehyde (MDA) (een produkt van lipid peroxidatie), de accumulatie van porfyrynes en de activiteit van de enzymen URO-D en porfobilinogeen deaminase (PBG-D) in levers van C57BL/10 muizen werden gemeten over een periode van 14 weken. Peroxidatie van lipid-membranen treedt slechts op in aanwezigheid van vrije zuurstof radicalen. Als bovendien ijzer aanwezig is, wordt via de Haber-Weiss reactie de productie van deze radicalen versterkt. Daarnaast werd de fractie ijzer met laag moleculair gewicht (LMW-ijzer) gemeten, aangezien deze fractie een afspiegeling vormt van de hoeveelheid "vrij" ijzer in de lever. Slechts deze fractie van ijzer kan waarschijnlijk een rol van betekenis spelen in het optreden van schadelijke processen in de lever. De voornaamste conclusie was dat DFx de totale hoeveelheid ijzer, de accumulatie van porfyrynes, de inhibitie van URO-D activiteit, de stimulatie van PBG-D activiteit, de productie van MDA en de hoeveelheid LMW-ijzer in levers van C57BL/10 muizen verminderde. Bovendien was er een lineair verband tussen de productie van MDA en de hoeveelheid LMW-ijzer. Deze bevinding suggereert dat DFx een belangrijke rol speelt bij het verminderen van de hoeveelheid ijzer die beschikbaar is voor de productie van vrije zuurstof radicalen. De activiteit van het enzym PBG-D, één van de enzymen die aan URO-D voorafgaat in de synthese van heem, was ook verhoogd bij experimentele



uroporfyrie. Dit kan een extra verklaring geven voor de uroporfyrine accumulatie in levers van C57BL/10 muizen. Mede op grond van recente literatuur-gegevens werd verondersteld dat uroporfyrinogeen en/of andere metabolieten, in aanwezigheid van ijzer, kunnen oxideren tot produkten die het enzym URO-D remmen, waardoor uiteindelijk de accumulatie van uroporfyrines in de lever verklaard kan worden.

In *Hoofdstuk 5* werd in het beloop van 5/49 (10%) patienten met PCT een hepatocellulair carcinoom (HCC) vastgesteld. Factoren die gerelateerd waren met een verhoogde kans op het krijgen van een HCC bij PCT waren: a) Een lange symptomatische periode voordat behandeling werd ingesteld, en b) de aanwezigheid van chronisch-actieve hepatitis en/of fibrose graad 3 of cirrhose in lever biopsieën.

In hepatocyten van patienten met PCT (zowel met F-PCT als met S-PCT) werden ook uroporfyrine kristallen gevonden. Deze uroporfyrine kristallen werden, evenals in levers van proefdieren met experimentele uroporfyrie, alleen gevonden in hepatocyten waarin ook reeds ijzer (vooral in de vorm van ferritine) aanwezig was. Dit leidde tot de conclusie dat ijzer ook een belangrijke rol speelt in de pathogenese van de humane vorm van uroporfyrie, PCT.

In *Hoofdstuk 6* werd de activiteit van het enzym PBG-D gemeten in erythrocyten van 47 patienten met F-PCT (23 patienten) en S-PCT (24 patienten). Een deel van deze patienten was symptomatisch en nog niet behandeld met aderlatingen, terwijl een ander deel van de patienten geen symptomen meer had na behandeling met aderlatingen. De activiteit van PBG-D was verhoogd in erythrocyten van F-PCT en S-PCT patienten, onafhankelijk van de aanwezigheid van huidsymptomen. Door middel van de bepaling van de immunologische reaktiviteit van PBG-D kon worden vastgesteld dat het mechanisme van deze verhoogde PBG-D activiteit kon worden verklaard, enerzijds door een verminderde afbraak van het PBG-D enzym, en anderzijds door een toename van de absolute hoeveelheid PBG-D enzym.

In *Hoofdstuk 7* werden alle resultaten besproken en de overéénkomsten tussen experimentele uroporfyrie en beide vormen van PCT (F-PCT en S-PCT) aangegeven. Tenslotte werden suggesties gedaan voor toekomstig onderzoek.



## CHAPTER 9

## References

- (1) Kappas A, Sassa S, Galbraith RA, Nordmann Y. The porphyrias. In: Scriver CR, Beaudet AL, Sly WS, Valle D, eds. *The metabolic basis of inherited disease*. New York: McGraw-Hill, 1989; pp. 1305-1365.
- (2) Kushner JP, Barbuto AJ, Lee GR. An inherited enzymatic defect in porphyria cutanea tarda. Decreased uroporphyrinogen decarboxylase activity. *J Clin Invest* 1976; 58: 1089-1097.
- (3) Elder GH, Lee GB, Tovey JA. Decreased activity of hepatic uroporphyrinogen decarboxylase in sporadic porphyria cutanea tarda. *N Engl J Med* 1978; 229: 274-278.
- (4) Felsher BF, Carpio NM, Englekling DW, Nunn AT. Decreased hepatic uroporphyrinogen decarboxylase activity in porphyria cutanea tarda. *N Engl J Med* 1982; 306: 766-769.
- (5) Ippen H. Allgemeinsymptome der späten hautporphyrie (porphyria cutanea tarda) als hinweise für deren behandlung. *Dtsch Med Wochenschr* 1961; 86: 127-133.
- (6) Bottomley SS, Muller-Ebenhard U. Pathophysiology of heme synthesis. *Semin Hematol* 1988; 25: 282-302.
- (7) Nordmann Y, de Verneuil H, Deybach JC, Delfau MH, Grandchamp B. Molecular genetics of porphyrias. *Ann Med* 1990; 22: 387-391.
- (8) Ades IZ, Stevens TM, Drew PD. Biogenesis of embryonic chick liver  $\delta$ -aminolevulinic synthase: regulation of the level of mRNA by hemin. *Arch Biochem Biophys* 1987; 253: 297-304.
- (9) De Matteis F. Toxicological aspects of liver heme biosynthesis. *Semin Hematol* 1988; 25: 321-329.
- (10) Spikes JD. Porphyrins and related compounds as photodynamic sensitizers. *Ann NY Acad Sci* 1975; 244: 496-508.
- (11) Lim HW, Perez HD, Goldstein IM, Gigli I. Complement-derived chemotactic activity is generated in human serum containing uroporphyrin after irradiation with 405 nm light. *J Clin Invest* 1981; 67: 1072-1077.
- (12) Elder GH, Smith SG, Smyth SJ. Laboratory investigation of the porphyrias. *Ann Clin Biochem* 1990; 27: 395-410.
- (13) Brodie MJ, Goldberg A. Acute hepatic porphyrias. *Clin Haematol* 1980; 9: 253-272.
- (14) Thunell S, Floderus Y, Henrichson A, Moore MR, Meissner P, Sinclair J. Alcoholic beverages in acute porphria. *J Stud Alcohol* 1992; 53: 272-276.
- (15) Poh-Fitzpatrick MB. Pathogenesis and treatment of photocutaneous manifestations of the porphyrias. *Semin Liver Dis* 1982; 2: 164-176.
- (16) Elder GH, Smith SG, Herrero C, Lecha M, Mascaro JM, Muniesa AM, Czarniecki DB, Brenan J, Poulos V, de Salamanca RE. Hepatoerythropoietic porphyria: a new uroporphyrinogen decarboxylase defect or homozygous porphyria cutanea tarda. *Lancet* 1981; i: 916-919.
- (17) Nordmann Y, Grandchamp B, de Verneuil H, Phung L, Cartigny B, Fontaine G. Harderoporphyria: a variant hereditary coproporphyria. *J Clin Invest* 1983; 72: 1139-1149.
- (18) Mustajoki P, Tenhunen R, Niemi KM, Nordmann Y, Kaäriäinen H, Norio R. Homozygous variegate porphyria. A severe skin disease of infancy. *Clin Genet* 1987; 32: 300-305.

- (19) Deybach JC. Enzymatic studies on lymphocytes in human porphyrias. In: Nordmann Y, ed. *Porphyrias and porphyria*. Paris: INSERM-John Libby, 1986: pp. 163-174.
- (20) Llewellyn DH, Smyth SJ, Elder GH, Hutchesson AC, Rattenbury JM, Smith MF. Homozygous acute intermittent porphyria: compound heterozygosity for adjacent base transitions in the same codon of the porphobilinogen deaminase gene. *Hum Genet* 1992; 89: 97-98.
- (21) Kordac V, Martasek P, Zeman J, Rubin A. Increased erythrocyte protoporphyrin in homozygous variegate porphyria. *Photodermatol* 1985; 2: 257-259.
- (22) Day RS, Eales L, Meissner D. Coexistent variegate porphyria and porphyria cutanea tarda. *N Engl J Med* 1982; 307: 36-41.
- (23) McKoll KEL, Thompson GG, Moore MR, Goldberg A, Church SE, Quadri MR, Youngs GR. Chester porphyria. Biochemical studies of a new form of acute porphyria. *Lancet* 1985; ii: 796-799.
- (24) De Verneuil H, Aitken G, Nordmann Y. Familial and sporadic porphyria cutanea. Two different diseases. *Hum Genet* 1978; 44: 145-151.
- (25) Elder GH. Human uroporphyrinogen decarboxylase defects. In: Orfanos CE, Stadler R, Gollnick H, eds. *Dermatology in five continents*. Berlin: Springer-Verlag, 1988: pp. 857-860.
- (26) Held JL, Sassa S, Kappas A, Harber LC. Erythrocyte uroporphyrinogen decarboxylase activity in porphyria cutanea tarda: a study of 40 consecutive patients. *J Invest Dermatol* 1989; 93: 332-334.
- (27) Kószó F, Morvay M, Dobozy A, Simon N. Erythrocyte uroporphyrinogen decarboxylase activity in 80 unrelated patients with porphyria cutanea tarda. *Brit J Dermatol* 1992; 126: 446-449.
- (28) D'Alessandro L, Griso D, Biolcati G, Macrì A, Topi GC. Incidence of hereditary porphyria cutanea tarda (PCT) in a sample of the Italian population. *Arch Dermatol Res* 1992; 284: 212-214.
- (29) Elder GH, Roberts AG, Enriques de Salamanca R. Genetics and pathogenesis of human uroporphyrinogen decarboxylase defects. *Clin Biochem* 1989; 22: 163-168.
- (30) Jackson AH, Sancovich HA, Ferramola AM, Evans N, Games DE, Matlin SA, Elder GH, Smith SG. Macrocyclic intermediates in the biosynthesis of porphyrins. *Philos Trans R Soc Lond Biol* 1976; 273: 191-206.
- (31) Mukerji SK, Pimstone NR. Evidence for two uroporphyrinogen decarboxylase isoenzymes in human erythrocytes. *Biochem Biophys Res Commun* 1987; 146: 1196-1203.
- (32) Kawanishi S, Seki Y, Sano S. Uroporphyrinogen decarboxylase. Purification, properties, and inhibition by polychlorinated biphenyl isomers. *J Biol Chem* 1983; 258: 4285-4292.
- (33) Elder GH, Tovey JA, Sheppard DM. Purification of uroporphyrinogen decarboxylase from human erythrocytes. Immunochemical evidence for a single protein with decarboxylase activity in human erythrocytes and liver. *Biochem J* 1983; 215: 45-55.
- (34) Elder GH, Urquhart AJ. Human uroporphyrinogen decarboxylase. Do tissue-specific isoenzymes exist? *Biochem Soc Trans* 1984; 12: 661-662.
- (35) De Verneuil H, Sassa S, Kappas A. Purification of uroporphyrinogen decarboxylase from human erythrocytes. A single enzyme catalyzing the four sequential decarboxylations of uroporphyrinogens I and III. *J Biol Chem* 1983; 258: 2454-2460.
- (36) Romana M, Dubart A, Beaupain D, Chabret C, Goossens M, Romeo PH. Structure of the gene for human uroporphyrinogen decarboxylase. *Nucleic Acids Res* 1987; 15: 7343-7356.
- (37) Smith AG, Francis JE. Investigations of rat liver uroporphyrinogen decarboxylase. Comparisons of porphyrinogens I and III as substrates and the inhibition by porphyrins. *Biochem J* 1981; 195: 241-250.

- (38) Luo J, Lim CK. Order of uroporphyrinogen III decarboxylation on incubation of porphobilinogen and uroporphyrinogen III with erythrocyte uroporphyrinogen decarboxylase. *Biochem J* 1993; 289: 529-532.
- (39) Lash TD. Action of uroporphyrinogen decarboxylase on uroporphyrinogen-III: a reassessment of the clockwise decarboxylation hypothesis. *Biochem J* 1991; 278: 901-903.
- (40) Romeo PH, Raich N, Dubart A, Beaupain D, Pryor M, Kushner J, Cohen-Solal M, Goossens M. Molecular cloning and nucleotide sequence of a complete human uroporphyrinogen decarboxylase cDNA. *J Biol Chem* 1986; 261: 9825-9831.
- (41) De Verneuil H, Grandchamp B, Foubert C, Weil D, N'Guyen VC, Gross MS, Sassa S, Nordmann Y. Assignment of the gene for uroporphyrinogen decarboxylase to human chromosome 1 by somatic cell hybridization and specific enzyme immunoassay. *Hum Genet* 1984; 66: 202-205.
- (42) McLellan T, Pryor MA, Kushner JP, Eddy RL, Shows TB. Assignment of uroporphyrinogen decarboxylase (*UROD*) to the pter-p21 region of human chromosome 1. *Cytogenet Cell Genet* 1985; 39: 224-227.
- (43) Dubart A, Mattei MG, Raich N, Beaupain D, Romeo PH, Mattei JF, Goossens M. Assignment of human uroporphyrinogen decarboxylase (*URO-D*) to the p34 band of chromosome 1. *Hum Genet* 1986; 73: 277-279.
- (44) Garey JR, Hansen JL, Harrison LM, Kennedy JB, Kushner JP. A point mutation in the coding region of uroporphyrinogen decarboxylase associated with familial porphyria cutanea tarda. *Blood* 1989; 73: 892-895.
- (45) Garey JR, Harrison LM, Franklin KF, Metcalf KM, Radisky ES, Kushner JP. Uroporphyrinogen decarboxylase: a splice mutation causes the deletion of exon 6 in multiple families with porphyria cutanea tarda. *J Clin Invest* 1990; 86: 1416-1422.
- (46) Sweeney GD. Porphyria cutanea tarda, or the uroporphyrinogen decarboxylase deficiency diseases. *Clin Biochem* 1986; 19: 3-15.
- (47) Moore MR, Barnardo D, Magnus IA, Turnbull AL, Beattie AD, Goldberg A. Hepatic  $\delta$ -aminolaevulinic acid synthetase activity in porphyria cutanea tarda. *Lancet* 1972; ii: 97-100.
- (48) Miyagi K, Cardinal R, Bossenmaier I, Watson CJ. The serum porphobilinogen and hepatic porphobilinogen deaminase in normal and porphyric individuals. *J Lab Clin Med* 1972; 78: 683-695.
- (49) Parera VE, Stella AM, Wider de Xifra EA, Fukuda H, Battle AM del C. Porphyrin biosynthesis and enzymic studies in erythrocytes from normals and porphyric humans. *Int J Biochem* 1980; 12: 947-953.
- (50) Brodie MJ, Moore MR, Thompson GG, Campbell BC, Goldberg A. Is porphobilinogen deaminase activity a secondary control mechanism in haem biosynthesis in humans? *Biochem Soc Trans* 1977; 5: 1466-1468.
- (51) Alleman MA, Wilson JHP, van den Berg JWO, Edixhoven-Bosdijk A, van Gastel-Quist LMH. Familial porphyria cutanea tarda: the pattern of porphyrins found from porphobilinogen by hemolysates. *Clin Chem* 1982; 28: 1144-1147.
- (52) Ventura E, Rocchi E, Gibertini P. Hepatic and erythrocyte uroporphyrinogen synthase and decarboxylase activities in porphyria cutanea tarda. *Ital J Gastroenterol* 1980; 12: 71-75.
- (53) Kondo M, Urata G, Shimizu Y. Decreased liver  $\delta$ -aminolaevulinic acid dehydratase activity in porphyria cutanea tarda and in alcoholism. *Clin Sci* 1983; 65: 423-428.
- (54) Grossman ME, Bickers DR, Poh-Fitzpatrick MB, Deleo VA, Harber LC. Porphyria cutanea tarda. Clinical features and laboratory findings in 40 patients. *Am J Med* 1979; 67: 277-286.
- (55) Mascaro JM, Herrero C, Lecha M, Muniesa AM. Uroporphyrinogen decarboxylase deficiencies: porphyria cutanea tarda and related conditions. *Semin Dermatol* 1986; 5: 115-124.

- (56) Friedman SJ, Doyle JA. Sclerodermoid changes of porphyria cutanea tarda: possible relationship to urinary uroporphyrin levels. *J Am Acad Dermatol* 1985; 13: 70-74.
- (57) Maynard B, Peters MS. Histologic and immunofluorescence study of cutaneous porphyrias. *J Cutan Pathol* 1992; 19: 40-47.
- (58) Pimstone NR. Porphyria cutanea tarda. *Semin Liver Dis* 1982; 2: 132-142.
- (59) Felsher BF, Kushner JP. Hepatic siderosis and porphyria cutanea tarda: relation of iron excess to the metabolic effect. *Semin Hematol* 1977; 14: 243-251.
- (60) Charlton RW, Jacobs P, Seftel H, Bothwell TH. Effect of alcohol on iron absorption. *Br Med J* 1964; 2: 1427-1429.
- (61) Shanley BC, Zail SS, Joubert SM. Effect of ethanol on liver  $\delta$ -aminolaevulinic synthetase activity and urinary porphyrin excretion in symptomatic porphyria. *Br J Haematol* 1969; 17: 389-396.
- (62) Doss M, von Tiepermann R, Stutz G, Teschke R. Alcohol-induced decrease in uroporphyrinogen decarboxylase activity in rat liver and spleen. *Enzyme* 1981; 26: 24-31.
- (63) Sixel-Dietrich F, Doss M. Hereditary uroporphyrinogen decarboxylase deficiency predisposing porphyria cutanea tarda (chronic hepatic porphyria) in females after oral contraceptive medication. *Arch Dermatol Res* 1985; 278: 13-16.
- (64) Baxi LV, Rubeo TJ, Katz B, Harber LC. Porphyria cutanea tarda and pregnancy. *Am J Obstet Gynecol* 1983; 146: 333-334.
- (65) Levere RD. Stilbestrol-induced porphyria: increase in hepatic  $\delta$ -aminolevulinic acid synthetase. *Blood* 1966; 28: 569-572.
- (66) Cam C, Nigogosyan G. Acquired toxic porphyria cutanea tarda due to hexachlorobenzene. Report of 348 cases caused by this fungicide. *JAMA* 1963; 183: 88-91.
- (67) Cripps DJ, Peters HA, Gocmen A, Dogramici I. Porphyria turcica due to hexachlorobenzene: a 20 to 30 year follow-up study on 204 patients. *Brit J Dermatol* 1984; 111: 413-422.
- (68) Marks GS. Exposure to toxic agents: the heme biosynthetic pathway and hemoproteins as indicator. *Crit Rev Toxicol* 1985; 15: 151-179.
- (69) Robinson PE, Mack GA, Remmers J, Levy R, Mohadjer L. Trends of PCB, hexachlorobenzene, and  $\beta$ -benzene hexachloride levels in the adipose tissue of the U.S. population. *Environ Res* 1990; 53: 175-192.
- (70) Von Creutzfeldt W, Beck K, Clotten R, Bianchi L. Die leber bei den hepatischen porphyrien, mit besonderer berücksichtigung der porphyria cutanea tarda. *Acta Hepatol Splenol* 1966; 13: 65-83.
- (71) Epstein JH, Redeker AG. Porphyria cutanea tarda. A study of the effect of phlebotomy. *N Engl J Med* 1968; 279: 1301-1304.
- (72) Lundvall O, Weinfeld A, Lundin P. Iron storage in porphyria cutanea tarda. *Acta Med Scand* 1970; 188: 37-53.
- (73) Cortés JM, Oliva H, Paradinas FJ, Hernandez-Guío C. The pathology of the liver in porphyria cutanea tarda. *Histopathology* 1980; 4: 471-485.
- (74) Lefkowitz JH, Grossman ME. Hepatic pathology in porphyria cutanea tarda. *Liver* 1983; 3: 19-29.
- (75) Rocchi E, Gibertini P, Cassanelli M, Pietrangelo A, Borghi A, Ventura E. Serum ferritin in the assessment of liver iron overload and iron removal therapy in porphyria cutanea tarda. *J Lab Clin Med* 1986; 107: 36-42.
- (76) Campo E, Bruguera M, Rodés J. Are there diagnostic histologic features of porphyria cutanea tarda in liver biopsy specimens? *Liver* 1990; 10: 185-190.

- (77) Lundvall O, Weinfeld A. Studies of the clinical and metabolic effects of phlebotomy treatment in porphyria cutanea tarda. *Acta Med Scand* 1968; 184: 191-199.
- (78) Chlumsky J, Malina L, Chlumská A. The effect of venesection therapy on liver tissue in porphyria cutanea tarda. *Acta Hepato-Gastroenterol* 1973; 20: 124-130.
- (79) Enriquez de Salamanca R, Rico R, Peña ML, Romero F, Olmos A, Jimenez J. Patterns of porphyrin excretion in porphyria cutanea tarda under venesection treatment. *Int J Biochem* 1980; 12: 861-868.
- (80) Rocchi E, Cassanelli M, Borghi A, Paolillo F, Pradelli M, Pellizzardi S, Vezzosi A, Gallo E, Baccarani Contri M, Ventura E. Liver iron overload and desferrioxamine treatment of porphyria cutanea tarda. *Dermatologica* 1991; 182: 27-31.
- (81) Lundvall O. The effect of replenishment of iron stores after phlebotomy therapy in porphyria cutanea tarda. *Acta Med Scand* 1971; 189: 51-63.
- (82) Felsher BF, Jones ML, Redeker AG. Iron and hepatic uroporphyrin synthesis. Relation in porphyria cutanea tarda. *JAMA* 1973; 226: 663-665.
- (83) Ginsburg AD, Margesson LJ, Feleki K. Porphyria cutanea tarda due to ferrous gluconate. *Can Med Assoc J* 1990; 143: 747-749.
- (84) Turnbull A, Baker H, Vernon-Roberts B, Magnus IA. Iron metabolism in porphyria cutanea tarda and in erythropoietic protoporphyria. *Q J Med* 1973; 166: 341-355.
- (85) Reizenstein P, Höglund S, Landegren J, Carlmark B, Forsberg K. Iron metabolism in porphyria cutanea tarda. *Acta Med Scand* 1975; 198: 95-99.
- (86) Klotz H, Klotz L, Frischauf H, Schnack H. Eisenkinetik bei porphyria cutanea tarda. *Dermatologica* 1968; 137: 97-106.
- (87) French TJ, Weir H, Dowdle E. Ferrokinetics in symptomatic porphyria. *S Afr J Lab Clin Med* 1971; 17: 62-65.
- (88) Sauer MAJGF, Funk DD. Iron overload in cutaneous porphyria. *Arch Int Med* 1969; 124: 190-196.
- (89) Seymour DG, Elder GH, Fryer A, Jacobs A, Williams GT. Porphyria cutanea tarda and haemochromatosis: a family study. *Gut* 1990; 31: 719-721.
- (90) Kushner JP, Edwards CQ, Dadone MM, Skolnick MH. Heterozygosity for HLA-linked hemochromatosis as a likely cause of the hepatic siderosis associated with sporadic porphyria cutanea tarda. *Gastroenterology* 1985; 88: 1232-1238.
- (91) Edwards CQ, Griffen LM, Goldgar DE, Skolnick MH, Kushner JP. HLA-linked hemochromatosis alleles in sporadic porphyria cutanea tarda. *Gastroenterology* 1989; 97: 972-981.
- (92) Beaumont C, Fauchet R, Nhu Phung L, de Verneuil H, GueGuen M, Nordmann Y. Porphyria cutanea tarda and HLA-linked hemochromatosis. Evidence against a systemic association. *Gastroenterology* 1987; 92: 1833-1838.
- (93) Kushner JP, Steinmuller DP, Lee GR. The role of iron in the pathogenesis of porphyria cutanea tarda. II Inhibition of uroporphyrinogen decarboxylase. *J Clin Invest* 1975; 56: 661-667.
- (94) Straka JG, Kushner JP. Purification and characterization of bovine hepatic uroporphyrinogen decarboxylase. *Biochemistry* 1983; 22: 4664-4672.
- (95) Mukerji SK, Pimstone NR, Burns M. Dual mechanism of inhibition of rat liver uroporphyrinogen decarboxylase activity by ferrous iron: its potential role in the genesis of porphyria cutanea tarda. *Gastroenterology* 1984; 87: 1248-1254.

- (96) Mukerji SK, Pimstone NR. *In vitro* studies of the mechanism of inhibition of rat liver uroporphyrinogen decarboxylase activity by ferrous iron under anaerobic conditions. *Arch Biochem Biophys* 1986; 244: 619-629.
- (97) Smith AG, Francis JE. Synergism of iron and hexachlorobenzene inhibits hepatic uroporphyrinogen decarboxylase in inbred mice. *Biochem J* 1983; 214: 909-913.
- (98) Blekkenhorst GH, Eales L, Pimstone NR. Activation of uroporphyrinogen decarboxylase by ferrous iron in porphyria cutanea tarda. *S Afr Med J* 1979; 56: 918-920.
- (99) Woods JS, Kardish R, Fowler BA. Studies on the action of porphyrinogenic trace metals on the activity of hepatic uroporphyrinogen decarboxylase. *Biochem Biophys Res Commun* 1981; 103: 264-271.
- (100) Wainstok de Calmanovici R, Ríos de Molina M del C, San Martín de Viale LC. The role of iron in the hexachlorobenzene induced porphyria. I. Studies on different types of iron and its relation with porphyrinogen carboxy-lyase decrease. *Acta Physiol Pharmacol Latinoam* 1985; 35: 481-491.
- (101) Elder GH, Urquhart AJ, de Salamanca RE, Munoz JJ, Bonkowsky HL. Immunoreactive uroporphyrinogen decarboxylase in the liver in porphyria cutanea tarda. *Lancet* 1985; i: 229-232.
- (102) Mukerji SK, Pimstone NR, Tan KT. A potential biochemical explanation for the genesis of porphyria cutanea tarda. Studies on the inherent biochemical defect in highly purified human erythrocyte uroporphyrinogen decarboxylase and its amplification by iron. *FEBS Lett* 1985; 189: 217-220.
- (103) Cram DL, Epstein JH, Tuffanelli DL. Lupus erythematosus and porphyria. *Arch Dermatol* 1973; 108: 779-784.
- (104) Clemmensen O, Thomsen K. Porphyria cutanea tarda and systemic lupus erythematosus. *Arch Dermatol* 1982; 118: 160-162.
- (105) Weatherhead L, Adam J. Discoid lupus erythematosus. Coexistence with porphyria cutanea tarda. *Int J Dermatol* 1985; 24: 453-455.
- (106) Rook A, Champion RH. Porphyria cutanea tarda and diabetes. *Brit Med J* 1960; 1: 860-861.
- (107) Franks AG, Pulini M, Bickers DR, Rayfield EJ, Harber LC. Carbohydrate metabolism in porphyria cutanea tarda. *Am J Med Sci* 1979; 277: 163-171.
- (108) Calcinaro F, Basta G, Lisi P, Cruciani C, Pietropaolo M, Santeusano F, Falorni A, Calafiore R. Insulin resistance in porphyria cutanea tarda. *J Endocrinol Invest* 1989; 12: 393-399.
- (109) Day RS, Eales L. Porphyrins in chronic renal failure. *Nephron* 1980; 26: 90-95.
- (110) Goldsman CI, Taylor JS. Porphyria cutanea tarda and bullous dermatoses associated with chronic renal failure: a review. *Cleve Clin Q* 1983; 50: 151-161.
- (111) Harlan SL, Winkelmann RK. Porphyria cutanea tarda and chronic renal failure. *Mayo Clin Proc* 1983; 58: 467-471.
- (112) McColl KEL, Simpson K, Laiwah AY, Thompson GG, McDougall A, Moore MR. Haemodialysis-related porphyria cutanea tarda - treatment failure with charcoal hemoperfusion. *Photodermatol* 1986; 3: 169-173.
- (113) Anderson CD, Rossi E, Garcia-Webb P. Porphyrin studies in chronic renal failure patients on maintenance hemodialysis. *Photodermatol* 1987; 4: 14-22.
- (114) Seubert S, Seubert A, Rumpf KW, Kiffe H. A porphyria cutanea tarda-like distribution pattern of porphyrins in plasma, hemodialysate, hemofiltrate, and urine of patients on chronic hemodialysis. *J Invest Dermatol* 1985; 85: 107-109.
- (115) Gebril M, Weinkove C, Ead R, McDonald K, Morton R. Plasma porphyrins in chronic renal failure. *Nephron* 1990; 55: 159-163.



- (116) Waldo ED, Tobias H. Needle-like cytoplasmic inclusions in the liver in porphyria cutanea tarda. *Arch Pathol* 1973; 96: 368-371.
- (117) Ostrowski J, Michalak T, Zawirska E, Kostrzewska E, Błaszczyk M, Gregor A. The function and morphology of the liver in porphyria cutanea tarda. *Ann Clin Res* 1984; 16: 195-200.
- (118) Timme AH, Dowdle EB, Eales L. Symptomatic porphyria. Part I. The pathology of the liver in human symptomatic porphyria. *S Afr Med J* 1974; 48: 1803-1807.
- (119) Kosaka Y, Hagiwara M, Akeda S, Tameda Y, Tsujita E, Okuda Y, Shiomi Y, Takase K, Hashizume M, Kitajima T, Kobayashi M, Kuniyoshi M. Porphyria cutanea tarda with special reference to ultrastructural findings of the liver. *Jpn J Gastroenterol* 1981; 78: 1635-1643.
- (120) James KR, Cortés JM, Paradinas FJ. Demonstration of intracytoplasmic needle-like inclusions in hepatocytes of patients with porphyria cutanea tarda. *J Clin Pathol* 1980; 33:899-900.
- (121) Kemmer C, Riedel H, Köstler E, Pätzold K. Zur bedeutung parakristalliner nadelstrukturen für die diagnose der chronischen hepatischen porphyrie - licht- und elektronenmikroskopische untersuchungen an biopsiematerial. *Zentralbl Allg Pathol* 1983; 127: 253-264.
- (122) Chlumská A, Chlumsky J, Krtek V, Malina L. Crystalline inclusions in hepatocytes in patients with late cutaneous porphyria. *Vnitr Lek (Prague)* 1981; 27: 1110-1113.
- (123) Fakan F, Chlumská A. Demonstration of needle-shaped hepatic inclusions in porphyria cutanea tarda using the ferric ferricyanide reduction test. *Virchows Arch B Pathol Anat Histopathol* 1987; 411: 365-368.
- (124) Uthemann H, Kotitschke R, Lissner R, Goerz G. Serologische hepatitis-B-marker bei porphyria cutanea tarda. *Dtsch Med Wochenschr* 1980; 105: 1718-1720.
- (125) Stölzel U, Köstler E, Meisel H, Richter B, Schmechta H, Porstmann B. Porphyria cutanea tarda and hepatitis B. *Dtsch Gesundh Wesen* 1983; 38: 1396-1399.
- (126) Salata H, Cortés JM, Enríquez de Salamanca R, Oliva H, Castro A, Kusak E, Carreño V, Hernandez Guío C. Porphyria cutanea tarda and hepatocellular carcinoma. Frequency of occurrence and related factors. *J Hepatol* 1985; 1: 477-487.
- (127) Rocchi E, Gibertini P, Cassanelli M, Pietrangelo A, Jensen J, Ventura E. Hepatitis B infection in porphyria cutanea tarda. *Liver* 1986; 6: 153-157.
- (128) Fargion S, Piperno A, Cappellini MD, Sampietro M, Fracanzani AL, Romano R, Caldarelli R, Marcelli R, Vecchi L, Fiorelli G. Hepatitis C virus and porphyria cutanea tarda: evidence of a strong association. *Hepatology* 1992; 16: 1322-1326.
- (129) Gafà S, Zannini A, Gabrielli C. Porphyria cutanea tarda and HIV infection: effect of zideovudine treatment in a patient. *Infection* 1992; 20: 373-374.
- (130) Berman J, Braun A. Incidence of hepatoma in porphyria cutanea tarda. *Rev Czech Med* 1962; 8: 290-295.
- (131) Kordac V. Frequency of occurrence of hepatocellular carcinoma in patients with porphyria cutanea tarda in long-term followup. *Neoplasma* 1972; 19: 135-139.
- (132) Solis JA, Betancor P, Campos R, Enríquez de Salamanca R, Rojo P, Marin I, Schüller A. Association of porphyria cutanea tarda and primary liver cancer: report of ten cases. *J Dermatol* 1982; 9: 131-137.
- (133) Topi GC, D'Alessandro Gandolfo L, Griso D, Morini S. Porphyria cutanea tarda and hepatocellular carcinoma. *Int J Biochem* 1980; 12: 883-885.
- (134) Haberman HF, Rosenberg F, Menon IA. Porphyria cutanea tarda: comparison of cases precipitated by alcohol and estrogens. *Can Med Assoc J* 1975; 113: 653-655.

- (135) Malina L, Chlumsky J. A comparative study of the results of phlebotomy and low-dose chloroquine treatment in porphyria cutanea tarda. *Acta Derm Venereol* (Stochh) 1981; 61: 346-350.
- (136) Ashton RE, Hawk JLM, Magnus IA. Low-dose oral chloroquine in the treatment of porphyria cutanea tarda. *Br J Dermatol* 1984; 111: 609-613.
- (137) De Verneuil H, Bourgeois F, de Rooij F, Siersema PD, Wilson JHP, Grandchamp B, Nordmann Y. Characterization of a new mutation (R292G) and a deletion at the human uroporphyrinogen decarboxylase locus in two patients with hepatoerythropoietic porphyria. *Hum Genet* 1992; 89: 548-552.
- (138) De Verneuil H, Grandchamp B, Beaumont C, Picat C, Nordmann Y. Uroporphyrinogen decarboxylase structural mutant (Gly<sup>281</sup>→Glu) in a case of porphyria. *Science* 1986; 234: 732-734.
- (139) Toback AC, Sassa S, Poh-Fitzpatrick MB, Schechter J, Zaider E, Harber LC, Kappas A. Hepatoerythropoietic porphyria: clinical, biochemical, and enzymatic studies in a three-generation family lineage. *N Engl J Med* 1987; 316: 645-650.
- (140) Elder GH, Evans JO, Matlin SA. The effect of the porphyrogenic compound, hexachlorobenzene, on the activity of uroporphyrinogen decarboxylase in the rat. *Clin Sci Mol Med* 1976; 51: 71-80.
- (141) Smith AG, Francis JE. Increased inhibition of hepatic uroporphyrinogen decarboxylase by hexachlorobenzene in male rats given the oestrogenic drugs diethylstilboestrol and chlorotrianisene. *Biochem Pharmacol* 1981; 30: 1849-1853.
- (142) Medline A, Bain E, Menon AJ, Haberman HF. Hexachlorobenzene and rat liver. *Arch Pathol* 1973; 96: 61-65.
- (143) Timme AH, Taljaard JF, Shanley BC, Joubert SM. Symptomatic porphyria. Part II. Hepatic changes with hexachlorobenzene. *S Afr Med J* 1974; 48: 1833-1836.
- (144) Mollenhauer MH, Johnson JH, Younger RL, Clark DE. Ultrastructural changes in liver of the rat fed hexachlorobenzene. *Am J Vet Res* 1975; 36: 1777-1781.
- (145) Böger A, Koss G, Koransky W, Naumann R, Frenzel H. Rat liver alternations after chronic treatment with hexachlorobenzene. *Virchows Arch B Pathol Anat Histopathol* 1979; 382: 127-137.
- (146) Smith AG, Francis JE, Dinsdale D, Manson MM, Cabral JRP. Hepatocarcinogenicity of hexachlorobenzene in rats and the sex difference in hepatic iron status and development of porphyria. *Carcinogenesis* 1985; 6: 631-636.
- (147) Taljaard JF, Shanley BC, Deppe WM, Joubert SM. Porphyrin metabolism in experimental hepatic siderosis in the rat. II. Combined effect of iron overload and hexachlorobenzene. *Brit J Haematol* 1972; 23: 513-519.
- (148) Louw M, Neethling AC, Percy VA, Carstens M, Shanley BC. Effects of hexachlorobenzene feeding and iron overload on enzymes of haem biosynthesis and cytochrome P450 in rat liver. *Clin Sci Mol Med* 1977; 53: 111-115.
- (149) Sweeney GD, Jones KG, Cole FM, Basford D, Krestynski F. Iron deficiency prevents liver toxicity of 2,3,7,8-tetrachlorodibenzo-*p*-dioxin. *Science* 1979; 204: 332-335.
- (150) Blekkenhorst GH, Day RS, Eales L. The effect of bleeding and iron administration on the development of hexachlorobenzene-induced rat porphyria. *Int J Biochem* 1980; 12: 1013-1017.
- (151) Ferioli A, Harvey C, De Matteis F. Drug-induced accumulation of uroporphyrin in chicken hepatocyte cultures. Structural requirements for the effect and role of exogenous iron. *Biochem J* 1984; 224: 769-777.
- (152) Alleman MA, Koster JF, Wilson JHP, Edixhoven-Bosdijk A, Slee RG, Kroos MJ, van Eijk HG. The involvement of iron and lipid peroxidation in the pathogenesis of HCB induced porphyria. *Biochem Pharmacol* 1985; 34: 161-166.

- (153) Wainstok de Calmanovici R, Billi SC, Aldonatti CA, San Martin de Viale LC. Effect of desferrioxamine on the development of hexachlorobenzene-induced porphyria. *Biochem Pharmacol* 1986; 35: 2399-2405.
- (154) Sinclair PR, Granick S. Uroporphyrin formation induced by chlorinated hydrocarbons (lindane, polychlorinated biphenyls, tetrachlorodibenzo-*p*-dioxin). Requirements for endogenous iron, protein synthesis and drug-metabolizing activity. *Biochem Biophys Res Commun* 1974; 61: 124-133.
- (155) Debets FMH, Hamers WJHMB, Strik JTTWA. Metabolism as a prerequisite for the porphyrinogenic action of polyhalogenated aromatics, with special reference to hexachlorobenzene and polybrominated biphenyls (Firemaster BP-6). *Int J Biochem* 1980; 12: 1019-1025.
- (156) De Verneuil H, Sassa S, Kappas A. Effects of polychlorinated biphenyl compounds, 2,3,7,8-tetrachlorodibenzo-*p*-dioxin, phenobarbital and iron on hepatic uroporphyrinogen decarboxylase. Implications for the pathogenesis of porphyria. *Biochem J* 1983; 214: 145-151.
- (157) Wainstock de Calvanovici R, Ríos de Molina M del C, Taira de Yamasato MC, Tomio JM, San Martin de Viale LC. Mechanism of hexachlorobenzene-induced porphyria in rats. Effect of phenobarbitone pretreatment. *Biochem J* 1984; 218: 753-763.
- (158) Carpenter HM, Williams DE, Henderson MC, Bender RC, Buhler DR. Hexachlorobenzene-induced porphyria in Japanese quail. Effect of pretreatment with phenobarbital or  $\beta$ -naphthoflavone. *Biochem Pharmacol* 1984; 33: 3875-3881.
- (159) Jones KG, Sweeney GD. Dependence of the porphyrinogenic effect of 2,3,7,8-tetrachlorodibenzo-*p*-dioxin upon inheritance of aryl hydrocarbon hydroxylase responsiveness. *Toxicol Appl Pharmacol* 1980; 53: 42-49.
- (160) Lui H, Sampson R, Sweeney GD. Hexachlorobenzene porphyria. In: Doss M, ed. *Porphyria in human diseases*. Basel: Karger, 1976: pp. 405-413.
- (161) Billi SC, Koss G, San Martin de Viale LC. Screening for the ability of hexachlorobenzene metabolites to decrease rat liver porphyrinogen carboxylase. *Res Commun Chem Pathol Pharmacol* 1986; 51: 325-336.
- (162) Stewart FP, Smith AG. Metabolism of the "mixed" cytochrome P-450 inducer hexachlorobenzene by rat liver microsomes. *Biochem Pharmacol* 1986; 35: 2163-2170.
- (163) Sinclair PR, Bement WJ, Bonkovsky HL, Lambrecht RW, Frezza JE, Sinclair JF, Uruquhart AJ, Elder GH. Uroporphyrin accumulation produced by halogenated biphenyls in chick-embryo hepatocytes. Reversal of the accumulation by piperonyl butoxide. *Biochem J* 1986; 237: 63-71.
- (164) Hahn ME, Gasiewicz TH, Linko P, Goldstein JA. The role of the *Ah* locus in hexachlorobenzene-induced porphyria. Studies in congenic C57BL/6J mice. *Biochem J* 1988; 254: 245-254.
- (165) Landers JP, Bunce NJ. Review article: the *Ah* receptor and the mechanism of dioxin toxicity. *Biochem J* 1991; 276: 273-287.
- (166) Jacobs JM, Sinclair PR, Bement WJ, Lambrecht RW, Sinclair JF, Goldstein JA. Oxidation of uroporphyrinogen by methylcholanthrene-induced cytochrome P-450. Essential role of cytochrome P-450d. *Biochem J* 1989; 258: 247-253.
- (167) Lambrecht RW, Sinclair PR, Gorman N, Sinclair JF. Uroporphyrinogen oxidation catalyzed by reconstituted cytochrome P450IA2. *Arch Biochem Biophys* 1992; 294: 504-510.
- (168) Nebert DW, Nelson DR, Coon MJ, Estabrook RW, Feyereisen R, Fujii-Kuriyama Y, Gonzalez FJ, Guengerich FP, Gunsalus IC, Johnson EF, Loper JC, Sato R, Waterman MR, Waxman DJ. The P450 superfamily: update on new sequences, gene mapping, and recommended nomenclature. *DNA Cell Biol* 1991; 10: 1-14.

- (169) Hahn ME, Goldstein JA, Linko P, Gasiewicz TA. Interaction of hexachlorobenzene with the receptor for 2,3,7,8-tetrachlorodibenzo-*p*-dioxin *in vitro* and *in vivo*. Evidence that hexachlorobenzene is a weak Ah receptor agonist. Arch Biochem Biophys 1989; 270: 344-355.
- (170) Landers JP, Birse LM, Nakai JS, Winhall MJ, Bunce NJ. Chemically induced hepatic cytosol from the Sprague-Dawley rat: evidence for specific binding of 2,3,7,8-tetrachlorodibenzo-*p*-dioxin to components kinetically distinct from the Ah receptor. Toxicol Lett 1990; 51: 295-302.
- (171) Voorman R, Aust SD. Specific binding of polyhalogenated aromatic hydrocarbon inducers of cytochrome P-450d to the cytochrome and inhibition of its estradiol 2-hydroxylase activity. Toxicol Appl Pharmacol 1987; 90: 69-78.
- (172) Francis JE, Smith AG. Polycyclic aromatic hydrocarbons cause hepatic porphyria in iron-loaded C57BL/10 mice: comparison of uroporphyrinogen decarboxylase inhibition with induction of alkoxyphenoxazone dealkylations. Biochem Biophys Res Commun 1987; 146: 13-20.
- (173) Greig JB, Francis JE, Kay SJE, Lovell DP, Smith AG. Incomplete correlation of 2,3,7,8-tetrachlorodibenzo-*p*-dioxin hepatotoxicity with Ah phenotype in mice. Toxicol Appl Pharmacol 1984; 74: 17-25.
- (174) De Matteis F. Role of iron in the hydrogen peroxide-dependent oxidation of hexahydroporphyrins (porphyrinogens): a possible mechanism for the exacerbation by iron of hepatic uroporphyrin. Mol Pharmacol 1988; 33: 463-469.
- (175) Smith AG, Cabral JRP, de Matteis F. A difference between two strains of rats in their liver non-haem iron content and in their response to the porphyrinogenic effect of hexachlorobenzene. Chem Biol Interact 1979; 27: 353-363.
- (176) San Martin de Viale LC, Viale AA, Nacht S, Grinstein M. Experimental porphyria induced in rats by hexachlorobenzene. A study of the porphyrins excreted by urine. Clin Chim Acta 1970; 28: 13-23.
- (177) Hershko Ch, Eilon L. The effect of sex difference on iron exchange in the rat. Brit J Haematol 1974; 28: 471-482.
- (178) Jones KG, Sweeney GD. Association between induction of aryl hydrocarbon hydroxylase and depression of uroporphyrinogen decarboxylase activity. Res Commun Chem Pathol Pharmacol 1977; 17: 631-637.
- (179) Urquhart AJ, Elder GH, Roberts AG, Lambrecht RW, Sinclair PR, Bement WJ, Gorman N, Sinclair JA. Uroporphyrin produced in mice by 20-methylcholanthrene and 5-aminolaevulinic acid. Biochem J 1988; 253: 357-362.
- (180) Sinclair P, Lambrecht R, Sinclair J. Evidence for cytochrome P450-mediated oxidation of uroporphyrinogen by cell-free liver extracts from chick embryos treated with 3-methylcholanthrene. Biochem Biophys Res Commun 1987; 146: 1324-1329.
- (181) De Matteis F, Harvey C, Reed C, Hempenius R. Increased oxidation of uroporphyrinogen by an inducible liver microsomal system. Possible relevance to drug-induced uroporphyrin. Biochem J 1988; 250: 161-169.
- (182) Lambrecht RW, Jacobs JM, Sinclair PR, Sinclair JF. Inhibition of uroporphyrinogen decarboxylase activity. The role of cytochrome P-450-mediated uroporphyrinogen oxidation. Biochem J 1990; 269: 437-441.
- (183) Rios de Molina M del C, Wainstock de Calmanovici R, San Martin de Viale LC. Investigations on the presence of porphyrinogen carboxy-lyase inhibitor in the liver of rats intoxicated with hexachlorobenzene. Int J Biochem 1980; 12: 1027-1032.
- (184) Cantoni L, Dal Fiume D, Rizzardini M, Ruggieri R. In vitro inhibitory effect on porphyrinogen carboxylyase of liver extracts from TCDD treated mice. Toxicol Lett 1984; 20: 211-217.

- (185) Smith AG, Francis JE. Chemically-induced formation of an inhibitor of hepatic uroporphyrinogen decarboxylase in inbred mice with iron overload. *Biochem J* 1987; 246: 221-226.
- (186) Green-Thompson RP, Kimmitt SM, Marks GS. Inhibition of chick embryo hepatic uroporphyrinogen decarboxylase by components of xenobiotic-treated chick embryo hepatocytes in culture. II. *Can J Physiol Pharmacol* 1992; 70: 939-942.
- (187) Lambrecht RW, Sinclair PR, Bement WJ, Sinclair JF, Carpenter HM, Buhler DR, Urquhart AJ, Elder GH. Hepatic uroporphyrin accumulation and uroporphyrinogen decarboxylase activity in cultured chick-embryo hepatocytes and in Japanese quail (*Coturnix coturnix japonica*) and mice treated with polyhalogenated aromatic compounds. *Biochem J* 1988; 253: 131-138.
- (188) Elder GH, Tovey JA, Sheppard DM. Purification of uroporphyrinogen decarboxylase from human erythrocytes. Immunochemical evidence for a single protein with decarboxylase activity in human erythrocytes and liver. *Biochem J* 1983; 215: 45-55.
- (189) Jacobs JM, Sinclair PR, Lambrecht RW, Sinclair JF, Jacobs NJ. Role of inducer binding in cytochrome P-450IA<sub>2</sub>-mediated uroporphyrinogen oxidation. *J Biochem Toxicol* 1990; 5: 193-199.
- (190) Jacobs JM. Studies on hepatic uroporphyrinogen oxidation and its role in the uroporphyrin caused by the polyhalogenated aromatic hydrocarbons. Ph.D. dissertation, 1989. Dartmouth College, Hanover, NH, USA.
- (191) Smith AG, de Matteis F. Oxidative injury mediated by the hepatic cytochrome P-450 system in conjunction with cellular iron. Effects on the pathway of haem biosynthesis. *Xenobiotica* 1990; 20: 865-877.
- (192) Urquhart AJ, Elder GH. Hexachlorobenzene-induced oxygen activation by mouse liver microsomes: Comparison with phenobarbitone and 20-methylcholanthrene. *Biochem Pharmacol* 1987; 36: 3795-3796.
- (193) Halliwell B, Gutteridge JMC. The importance of free radicals and catalytic metal ions in human diseases. *Mol Aspects Med* 1985; 8: 89-193.
- (194) Smith AG, Francis JE, Cabral JRP, Carthew P, Manson MM, Stewart FP. Iron-enhancement of the hepatic porphyria and cancer induced by environmental polyhalogenated aromatic chemicals. In: Poli G, Cheeseman KH, Dianzani MU, Slater TF, eds. Free radicals in the pathogenesis of liver injury. *Adv Biosci.* Oxford: Pergamon Press, 1989; 76: pp. 203-214.
- (195) Rizzardini M, Graziani A, Carugo C, Cantoni L. Investigations on the role of free radical processes in hexachlorobenzene-induced porphyria in mice. *J Biochem Toxicol* 1988; 3: 33-46.
- (196) Visser O, van den Berg JWO, Edixhoven-Bosdijk A, Koole-Lesuis R, Rietveld T, Wilson JHP. Development of hexachlorobenzene porphyria in rats: time sequence and relationship with lipid peroxidation. *Food Chem Toxicol* 1989; 27: 317-321.
- (197) Mukerji SK, Pimstone NR. Free radical mechanism of oxidation of uroporphyrinogen in the presence of ferrous iron. *Arch Biochem Biophys* 1990; 281: 177-184.
- (198) Freeman BA, Crapo JD. Biology of disease: free radicals and tissue injury. *Lab Invest* 1982; 47: 412-426.
- (199) Aust SD, Svingen BA. The role of iron in enzymatic lipid peroxidation. In: Pryor WA, ed. Free radicals in biology. New York: Academic Press, 1982: pp. 1-28.
- (200) Francis JE, Smith AG. Oxidation of uroporphyrinogens by hydroxyl radicals. Evidence for nonporphyrin products as potential inhibitors of uroporphyrinogen decarboxylase. *FEBS Lett* 1988; 233: 311-314.
- (201) Jacobs JM, Sinclair PR, Lambrecht RW, Sinclair JF. Effects of iron-EDTA on uroporphyrinogen oxidation by liver microsomes. *FEBS Lett* 1989; 250: 349-352.

- (202) Sinclair PR, Jacobs JM, Deam SM, Lambrecht RW, Sinclair JF, Elder GH. Relationship between lucigenin-enhanced chemiluminescence and uroporphyrinogen oxidation in mouse and chick embryo liver microsomes. *Biochem Pharmacol* 1990; 39: 1828-1830.
- (203) Kozlov AV, Yegorov DY, Vladimirov YA, Azizova OA. Intracellular free iron in liver tissue and liver homogenate: studies with electron paramagnetic resonance on the formation of paramagnetic complexes with desferal and nitric oxide. *Free Rad Biol Med* 1992; 13: 9-16.
- (204) Wilson JHP, van den Berg JWO, Edixhoven-Bosdijk A, van Gastel-Quist LHM. Preparation of porphyrin methyl esters for high pressure liquid chromatography. *Clin Chim Acta* 1978; 89: 165-167.
- (205) Lim CK, Li F, Peters TJ. Review. High-performance liquid chromatography of porphyrins. *J Chromatogr* 1988; 429: 123-153.
- (206) Straka JG, Kushner JP, Pryor MA. Uroporphyrinogen decarboxylase. A method for measuring enzyme activity. *Enzyme* 1982; 28: 170-182.
- (207) Jordan PM. Uroporphyrinogen III Cosynthetase: A direct assay method. *Enzyme* 1982; 28: 158-166.
- (208) Wilson JHP, de Rooy FWM, te Velde K. Acute intermittent porphyria in the Netherlands: heterogeneity of the enzyme porphobilinogen deaminase. *Neth J Med* 1986; 29: 393-399.
- (209) De Rooij FWM, Hamer CM, Wilson JHP. Purification of porphobilinogen deaminase from human erythrocytes by fast protein liquid chromatography. *Clin Chim Acta* 1987; 162: 61-68.
- (210) De Rooij FWM, Hamer CM, Wilson JHP. Heterogeneity in acute intermittent porphyria: biochemical for family related variation in the mutant enzyme porphobilinogen deaminase. In: Topi GC, D'Alesandro Gandolfo L, eds. Rome: Bolletino Dell'istituto Dermatologica S. Gallicano, 1987; 8: pp. 175-180.
- (211) Harris DC. Iron exchange between ferritin and transferrin in vitro. *Biochemistry* 1978; 17: 3071-3078.
- (212) Voogd A, Sluiter W, van Eijk HG, Koster JF. Low molecular weight iron and the oxygen paradox in isolated rat hearts. *J Clin Invest* 1992; 90: 2050-2055.
- (213) Bradford MM. A rapid and sensitive method for the quantitation of microgram quantities of protein utilizing the principle of protein-dye binding. *Anal Biochem* 1976; 72: 248-254.
- (214) Lowry OH, Rosebrough NJ, Farr AL, Randall RJ. Protein measurement with the folin phenol reagent. *J Biol Chem* 1951; 193: 265-275.
- (215) Kornbrust DJ, Mavis RD. Relative susceptibility of microsomes from lung, heart, liver, kidney, brain and testes to lipid peroxidation: correlation with vitamin E content. *Lipids* 1980; 15: 315-322.
- (216) Lillie RD, Fullmer HM. *Histopathologic technic and practical histochemistry*, New York: McGraw-Hill, Inc., 4th ed., 1976.
- (217) Scheuer PJ, Williams R, Muir AR. Hepatic pathology in relatives of patients with haemochromatosis. *J Pathol Bacteriol* 1962; 84: 53-64.
- (218) Anthony PP, Vogel CL, Barker LF. Liver cell dysplasia: a premalignant condition. *J Clin Pathol* 1973; 26: 217-223.
- (219) Sorber CWJ, de Jong AAW, den Breejen NJ, de Bruijn WC. Quantitative energy-filtered image analysis in cytochemistry. I. Morphometric analysis of contrast-related images. *Ultramicroscopy* 1990; 32: 55-68.
- (220) Sorber CWJ, van Dort JB, Ringeling PC, Cleton-Soeteman MI, de Bruijn WC. Quantitative energy-filtered image analysis in cytochemistry. II. Morphometric analysis of element-distribution images. *Ultramicroscopy* 1990; 32: 69-79.

- (221) Cleton MI, Frenkel EJ, de Bruijn WC, Marx JJM. Determination of iron to phosphorus ratios of iron storage compounds in patients with iron overload: a chemical and electron probe X-ray microanalysis. *Hepatology* 1986; 6: 848-851.
- (222) Ploem JS. Reflection contrast microscopy as a tool for investigation of the attachment of living cells to a glass surface. In: van Furth R (ed). *Mononuclear phagocytes in immunity, infection and pathology*. Blackwell, Oxford, 1975: pp. 405-421.
- (223) Cornelese-ten Velde I, Prins FA. New sensitive light microscopical detection of colloidal gold on ultrathin sections by reflection contrast microscopy: combination of reflection contrast and electron microscopy in post-embedding immunogold histochemistry. *Histochemistry* 1990; 94: 61-71.
- (224) Cleton MI, Mostert LJ, Sorber LWJ, de Jong AAW, de Jeu-Jaspars CMH, de Bruijn WC. Effect of phlebotomy on the ferritin iron content in the rat liver as determined morphometrically with the use of electron energy loss spectroscopy. *Cell Tissue Res* 1989; 256: 601-605.
- (225) Samokyszyn VM, Thomas CE, Reif DW, Saito M and Aust SD. Release of iron from ferritin and its role in oxygen radical toxicities. *Drug Metab Rev* 1988; 19: 283-303.
- (226) Petyka ZJ, Kostich ND, Dhar GJ. Location of iron and porphyrin in the liver in porphyria cutanea tarda. *Acta Histochem (Jena)* 1978; 63: 168-176.
- (227) Goldberg L, Smith JP, Martin LE. The effects of intensive and prolonged administration of iron parenterally in animals. *Br J Exp Pathol* 1957; 38: 297-311.
- (228) Dunn WL. Iron-loading, fibrosis and hepatic carcinogenesis. *Arch Pathol* 1967; 83: 258-266.
- (229) Pechet GS. Parenteral iron overload. Organ and cell distribution in rats. *Lab Invest* 1969; 20: 119-126.
- (230) Van Wyk CP, Linder-Horowitz M, Munro HN. Effect of iron loading on non-heme iron compounds in different cell populations. *J Biol Chem* 1971; 246: 1025-1031.
- (231) Hultcrantz R, Arborgh B. Studies on the rat liver following iron overload. 1. Fine structural appearance. *Acta Path Microb Immun Scand A* 1978; 86: 143-155.
- (232) Parmley RT, May ME, Spicer SS, Buse MG, Alvarez CJ. Ultrastructural distribution of inorganic iron in normal and iron-loaded hepatic cells. *Lab Invest* 1981; 44: 475-485.
- (233) Smith AG, Carthew P, Francis JE, Edwards RE, Dinsdale D. Characterization and accumulation of ferritin in hepatocyte nuclei of mice with iron overload. *Hepatology* 1990; 12: 1399-1405.
- (234) Cheeseman KH, Proudfoot KA, Maddix SP, Collins MM, Milia A, Slater TF. Low rate of NADPH/ADP-iron dependent lipid peroxidation in hepatic microsomes of DBA/2 mice. *FEBS Lett* 1985; 184: 343-346.
- (235) Munro HN, Linder MC. Ferritin: structure, biosynthesis, and role in iron metabolism. *Physiol Rev* 1978; 58: 317-396.
- (236) Sweeney G, Basford D, Rowley B, Goddard G. Mechanisms underlying the hepatotoxicity of 2,3,7,8-tetrachlorodebenzo-*p*-dioxin. *Banbury Rep* 1984; 18: 225-237.
- (237) Rowley B, Sweeney GD. Release of ferrous iron from ferritin by liver microsomes: a possible role in the toxicity of 2,3,7,8-tetrachlorodibenzo-*p*-dioxin. *Can J Biochem Cell Biol* 1984; 62: 1293-1300.
- (238) Koster JF, Slee RG. Ferritin, a physiological iron donor for microsomal lipid peroxidation. *FEBS Lett* 1986; 199: 85-88.
- (239) Jacobs A. Low molecular weight intracellular iron transport compounds. *Blood* 1977; 50: 433-439.
- (240) Egyed A. Cellular iron metabolism: aspects of regulation. In: Saltman P, Henegauer J. eds. *The biochemistry and physiology of iron*. Amsterdam: Elsevier North Holland, Inc., 1982: pp. 103-119.

- (241) Morley CGD, Rewers K, Bezkorovainy A. The pathway of iron from serum transferrin to liver ferritin in the rat. In: Saltman P, Henegauer J. eds. *The biochemistry and physiology of iron*. Amsterdam: Elsevier North Holland, Inc., 1982: pp. 171-172.
- (242) Fontecave M, Pierre JL. Iron metabolism: the low-molecular-mass iron pool. *Biol Metal* 1991; 4: 133-135.
- (243) Cadenas E. Biochemistry of oxygen toxicity. *Annu Rev Biochem* 1989; 58: 79-110.
- (244) Wills ED. Lipid peroxide formation in microsomes. The role of non-haem iron. *Biochem J* 1969; 113: 325-332.
- (245) Braughler JM, Chase RL, Pregonzer JF. Oxidation of ferrous iron during peroxidation of lipid substrates. *Biochim Biophys Acta* 1987; 921: 457-464.
- (246) Hentze MW, Caughman SW, Casey JL, Koeller DM, Rouault TA, Harford JB, Klausner RD. A model for the structure and functions of iron-responsive elements. *Gene* 1988; 72: 201-208.
- (247) Kondo M, Smimizu Y. The effects of ethanol, estrogen, and hexachlorobenzene on the activities of hepatic  $\delta$ -aminolevulinic acid synthetase,  $\delta$ -aminolevulinic acid dehydratase, and uroporphyrinogen decarboxylase in male rats. *Arch Toxicol* 1986; 59: 141-145.
- (248) Stein JA, Tschudy DP, Corcoran PL, Collins A.  $\delta$ -Aminolevulinic acid synthase. III. Synergistic effect of chelated iron on induction. *J Biol Chem* 1970; 245: 2213-2218.
- (249) Beaumont C, Grandchamp B, Bogard M, de Verneuil H, Nordmann Y. Porphobilinogen deaminase is unstable in the absence of its substrate. *Biochim Biophys Acta* 1986; 882: 384-388.
- (250) Johnson PJ, Williams R. Cirrhosis and the aetiology of hepatocellular carcinoma. *J Hepatol* 1987; 4: 140-147.
- (251) Review by an international group. Acute and chronic hepatitis revisited. *Lancet* 1977; ii: 914-919.
- (252) Deugnier YM, Loréal O, Turlin B, Guyader D, Jouanolle H, Moirand R, Jacquelinet C, Brissot P. Liver pathology in genetic hemochromatosis: a review of 135 homozygous cases and their biochemical correlations. *Gastroenterology* 1992; 102: 2050-2059.
- (253) Cleton-Soeteman MI, Sindram JW. The human liver in iron overload. A morphological and functional study. Ph.D. dissertation, 1986. University of Utrecht, Utrecht, The Netherlands.
- (254) Zuyderhoudt FMJ, Sindram JW, Marx JJM, Jöring GGA, van Gool J. The amount of ferritin and hemosiderin in the livers of patients with iron-loading diseases. *Hepatology* 1983; 3: 232-235.
- (255) Niederau C, Fischer R, Sonnenberg A, Stremmel W, Trampisch HJ, Strohmeyer G. Survival and causes of death in cirrhotic and in noncirrhotic patients with primary hemochromatosis. *N Engl J Med* 1985; 313: 1256-1262.
- (256) Anderson PM, Reddy RM, Anderson KE, Desnick RJ. Characterization of the porphobilinogen deaminase deficiency in acute intermittent porphyria. Immunological evidence for heterogeneity of the genetic defect. *J Clin Invest* 1981; 68: 1-12.
- (257) Ostrowski J. Erythrocyte porphobilinogen deaminase activity in liver disease. *Gastroenterology* 1987; 92: 845-851.
- (258) Epstein O, Lahav M, Schoenfeld N, Nemes L, Shaklai M, Atsmon A. Erythrocyte uroporphyrinogen synthase activity as a possible diagnostic aid in the diagnosis of lymphoproliferative diseases. *Cancer* 1983; 52: 828-832.
- (259) Anderson KE, Sassa S, Peterson CM, Kappas A. Increased erythrocyte uroporphyrinogen-I-synthase,  $\delta$ -aminolevulinic acid dehydratase and protoporphyrin in hemolytic anemias. *Am J Med* 1977; 63: 359-364.



- (260) Cretien S, Dubart A, Beaupain D, Raich N, Grandchamp B, Rosa J, Goossens M, Romeo PH: Alternative transcription and splicing of the human porphobilinogen deaminase gen result either in tissue-specific or in housekeeping expression. *Proc Natl Acad Sci USA* 1988; 85: 6-10.
- (261) Sinclair PR, Bement WJ, Lambrecht RW, Gorman N, Sinclair JF. Chlorinated biphenyls induce cytochrome P450IA2 and uroporphyrin accumulation in cultures of mouse hepatocytes. *Arch Biochem Biophys* 1990; 281: 225-232.
- (262) Madra S, Smith AG. Induction of cytochrome P450 activities by polychlorinated biphenyls in isolated mouse hepatocytes. *Biochem Pharmacol* 1992; 44: 455-464.
- (263) Bissel DM, Arenson DM, Maher JJ, Roll FJ. Support of cultured hepatocytes by a laminin-rich gel. Evidence for a functionally significant subendothelial matrix in normal rat liver. *J Clin Invest* 1987; 79: 801-812.
- (264) Debets F, Reinders JH, Koss G, Seidel J, Strik A. Effects of dietary antioxidants on the biotransformation and porphyrinogenic action of hexachlorobenzene in two strains of rats. *Chem Biol Interact* 1981; 37: 77-94.



## List of publications related to this thesis:

Siersema PD, Wilson JHP.

De porfyrieën.

Ned Tijdschr Geneesk 1989; 133: 2542-2547.

Siersema PD, de Rooij FWM, Edixhoven-Bosdijk A, Wilson JHP.

Erythrocyte porphobilinogen deaminase activity in porphyria cutanea tarda.

Clin Chem 1990; 36: 1779-1783.

Wilson JHP, Siersema PD.

Geneesmiddelen bij acute porfyrie.

Geneesmiddelenbulletin 1990; 24: 35-40.

Siersema PD, van Helvoirt RP, Ketelaars DAM, Cleton MI, de Bruijn WC, Wilson JHP, van Eijk HG.  
Iron and uroporphyrin in hepatocytes of inbred mice in experimental porphyria: a biochemical and morphological study.

Hepatology 1991; 14: 1179-1188.

Siersema PD, de Rooij FWM, Edixhoven-Bosdijk A, Wilson JHP.

The activity of erythrocyte porphobilinogen deaminase in familial and sporadic forms of porphyria cutanea tarda.

In: Vermeer BJ, Wuepper KD, van Vloten WA, Baart de la Faille H, van der Schroeff JG (eds):  
Metabolic disorders and nutrition correlated with the skin.

Curr Probl Dermatol 1991; 20: 116-122.

Siersema PD, de Rooij FWM, Wilson JHP, van Helvoirt RP, van Eijk HG.

De porfyrieën in klinisch-chemisch perspectief.

Tijdschr NVKC 1991; 16: 16-22.

Siersema PD, ten Kate FJW, Mulder PGH, Wilson JHP.

Hepatocellular carcinoma in porphyria cutanea tarda: frequency and factors related to its occurrence.

Liver 1992; 12: 56-61.

Siersema PD, van Helvoirt RP, Cleton-Soeteman MI, de Bruijn WC, Wilson JHP, van Eijk HG.

The role of iron in experimental porphyria and porphyria cutanea tarda.

Biol Trace Elem Res 1992; 35: 65-72.

De Verneuil H, Bourgeois F, de Rooij F, Siersema PD, Wilson JHP, Grandchamp B, Nordmann Y.

Characterization of a new mutation (R292G) and a deletion at the human uroporphyrinogen decarboxylase locus in two patients with hepatoerythropoietic porphyria.

Hum Genet 1992; 89: 548-552.

Van Gelder W, Siersema PD, Voogd A, de Jeu-Jaspars NCM, van Eijk HG, Koster JF, de Rooij FWM, Wilson JHP.

The effect of desferrioxamine on iron metabolism and lipid peroxidation in hepatocytes of C57BL/10 mice in experimental uroporphyrin.

Biochem Pharmacol 1993; 46: 221-228.

Siersema PD, Cleton-Soeteman MI, de Bruijn WC, ten Kate FJW, van Eijk HG, Wilson JHP.

Ferritin accumulation and uroporphyrin crystal formation in hepatocytes of C57BL/10 mice: a time-course study.

Cell Tissue Res 1993, in press.

Siersema PD, de Man RA, Wilson JHP, Alleman MA, Mulder AH, de Rooij FWM.

Porphyria cutanea tarda and focal nodular hyperplasia: the role of estrogens.

Eur J Gastroenterol Hepatol 1993, in press.

Siersema PD, Cleton-Soeteman MI, Rademakers LHPM, ten Kate FJW, Marx JJM, de Bruijn WC, van Eijk HG, Wilson JHP.

The liver in porphyria cutanea tarda: a morphological and morphometrical study.

In preparation.



## Curriculum Vitae (in Dutch)

- 20 november 1959 Geboren te Delft
- 1978 Eindexamen VWO-B, Erasmus College, Zoetermeer  
Aanvang studie Geneeskunde, Erasmus Universiteit, Rotterdam
- februari-juli 1981 Keuze-onderzoek Immunologie  
Department of Experimental Pathology, St Mary's Hospital,  
London, UK (Head: Prof. J.F. Mowbray)
- juni-september 1982 Stage Chirurgie  
Department of Surgery, Hadassah University Hospital, Jerusalem,  
Israel (Head: Prof. Z. Eyal)
- juli-december 1983 Stage Cardiologie  
Division of Cardiovascular Medicine, Henry Ford Hospital, Detroit,  
USA (Head: Dr S. Goldstein)
- 1981-1985 Student-assistent  
Chemische Pathologie, Erasmus Universiteit, Rotterdam  
(Hoofd: Prof. Dr H.G. van Eijk)
- 1983 Doctoraalexamen (Cum Laude)
- 1985 Artsexamen
- juni-december 1986 Senior House Officer  
Department of Medicine, Charing Cross Hospital, London, UK  
(Head: Prof. A. Guz)
- 1985-1990 Opleiding tot internist  
Afdeling Inwendige Geneeskunde II, Academisch Ziekenhuis  
Rotterdam-Dijkzigt (Opleider: Prof. J.H.P. Wilson)
- 1990-1992 Internist  
Afdeling Inwendige Geneeskunde II, Academisch Ziekenhuis  
Rotterdam-Dijkzigt (Hoofd: Prof. J.H.P. Wilson) en  
Afdeling Interne Oncologie, Dr Daniël den Hoed Kliniek,  
Rotterdam (Hoofd: Prof. Dr G. Stoter)
- sedert 1992 Opleiding tot gastro-enteroloog (registreerbaar per april 1994)  
Subafdeling Gastro-Enterologie van de Afdeling Inwendige  
Geneeskunde II, Academisch Ziekenhuis Rotterdam-Dijkzigt  
(Opleider: M. van Blankenstein)



## Verantwoording (Acknowledgement in Dutch)

De afgelopen jaren had ik het voorrecht om, onder leiding van Henk van Eijk en Paul Wilson, te mogen bijdragen aan het in dit proefschrift beschreven werk.

Dit werk was niet mogelijk geweest zonder de medewerking van vele patiënten met porfyria cutanea tarda. Samen deelden wij de hoop wat beter te begrijpen wat "porfyrie" is.

In samenwerking met een aantal mede-auteurs werden de resultaten beschreven in verschillende publikaties. Hun namen staan vermeld bij de respectievelijke hoofdstukken. Samen met hen, maar ook met Peter Hoefkens, Rita Koole-Lesuis, Martin Kroos, Johan van Lier, Lianne Sorber, Kor te Velde en Gardi Voortman kon al het werk verricht worden. Patricia Stewart zorgde voor de correcte Engelse spelling.

Blijven de namen van hen die dicht om mij heen staan en die voor mij en voor wie ik zorg(d)(en). Met hen deel ik een diep gevoel van liefde en vertrouwen.

